AN EXPERIMENTAL STUDY INTO THE DYNAMIC
BEHAVIOR OF HEMISPHERICAL SHELLS
SUBJECTED TO EXTERNAL AND INTERNAL
LOADINGS.

Panagiotis Romanos

AN EXPERIMENTAL STUDY

INTO THE DYNAMIC BEHAVIOR OF HEMISPHERICAL SHELLS

SUBJECTED TO EXTERNAL AND INTERNAL LOADING

By

PANAGIOTIS ROMANOS

Lieutenant, Hellenic Navy, B.S. Greek Naval Academy (1963)

Submitted in partial fulfillment of the requirements for the
degree of Ocean Engineer   and the degree of Master of Science
in Mechanical Engineering

at the

MASSACHUSETTS INSTITUTE OF TECHNOLOGY

June,1973

An Experimental Study Into The Dynamic
Behavior of Hemispherical Shells Subjected
To External And Internal Loading

by

Panagiotis Romanos

Abstract

An experimental investigation into the dynamic
behavior of fully clamped hemispherical shells subjected
to uniformly distributed external and internal impulsive
loading is reported. The applied loads were sufficient
to cause plastic flow of the material. The materials
used were mild steel 1020 and aluminum 6061-T6. The
deflections of internally loaded specimens showed a lin-
ear variation with the initial velocity, while the de-
flections of the externally loaded specimens vary non-
linearly with velocity after a certain value of the
latter; this may be useful in evaluating a "buckling
threshold". The externally loaded specimens exhibited
a number of modes of deformation in the meridional

direction which is much less than the number of modes

of deformation in the circumferential direction.

Thesis Advisor: Norman Jones

Title: Associate Professor Naval Architecture and
        Marine Engineering

Acknowledgements

I take this opportunity to express my deep gratitude to Professor Norman Jones for his invaluable help and encouragement during the completion of this work.

Many thanks are due to Fred Merlis and Earl Wassmouth of the Aeronautics Department for their help in the experiments and equipment construction, and to Professor Ermett Witmer for the permission to use the experimental facilities.

Thanks are also due to Antonio Cunha, Theodosios Boufounos, Theodoros Achtarides and Dwight Okawa for their help in conducting the experiments.

Thanks are also extended to Andrew Summers who taught me how to use the experimental facilities and whose work proved to be extremely useful.

Finally, I thank Mrs. Ann Kim and Mrs. Katerina Litinas for their expert typing of the manuscript.

TABLE OF CONTENTS

LIST OF TABLES

LIST OF FIGURES

INTRODUCTION

The considerable attention which has been given
in recent years to the problem of instability of shell
structures, is primarily due to their increasing use
in hydrospace vehicles, nuclear reactors and space ve-
hicles. For example, complete spheres are used for
deep submersibles, while spherical caps or hemispheres
are used in order to form the ends of the pressure hulls
of submarines.

These hydrospace vehicles as well as other struc-
tures are often subjected to high intensity loading which
may be applied either dynamically or statically. Such
high loadings can be caused by deep diving, collision,
water wave impacts or high explosive effects, the latter
being usually associated with naval vessels in wartime.

Although considerable work has been so far devoted
to instability of shells subjected to static loadings,
the work done on dynamic loading is limited. For the
case of hemispherical shells which is the subject of
this investigation, a literature survey showed that the
subject of instability of hemispherical shells subjected
to external dynamic loading has been barely dealt with
up to now. In Reference (1) some experimental work has
been done on the dynamic behavior of hemispherical shells

subjected to dynamic external loading; two types of
dynamic tests were examined, of which one involved blast-
induced dynamic buckling and permanent deformation of the
shell, while the second involved producing permanent de-
formation by projectile impact coincident with the axis
of symmetry of the hemispherical shell. Hence in both
cases, the loading was not uniformly distributed over
the surface of the shell.

In Reference (2), theoretical work has been done
on elastic-plastic buckling of shells under dynamic load-
ing, with the case of hemispherical shells included.
This is the only theoretical work on dynamic instability
of hemispherical shells subjected to external loading
that the author is aware of.

It is the purpose of a major part of the present
investigation to study the experimental behavior of
clamped hemispherical shells subjected to externally
applied impulsive loading. It is hoped that the results
presented herein will help in developing new theories
on this subject or confirming already existing theories
as those of Reference (2).

The remainder of this work is devoted in the in-
vestigation of the dynamic behavior of clamped hemisphe-
rical shells subjected to internal loading. This forms

a continuation of work reported in References (3), (4)
and (5) and differs in the specimen geometry (primarily
the ratio of radius to the thickness of the hemisphere).
The dynamic internal loading of hemispherical shells has
an important application in the case of an internal ex-
plosion occurring in pressure vessels or reactor vessels.

Notation Used

h_n nominal explosive thickness

h_a measured average explosive thickness

H average thickness of hemispherical specimen

I_{sp} specific impulse of the explosive

M_{os} equal to $\sigma_{os} H^2/4$, is the static collapse moment of the hemispherical specimen

m_s loaded mass of the hemispherical specimen

R_s mean radius of the hemispherical specimen

R_e radius formed between the hemispherical part of the specimen and the flange

V_{os} impulse velocity imparted to hemisphere

W_e weight of explosive used

W permanent radial deflection, maximum value of deflections for internally loaded specimens and average value of deflections for externally loaded specimens

ρ_s density of specimen material

σ_{os} average static yield stress of hemispherical specimen

-4-

λ equal to $\dfrac{\sigma_{os}(V_{os})^2 R_s^2}{M_{os}}$, is a non-dimensional

parameter used to relate results to one another

2α overall angle of the hemisphere which is covered

by explosive

EXPERIMENTAL PROCEDURE

Twenty eight hemispherical specimens were used in this study. The general dimensions of these specimens are shown in figure 1 . Twenty one of the specimens were made from hot rolled mild steel 1020 and the remaining seven from aluminium 6061-T6. The specific dimensions for each specimen used are shown in table 1. The specimens were initially hydroformed from plates of 1/4" thickness, using a Cincinatti Milling Hydroform machine, which gave the hemispherical shape to the flat plates. The aluminium specimens were hydroformed while being in the zero heat treatment condition and were heat treated after the hydroforming, the T6 condition. The steel specimens were annealed after hydroforming. Then all the specimens were machined in order to be brought down to the dimensions required. Unfortunately, although the initial order was to machine the specimens at a maximum thickness of 0.145", due to an error of the machining company the maximum thickness obtained was only 0.090". Thus the specimens delivered were 10 steel specimens of 0.070" thickness, 11 steel specimens of 0.090" and 7 aluminium specimens of 0.090" thickness.

Initially the specimens were measured by the apparatus shown in figure 7. This apparatus consists of a dial gage with stem travel of 3" and with subdivisions of

0.001",which is attached permanently on the head of a

milling machine.Each specimen was marked before the

measurement, so that in the measurements taken after

deformation points corresponding to the same meridional

direction could be measured. The axis of the dial gage

was inclined by 20° to the vertical direction, so that

the part of the hemisphere which is near the flage can be

measured. The table on which the specimen to be measured

was resting could be rotated 360° in increments of one

degree and it could travel longitudinally with increments

of 0.001". The specimen was placed in the center of the

table and the dial gage was arranged in such a way that its

needle would pass through the center of the revolving plate

and therefore through the top of the hemispherical specimen

when it was centered on the plate. The specimens were held

firmly on the table by three cap screws placed every 90

degrees. For the specimens which were to be externally

loaded initial measurements were taken every 30° degrees,

and in each such position of the specimen 20 points were

measured starting from a point nearest to the edge of the

flange and ending to the top of the hemispherical part.

For the specimens which were to be internally loaded

initial measurements were taken every 45 degrees and in 15

points in the meridional direction up to the top of the

hemispherical part. The dial gage was adjusted to indicate zero on the top of the plate where the specimen was resting, so that the measurements gave the distance from the surface of the specimen to the top of the plate. In order to get the vertical distance of each point measured from the top of the plate the dial gage indication was multiplied by cos 20° since as mentioned above the dial gage had an inclination of 20° to the vertical. Similarly, the longitudinal position of each measured point was found by subtracting the product of the dial gage indication times sin 20° from the longitudinal travel of the table which was measured from the edge of the specimen's flange. A further explanation of how these measurement conversions were made is given in appendix I. The thickness of the specimen was measured by the device shown in two views in figures 8 and 9. Thirty eight measurements were taken in each specimen, in two intersecting at right angles meridional directions. Of the nineteen measurements in each of these directions eleven were on the hemispherical part and the remainder 8 in the flange. The twenty two measurements taken on the hemispherical part of each specimen were averaged and this average thickness is shown as H in table 1. From this table it can be seen that only specimens 13 17 and 18 have an average thickness which is slightly less than the required, which would be 0.088 since the required

thickness tolerance was 0.002" and the nominal thickness of the mentioned specimens was 0.090".

After the initial measurements were taken, the area of the specimen which were to be exposed to the dynamic load was covered by polyurethene foam, of 1/4 inch thickness, of polyester type, with density 0.032 grams/cm3. This foam was glued in place with Dupont # 4684 cement, and it acted as an attenuator which prevents spalling of the material which would happen due to the explosion. Next, the explosive was cut in four pieces which had the form of spherical triangles and the thickness of each of the pieces cut was measured on seven points (six around the perimeter and one in the middle) for tests 1 to 24 and on four points (three in the corners and one in the middle) for tests 25 to 28. The device with which the explosive thickness was measured is shown in figure 10 and it consists of a flat plate made of glass and a dial gage placed with its stem vertical to the plate and with its measuring point substituted by a wooden pad, so that it will not exert a localized high pressure on the explosive. The explosive thickness were found varying from 0.0060" to 0.0125" for explosive of nominal thickness 0.010", from 0.0152" to 0.0196" for explosive of nominal thickness 0.015" and from 0.028" to 0.0335" for explosive of nominal thickness 0.030".

The average thickness of the explosive used in each test
is also shown in table 1. The explosive was then weighed
with a scale of accuracy 0.01 gram and was glued on the top
of the foam attenuator. In all tests from 1 to 24 the
edge of the explosive after it was glued on the foam had
a vertical distance from the top of the flange of 1/4" for
the externally loaded specimens and 1/4" from the bottom
of the flange for the internally loaded specimens; from this
distance the angle formed by the radii of the spherical
surface which pass from the edges of the explosive was
found for each specimen after drawing the initial profile
of the specimen as described in appendix I. The angles so
measured are shown in table 1. In tests 25 to 28 the angle
mentioned above was specified and is also shown in table 1.

After the explosive had been firmly glued on the
foam attenuator, the specimen was bolted in the clamping
devices which are shown in figures 2 and 3. Figure 2 shows
the clamping device used for external loading and figure 3
shows the clamping device used for internal loading. Both
clamping devices were case hardened in order to protect
the serrations which prevented the slippage of the specimens.
The specimen was bolted between the two parts of the
clamping devices with 16 heat treated steel bolts of 1/4"
diameter and twenty threads per inch. The lower part of the

clamping device was then secured on the test table which
is shown in figure 4 by 4 small steel clamps as shown in the
arrangement of figure 5. Figure 5 shows the arrangement
used for internal loading. The only difference in the
external loading arrangement is that the hemispherical part
of the specimen is upwards instead of downwards as shown
in figure 5.

The explosive used in all the experiments came
from the same order and it was calibrated as described in
detail in appendix II. An explosive leader of dimensions
30 inches by 0.25 inches by 0.015 inches was used in the
experiments. One end of the leader over an area of 0.5"X0.25"
was pressed firmly on the middle of the hemispherical
specimen in such a way as to join the four parts of the
explosive which had been previously glued on the foam
attenuator. The other end of the explosive leader was folded
over a length of 1.5 inches and on this end was pressed a
number six blasting cap which detonated the the explosive.
The blasting cap was put into the hole of a metal block under
which the end of the explosive leader was placed. With this
arrangement the specimen was not affected by the impulse due
to the blasting cap. The overall testing arrangement is shown
in figure 6 with the specimen arranged for external loading.

After each experiment, the deformed specimen was

-11-

measured with the same apparatus which was used for the initial measurements as mentioned above and is shown in figure 7. Since the external surface of the specimens were used for the measurements, the externally loaded specimens were washed with pure aceton, so that all remaining parts of burned attenuator were removed and the specimens were completely clean during the measurements. In these measurements only the points along one semicircle were measured, for which the initial measurements had shown the greatest variation between the two parts of the semicircle; this corresponds to the worst possible variation in the radius measurements made. For the internally loaded specimens the same number of points were measured after deformation as the ones of the initial measurements. For the externally loaded specimens, because of the buckling phenomenon, irregular shapes were observed and hence eighty points were measured on a semicircle, so that an accurate deformation profile could be drawn. In addition, for the externally loaded specimens measurements were taken at two distances from the edge of the flange, every 10 degrees around the periphery so that deformation profiles in the sense of circles which before deformation were parallel to the base could be obtained. The details of how the deformation profiles were obtained and drawings of deformation profiles for each of the

specimens are given in appendix I .

The data obtained with this experimental investigation are shown in tables 1, 2 and 3 and plotted in figures 11, 12, 13, and 14. Sample calculations for obtaining these data are shown in appendix I.
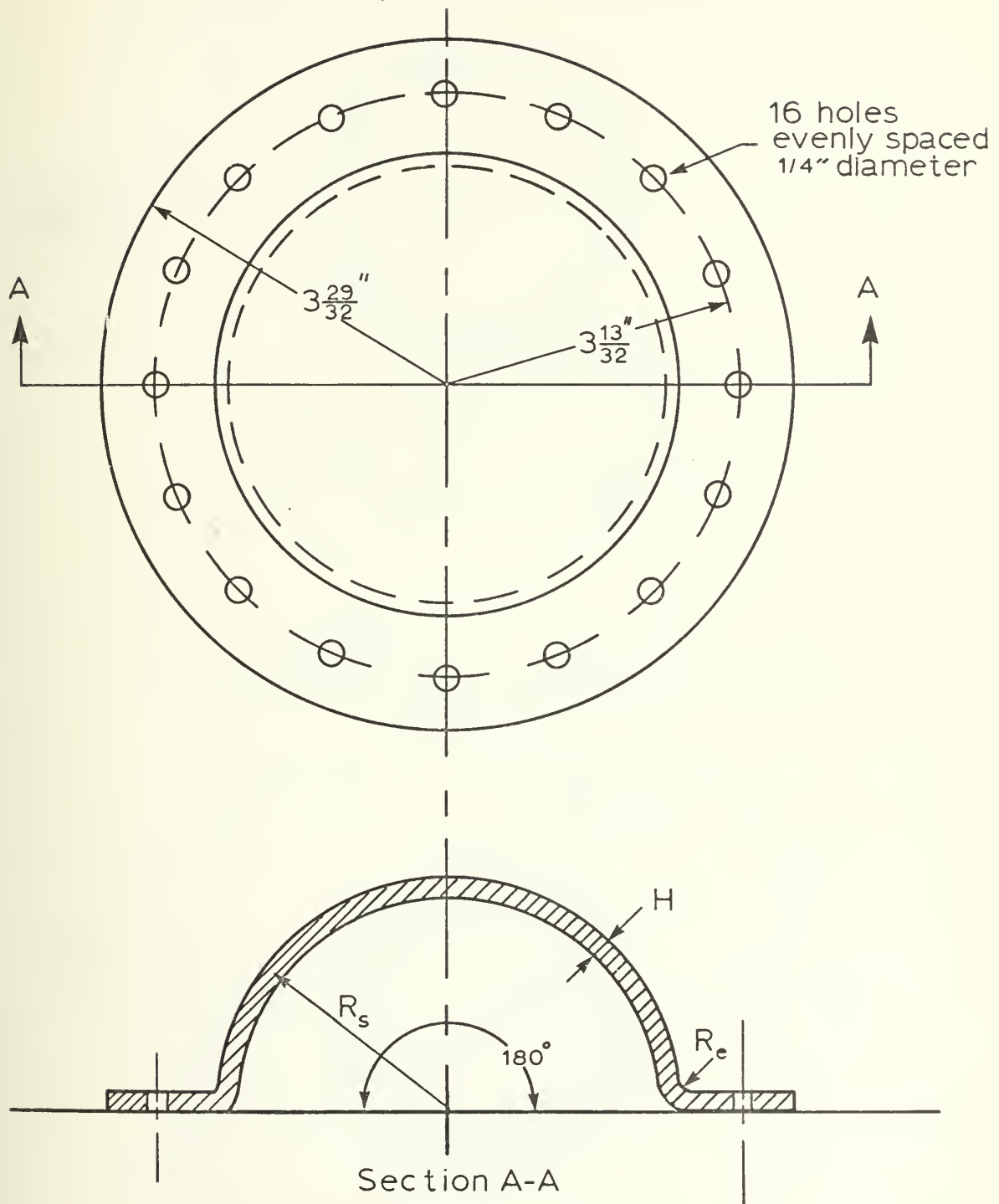
FIGURE 1: General specimen geometry
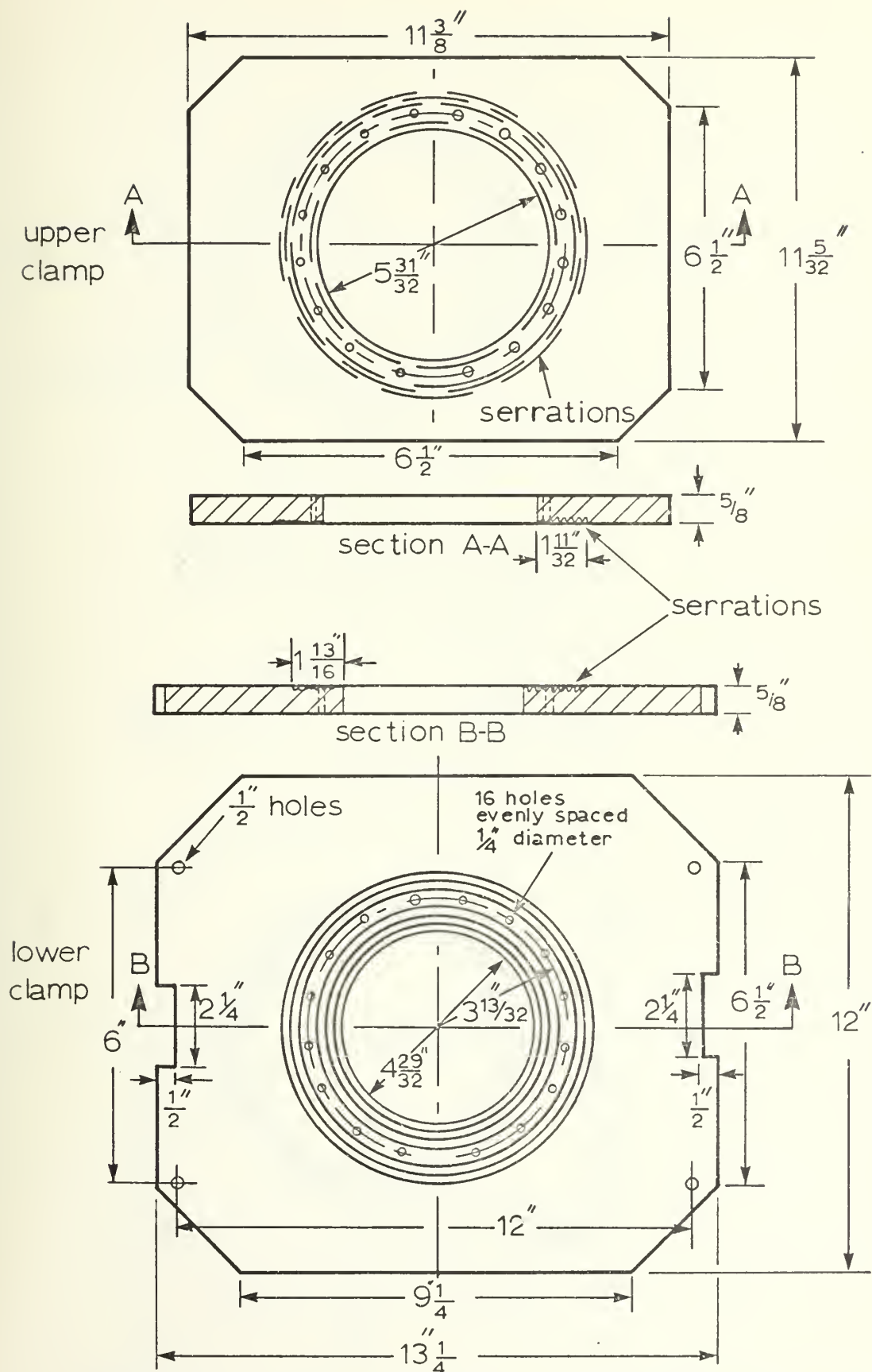
FIGURE 2: Clamping device for external loading

-15-

FIGURE 3: Clamping device for internal loading

-16-
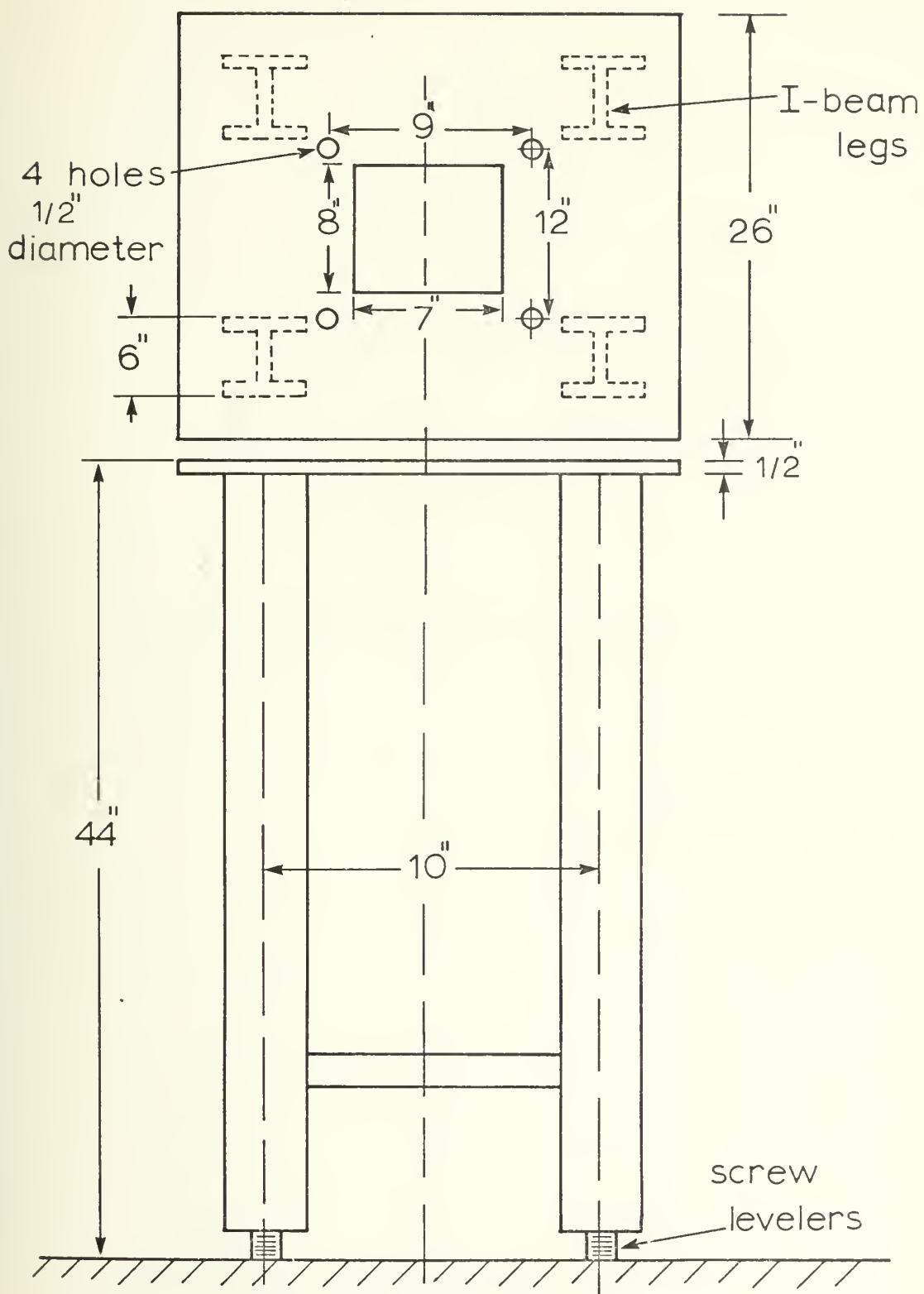
FIGURE 4: Test table

-17-
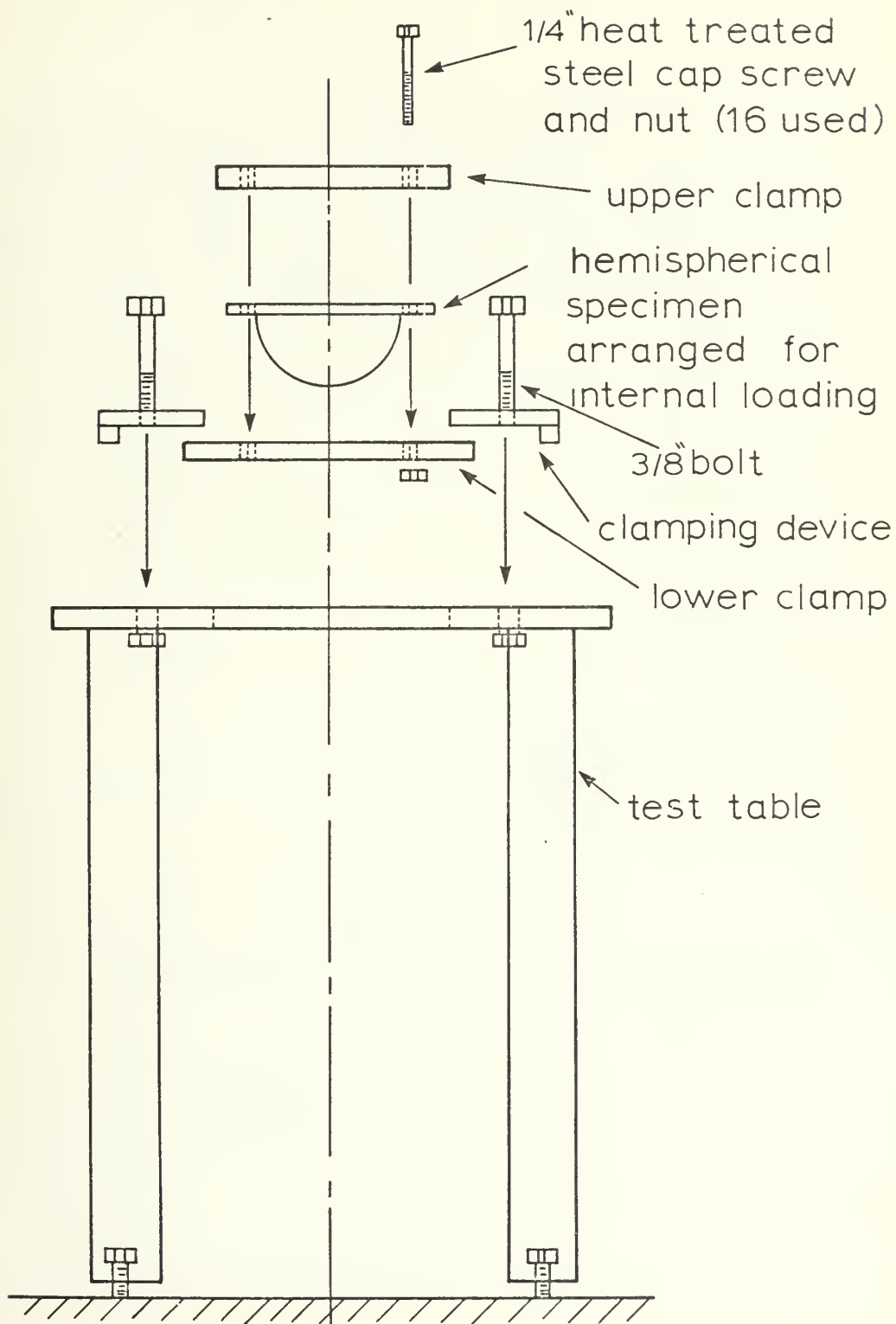
FIGURE 5: Clamping arrangement

-18-
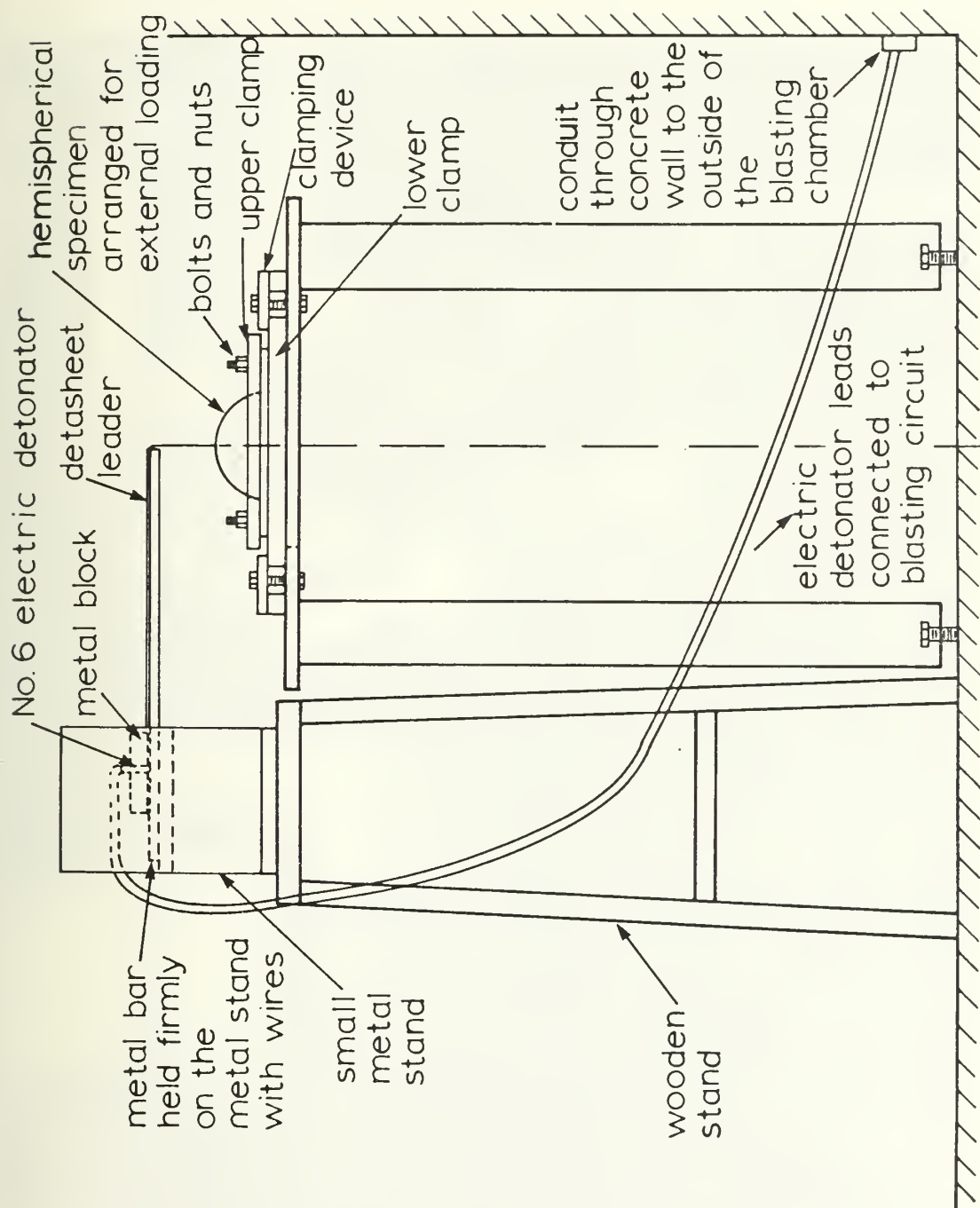
FIGURE 6: Testing arrangement

No. 6 electric detonator

hemispherical specimen arranged for external loading

bolts and nuts

upper clamp

clamping device

lower clamp

conduit through concrete wall to the outside of the blasting chamber

detasheet leader

metal block

metal bar held firmly on the metal stand with wires

small metal stand

electric detonator leads connected to blasting circuit

wooden stand

-19-

Figure 7

Figure 8

-21-

Figure 9

-22-

Figure 10

-23-
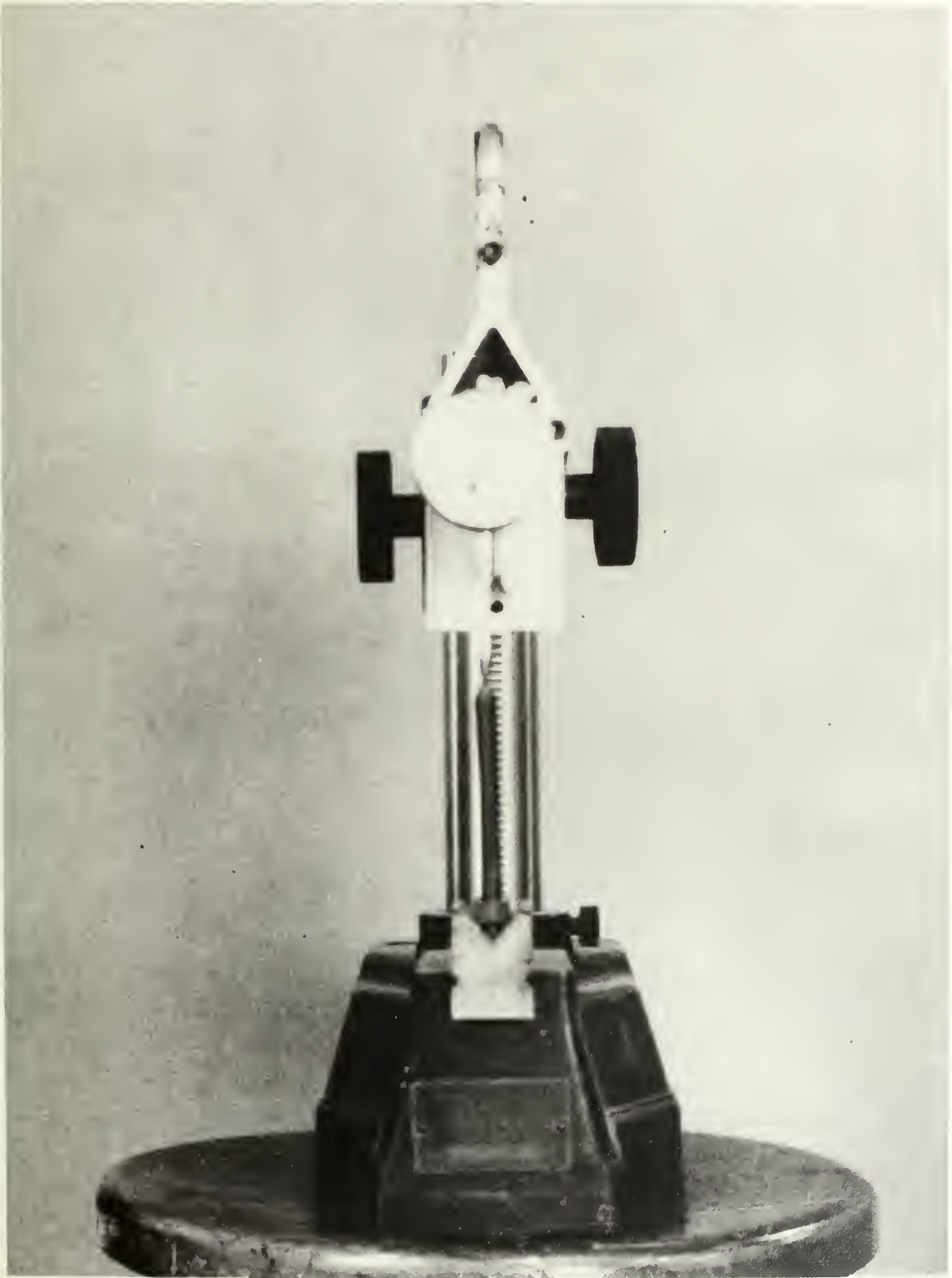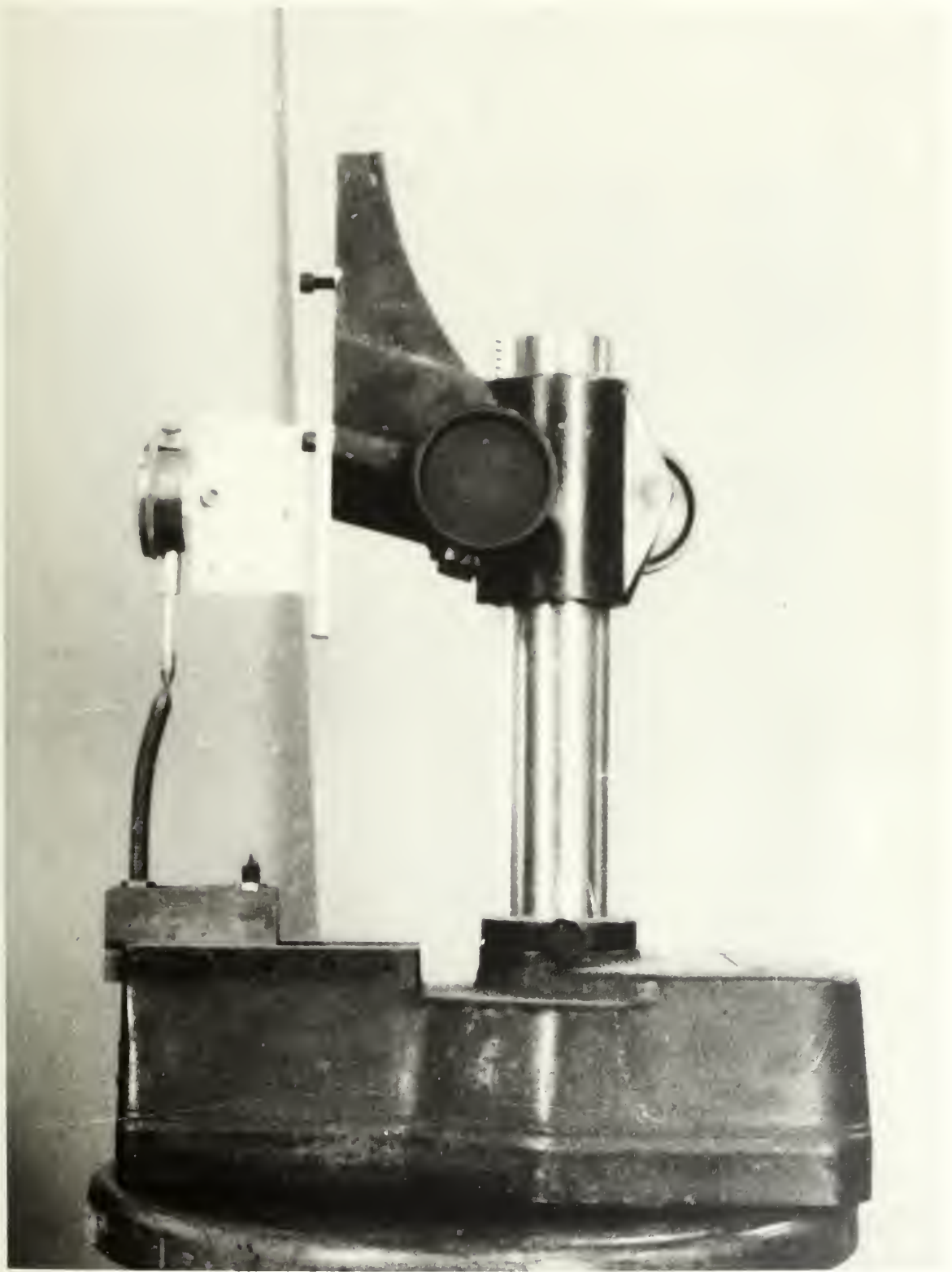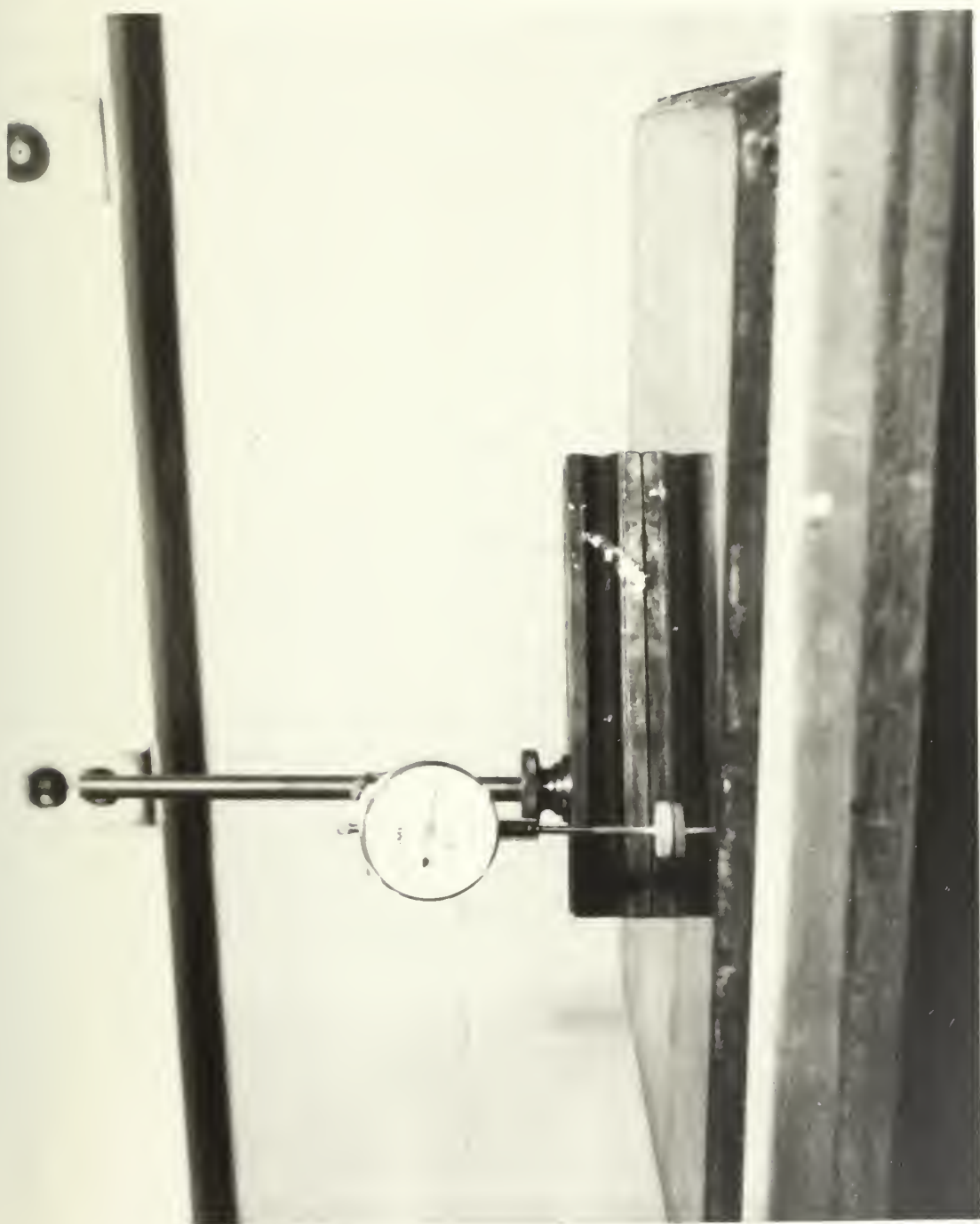
TABLE 1

SPECIMEN CHARACTERISTICS AND EXPERIMENTAL DATA

Test No.	Material	Type of Loading	R_e (in)	R_s (in)	H (in)	$\frac{R_s}{H}$	α (degrees)	h_n (in)	h_a (in)	W_e (grams)
1	M.S.	E	7/16	Part of explosive didn't detonate			83	0.020	--	20.89
2	M.S.	E	7/16	2.575	0.0708	36.339	83	0.020	0.01952	20.70
3	M.S.	E	7/16	Specimen failed completely			83	0.030	--	33.38
4	M.S.	E	7/16	2.556	0.0713	35.848	83	0.025	0.02799	28.75
5	M.S.	E	7/16	Part of explosive didn't detonate			83	0.015	--	18.31
6	M.S.	E	7/16	2.5604	0.070045	36.34	83	0.015	0.01763	18.48
7	M.S.	I	7/16	2.5596	0.06872	37.24	84.5	0.015	0.01779	11.40
8	M.S.	I	7/16	Specimen failed completely			84.5	0.030	--	22.38

TABLE 1 (cont'd)

SPECIMEN CHARACTERISTICS AND EXPERIMENTAL DATA

Test No.	Mate-rial	Type of Loading	R_e (in)	R_s (in)	H (in)	$\frac{R_s}{H}$	α (degrees)	h_n (in)	h_a (in)	W_e (grams)
9	M.S.	I	7/16	2.5589	0.06805	37.6	84.5	0.025	0.02709	18.01
10	M.S.	I	7/16	See remarks on end of table			84.5	0.020	--	12.85
11	M.S.	E	13/32	2.572	0.09032	28.477	82.2	0.030	0.031	33.46
12	M.S.	E	13/32	2.5709	0.09047	28.417	82.2	0.015	0.01717	18.37
13	M.S.	E	13/32	2.5659	0.08732	29.38	82.2	0.025	0.02751	28.78
14	M.S.	E	13/32	See remarks on end of table			82.2	0.035	--	39.73
15	M.S.	I	13/32	2.5655	0.08996	28.517	84.1	0.015	0.01713	11.90
16	M.S.	I	13/32	2.5564	0.09023	28.332	84.1	0.030	0.03137	21.88

TABLE 1 (cont'd)

SPECIMEN CHARACTERISTICS AND EXPERIMENTAL DATA

Test No.	Mate-rial	Type of Loading	R_e (in)	R_s (in)	H (in)	$\frac{R_s}{H}$	α (degrees)	h_n (in)	h_a (in)	W_e (grams)
17	M.S.	I	13/32	2.5563	0.08766	29.16	84.1	0.025	0.02688	18.83
18	M.S.	I	13/32	2.5569	0.0873	29.29	84.1	0.035	0.03667	25.63
19	M.S.	E	13/32	2.555	0.0911	28.046	82.2	0.020	0.01979	21.89
20	M.S.	I	13/32	See remarks on end of table			84.1	0.020	--	14.00
21	M.S.	E	13/32	2.5691	0.08997	28.555	82.2	0.030	0.03066	34.11
22	Al.	E	5/32	Specimen failed com-pletely			82.2	0.015	--	18.62
23	Al.	I	5/32	See remarks on end of table			84.1	0.015	--	11.95
24	Al.	I	5/32	Explosive was found burning			84.1	0.010	--	6.93

TABLE 1 (cont'd)

SPECIMEN CHARACTERISTICS AND EXPERIMENTAL DATA

Test No.	Material	Type of Loading	R_e (in)	R_s (in)	H (in)	$\frac{R_e}{H}$	α (degrees)	h_n (in)	h_a (in)	W_e (grams)
25	Al.	I	5/32	Specimen failed completely			45	0.025	--	7.82
26	Al.	I	5/32	2.5596	0.09066	28.233	45	0.015	0.01609	4.20
27	Al.	I	5/32	Part of the explosive			30	0.015	--	1.98
28	Al.	I	5/32	2.5669	0.08923	28.769	60	0.015	0.01737	7.64

Remarks On TABLE 1

1. M.S. : Mild steel 1020

   Al. : Aluminum 6061-T6

   R_e : radius formed between spherical and flat part of each specimen as shown in Figure 1.

   H : Average thickness of hemisphere

   R_s : Average radius of the hemisphere as shown in Figure 1.

Remarks On Table 1

α   :   Angle formed by two radii of the hemisphere, one of which passes
         through the top of the hemispherical surface and the other through
         the lower edge of the explosive.

h_n :   nominal thickness of explosive used

h_a :   average thickness of explosive used

W_e :   weight of explosive used

E   :   refers to external loading

I   :   refers to internal loading

2.   In tests 10 and 20 the deformations measured after the tests were found less
     than those of 7 and 15, although larger amounts of explosive were used.   Hence
     the experimental results of tests 10 and 20 were considered unreliable.

3.   In tests 14 and 23 large cracks were developed around the edge of the specimen
     between the hemispherical and the flat part and hence the deformations were
     not measured.

TABLE 2

EXPERIMENTAL RESULTS

Test No.	$m_s \times 10^5 \dfrac{lb_f - sec^2}{in}$	I_t (lb_f-sec)	V_{os} (in/sec)	λ	W (in)	$\dfrac{W}{H}$	E_r (energy ratio)
2*	187.37	8.423	4,495	1,716	0.1366 (0.176)	1.927	217
4*	185.76	11.698	6,297	3,279	0.2638 (0.373)	3.699	425
6	184.17	7.519	4,083	1,415	0.1655 (0.222)	2.349	178
7	184.87	4.638	2,509	562	0.071	1.033	66
9*	182.96	7.328	4,005	1,458	0.117	1.719	172
11*	234.5	13.615	5,806	1,758	0.2449 (0.308)	2.711	361

TABLE 2 (cont'd)

EXPERIMENTAL RESULTS

Test No.	$m_s \times 10^5 \dfrac{lb_f\text{-}sec^2}{in}$	I_t (lb_f-sec)	V_{os} (in/sec)	λ	W (in)	$\dfrac{W}{H}$	E_r (energy ratio)
12*	234.7	7.475	3,185	527	0.0779 (0.095)	0.861	109
13	225.65	11.71	5,190	1,495	0.1598 (0.206)	1.83	289
15*	241.26	4.84	2,007	211	0.0325	0.361	43
16	240.27	8.903	3,705	709	0.108	1.197	147
17*	233.4	7.662	3,283	589	0.083	0.946	116
18*	232.5	10.331	4,443	1,089	0.1165	1.334	212
19	233.4	8.907	3,816	737	0.0921 (0.125)	1.0109	156

TABLE 2 (cont'd)

EXPERIMENTAL RESULTS

Test No.	$m_s \times 10^5 \dfrac{lb_f\text{-}sec^2}{in}$	I_t (lb$_f$-sec)	V_{os} (in/sec)	λ	W (in)	$\dfrac{W}{H}$	E_r (energy ratio)
21*	233.08	13.879	5,955	1,859	0.2495 (0.312)	2.773	380
26	27.22	1.709	6,279	767	0.1575	1.737	62
28	45.99	3.108	6,759	922	0.175	1.961	72

Remarks On TABLE 2

1. W for the internally loaded specimens is the maximum deflection measured on a semicircle, and for externally loaded specimens it is the average deflection measured on a semicircle, and inside parenthesis the maximum deflection measured is indicated.

Remarks On TABLE 2

2. The asterisk (*) in the side of the test numbers indicates that the observed maximum deflection was not in the top of the hemisphere.

TABLE 3

MODES OF DEFORMATION OF EXTERNALLY

LOADED SPECIMENS

Test No.	No. of Peaks In Meridional Semicircle	No. of Peaks In Circles Parallel To The Base
2	3	11
4	5	10
6	3	7
11	3	10
12	3	8
13	4	11
14	-	8
19	3	9
21	3	10

$W \times 10$
in

4
3
2
1

—— O H ≈ 0.070in
- - - △ H ≈ 0.090in

$V_{os} \times 10^{-3}$
in/sec

External loading

1 2 3 4 5 6 7

O 4
△ 21
11 △
△ 13
O 2
△ 19
O 6
△ 12

△ 15
O 7
△ 17
O 9
△ 16
18 △

Internal loading

Figure 11

Figure 12

Figure 13
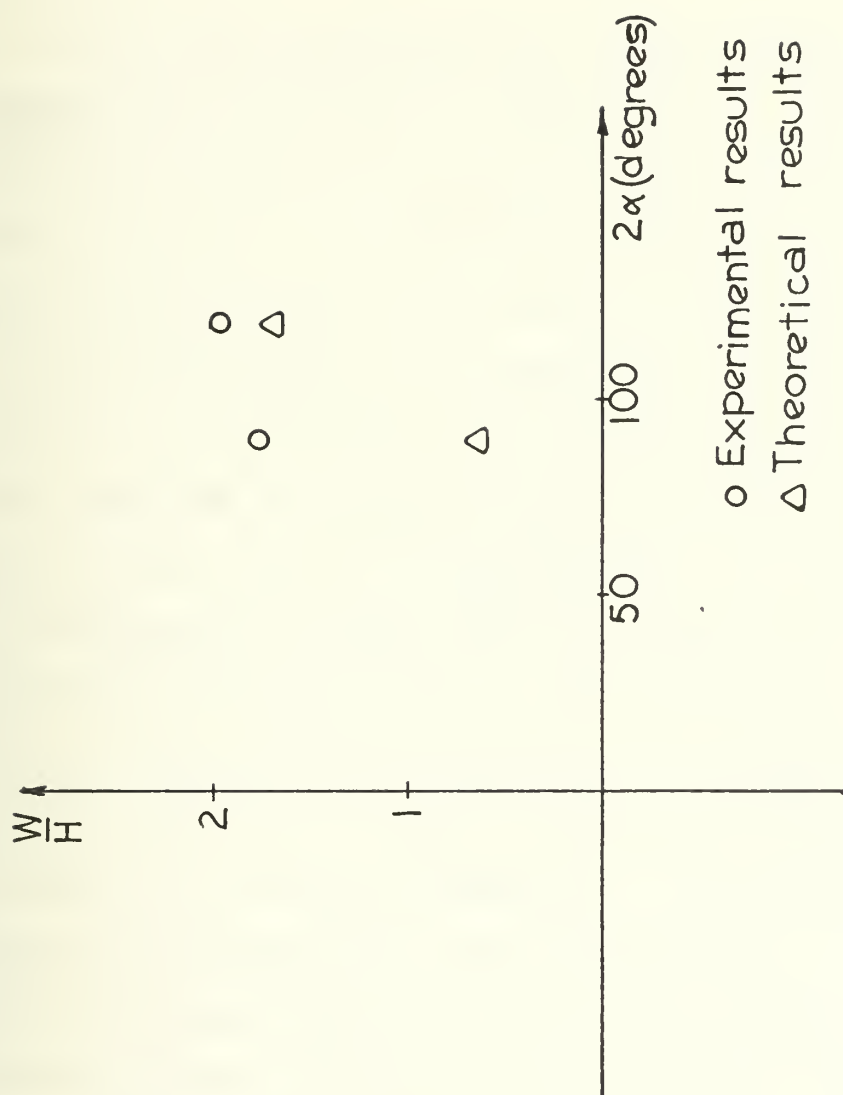
Figure 14

Experimental Results

·The results obtained in the present experimental
investigation are shown in Tables2 and 3, while some
experimental data used to evaluate those results are
given in Table 1. For the calculation of the quantities
shown in Table 2 the yield stress of the material used
for the fabrication of the specimens, as well as their
densities were required; for this purpose tensile tests
were conducted with tensile specimens from the materials
used and are reported in Appendix III. For the densities
of the materials average values of densities of the same
materials obtained in previous investigations were used,
and are also reported in Appendix III. Samples of the
calculations made in order to obtain the results shown
in Table 2 are shown in Appendix I. In Appendix I the
method of measuring the radial deflections is described,
tables of these deflections for each specimen are given
and deformation profiles in the meridional direction for
one measured semicircle are given for each specimen.
From the deformation profiles of the externally loaded
specimens in the meridional direction, the number of peaks
of the deformation profile were measured and are shown in
Table 3. For the externally loaded specimens two deform-
ation profiles in the circumferential sense were also

obtained for each specimen by the method described in
Appendix I and they are drawn also in the same Appendix
for each of the externally loaded specimens. The last
mentioned circumferential profiles were also drawn for
specimen 14 although the radial deformations of the speci-
men were not measured because of a large crack which
developed in the part between the spherical part and the
flange of the specimen; these profiles were drawn be-
cause it was considered useful to see the deformation pro-
files in the circumferential direction of this specimen
which was subjected to higher loading than the other speci-
mens of the same nominal thickness.

Discussion of Results

The deflections of the specimens used in the meri-
dional and circumferential direction which are presented
in form of tables and drawings in Appendix I show a cer-
tain non symmetry. This may be due to a number of factors.
The radius of the hemisphere measured on one semicircle in
the meridional direction was found varying a little so that
the shape was not perfectly circular. The thickness was
found varying by a little more than $\pm 0.002''$ which was the
tolerance initially required; moreover the thickness of the
specimens in the region between the hemispherical part and
the flange was less than the thickness of the rest of the
specimen and this can justify the comparatively high de-
flections measured in this region, since one would expect
to have deflections increasing as we go away from the
clamped region and not decreasing near this region and then
increasing again. The main factor to which the non sym-
metry of deformation may be due to the variation in the
thickness of the explosive which is mentioned in the Ex-
perimental Procedure.

Since the energy ratios E_r calculated for all
specimens in the way shown in Appendix I and reported
in Table 2 vary from 43 to 425, the material elasticity
should not affect the overall structural response and the
energy dissipation can be considered as purely plastic.

From the deformation profiles for the externally loaded specimens which are presented in Appendix I, the conclusion may be drawn that the number of modes of deformation in the meridional direction is much less than in the circumferential direction as shown also in Table 3.

The experimental results are plotted in Figures 11 to 14. In Figure 11 the deflection of the specimen is plotted versus the velocity imparted to the specimen by the explosive. For the externally loaded specimens the average deflection was used while for the internally loaded specimens the average deflection was used. It can be seen from Figure 11 that for the same velocity V_{os}, the specimens with nominal thickness 0.070 in. exhibited deflection higher than those of nominal thickness 0.090 in., which, of course, was to be expected. Moreover, although the deflections of the internally loaded specimens show an almost linear variation with velocity, the deflection of the externally loaded specimens shows a strong non-linear variation with velocity after a certain point. This non-linearity is more pronounced in Figure 12 in which the same plotting as in Figure 11 is made, but using the maximum deflections of the externally loaded specimens. This implies that a "buckling threshold" could be found, which is the point

after which the slope of the deflection-velocity curve starts to change abruptly.

In Figure 13 the non dimentional deflection W/H is plotted against the non-dimensional impulse parameter λ. The values of $\frac{W}{H}$ and λ for each specimen were taken from Table 2. It can be seen from Figure 13 that the variation of the non-dimensional deflection $\frac{W}{H}$ with the non-dimensional impulse parameter λ is slightly non-linear. Also for the same value of λ the values of $\frac{W}{H}$ for the specimens with nominal thickness of 0.090 in., are higher than those for the specimens with a nominal thickness of 0.070 in.

Finally in Figure 14 the non-dimensional deflection $\frac{W}{H}$ is plotted against half of the included angle of the explosive α, for specimens 26 and 28, which were the only aluminum specimens for which results were obtained. These experimental points are too few for valid conclusions to be drawn. In Figure 14 the theoretical predictions for the values of $\frac{W}{H}$ which were calculated in Appendix I according to a method given in Reference (9) are also plotted. It can be seen that the theoretical prediction for the value of $\frac{W}{H}$ for specimen 26 is much less than the experimental value, while for specimen 28 a much better agreement was obtained.

-42-

CONCLUSIONS AND RECOMMENDATIONS

An experimental investigation into the dynamic behavior of fully clamped hemispherical shells subjected to uniformly distributed external and internal impulsive loading is reported herein. The applied loads were sufficiently high to cause plastic flow of the material. The materials used for the specimen fabrication were mild steel 1020 which is a highly strain rate sensitive material and aluminium 6061-T6 which is insensitive to strain rate. It was one of the purposes of this work to assess the influence of strain rate sensitivity of the materials on the structural response. However due to the small thicknesses of the delivered specimens this became impossible because complete failure of the aluminium specimens was observed at comparatively low loads.

It was observed that the deflections of the internally loaded specimens show a linear variation with the initial velocity imparted to the specimens by the explosive, while the deflections of the externally loaded specimens vary non-linearly with velocity after a certain value of the latter. This may imply that a "buckling threshold" could be calculated as the velocity for which the slope of the deflection vs velocity curve starts to change abruptly.

From the results of externally loaded specimens

it was observed that the number of modes of deformation in the meridional direction is much less than that in the circumferential direction.

It is recommended that some more tests be made with steel specimens of 0.070 in thickness so that the results obtained in this work can be verified, because for this thickness the number of successful tests made were only a few. Also it would be interesting to test thicker aluminium specimens with external load as well as steel specimens with the same thickness in order to find the behavior of aluminium specimens in buckling and to assess the influence of strain rate sensitivity of the material on the deformation; specimens of higher thicknesses will permit also the use of higher loadings without complete failure.

References

1. Witmer E.A., Pian T.H.H. and Balmer H.A.: "Dynamic Deformation and Buckling of Spherical Shells Under Blast and Impact Loading". Collected Papers on Instability of Shell Structures, NASA TN-D-1510, 1962.

2. Ahn, C.S. : "Elastic Plastic Buckling of Shells Under Dynamic Loading", Ph.D. Thesis, M.I.T. Department of Ocean Engineering, June 1972.

3. Giannotti, J.G. : "An Experimental Study into the Dynamic Behavior of Spherical Shells". M.S. Thesis, M.I.T. Department of Civil Engineering, June 1970.

4. Jones, N., Giannotti, J.G. and Grassit, K.E. : "An Experimental Study into the Dynamic Behavior of Spherical Shells and Shell Intersections", M.I.T. Department of Ocean Engineering, Report 71-15, 1971. Also Archiwum Bodowy Maszyn (Arch. of Mech. Eng.) 1972.

5. Summers, A.B. : "Experimental Dynamic Plastic Behavior of Shell Intersections". M.S. Thesis, M.I.T. Department of Ocean Engineering, February 1973.

6. Dumas, J.W. : "Dynamic Response of Cylindrical Shells to Impulsive Loading". Naval Engineer Thesis, M.I.T. Department of Ocean Engineering, 1970.

7. Jones, N., Dumas J.W., Giannotti, J.G. and Grassit K.E.:
    "The Dynamic Plastic Behavior of Shells" published in
    "Dynamic Response of Structures" edited by G. Herrmann
    and N. Perrone, Pergammon Press, 1972 pp. 1-29.

8. Daily, J.W., and Harleman, D.R.F.: "Fluid Dynamics",
    Addison-Wesley Publishing Co., Inc., Reading, Mass.
    1966.

9. Jones, N., and Walters, R.M., "A Comparison of Theory
    and Experiments on the Dynamic Plastic Behavior of
    Shells", Archives of Applied Mechanics, Vol. 24, Olszak
    Anniv. Vol., pp. 701-714, 1972.

APPENDIX I

EXPLANATION OF MEASUREMENT CONVERSIONS, DRAWING OF
INITIAL AND DEFORMATION PROFILES TABLES OF DEFLECTIONS
AND SAMPLE CALCULATIONS.

Explanation of Measurement Conversions

The manner and the apparatus with which the speci-
mens were measured before and after deformation were
described above. Figure I-1 shows a schematic diagram
of the measuring apparatus. In this figure the solid
arrow on the spherical surface indicates the stem of
the dial gauge with which the measurements were taken
and which had an inclination of 20° to the vertical as
shown. The dial gauge reading is the distance d ,
that is the distance from the spherical surface to the
top of the flat plate on which the specimen was resting.
The longitudinal travel of the table on which the flat
plate and the specimen were resting is shown as ℓ in
Figure I-1 and as mentioned before it could be measured
with accuracy of 0.001". In order to plot the initial
and deformation profiles, the distances x and y which
are shown in Figure I-1 were required. Distance x is
the horizontal distance of the measured point from a point
near the edge of the flange which was the zero of the
longitudinal travel of the table. From the geometry of
Figure I-1 we get:

$$y = d \cos 20^\circ$$
$$x = \ell - d \sin 20^\circ$$

For example with d = 1.1581 in. and ℓ = 1.875 in.
which were taken from initial measurements of specimen
11, we have:

y = 1.0082 in.   and   x = 1.4789 in.

In this way all the measurements taken before and
after deformation were converted and the coordinates of
each point obtained, so that they could be easily plotted.

Drawing of Initial and Deformation Profiles

After the measurements taken before and after de-
formation had been converted as described above, the
initial and deformation profiles of one semicircle (of
which the before deformation measurements showed the
highest variation) were drawn with a scale of 10 to 1.
From the initial profile so drawn the outside radius of
the hemisphere was measured at each point plotted and
from all these measurements the average outside radius
of the hemisphere was obtained. From this value of
average outside radius and the average thickness of
the hemisphere obtained as already mentioned, the mean
radius R_s of each specimen was obtained and is shown
in Table 1. From the drawings of initial and deforma-
tion profiles mentioned above, radial deflections of
the deformed specimen were obtained every 10 degrees
in the meridional direction. These deflection measure-
ments are shown for each specimen in Table I-1 to I-16.
The detailed measurements taken are not given in this
report because of their great volume.

For each specimen a deformation profile in the
meridional direction was drawn, which was based on the
radial deflections obtained as mentioned above and on
the average outside radius of each specimen.

The profiles so drawn are shown in figures in the end of this appendix and they are drawn from 10 degrees up to 170 degrees in the meridional direction. It should be mentioned here that due to the large radius due to machining in the part of the specimens between the hemisphere and the flange (which is shown as R_e in Table 1) and to the fact that in most specimens the thickness of the specimen in this part was found to be less than in the rest of the specimen, the deformations found there were longer than expected. From the profiles drawn in the meridional sense the number of peaks was measured and is shown in Table 3.

In the internally loaded specimens the edge of the flange exhibited a downward motion and this had to be taken into account in the calculation of the deflections of the hemisphere. For this reason the initial measurements of a point of the flange at a known distance from the edge were averaged and this average was subtracted from the average of the final measurements of points of the flange at the same distance from the edge. In this way the vertical movement of the flange at a known distance from the edge was found. In order to find the vertical motion of the hemisphere due to the deflection of the flange, the vertical movement of a point of the flange found as described above was multiplied by the

ratio of the distance of the cross section of the mid-
surface of the hemisphere with the flange from the edge
of the flange to the distance of the measured point
from the edge of the flange. The vertical motion of
the hemisphere due to the deflection of the inner edge
of the flange was subtracted from the vertical deflec-
tions of all measured points which had a distance from
the edge of the flange of more than 1.25 in. This dis-
tance of 1.25 in. was a little less than the calculated
in each case distance of the cross section of the mid-
surface of the hemispherical surface with the flange.
This correction as mentioned above was made to the re-
sults of all internally loaded specimens except of speci-
men 7 for which no deflection of the flange was found.

For the externally loaded specimens measurements
were taken after deformation in the sense of circles
initially parallel to the base at two constant dis-
tances from the edge of the flange. These distances
(indicated by letter ℓ in Figure I-1) were 1.5 in. and
2.5 in. for specimen 2 and 1.75 in. and 2.75 in. for all
other externally loaded specimens. An average value of
the distance x (as shown in Figure I-1) was obtained
from the initial measurements at each constant distance
ℓ and was subtracted from each x distance measured
after deformation; in this way the horizontal component

of the deflection of each measured point was obtained.
Next the average radius of each circle which was ini-
tially parallel to the base was obtained by subtracting
the average x value of initially measured points (at
constant distance ℓ) as mentioned above from the dis-
tance of the center of the hemisphere from the edge of
the flange. This circle was next drawn and the horizon-
tal deflections of the points measured every 10° were
plotted on radial lines from the periphery of the circle.
Thus, 36 points were obtained and a deformation profile
was drawn. For each externally loaded specimen two such
profiles were drawn corresponding to distances ℓ as
mentioned above, and they are shown in figures presented
in the end of this appendix. From these figures the
number of peaks observed in each profile was counted
and is shown in Table 3.

In Figure I-2 a photograph of specimen 14 after
deformation is shown. From this photograph the ripples
due to buckling are clearly shown, as well as the deep
crack in the right hand side, which is the reason for
not measuring the radial deflections of this specimen.
An explosive thickness of 0.035 in. was used for this
specimen.

In Figure I-3 a photograph of specimen 21 after
deformation is shown. The ripples due to buckling are

also clearly shown here, but are not as deep as those of specimen 14 of Figure II-2.

Sample Calculations

The velocity imparted to the hemispherical specimen by the explosive can be found by dividing the total impulse imparted to the specimen by the loaded mass of the specimen. The total impulse is obtained by multiplying the specific impulse of the explosive (as obtained in Appendix II) times the weight of explosive used.

$$I_t = I_{sp} \times W_e$$

where

I_t = Total impulse

I_{sp} = Specific impulse

W_e = Weight of explosive

Since the angle of the spherical surface 2α which is covered by the explosive is known (half of this angle is shown in Table 1 as $\alpha 1$, the loaded mass of the hemispherical specimen could be found from the formula:

$$\text{Loaded mass} = m_s = \rho_s \, 2\pi \, (R_s)^2 H (1 - \cos \alpha)$$

where

m_s = loaded mass of hemisphere

ρ_s = density of hemispherical specimen

R_s = mean radius of hemisphere (given in Table 1)

H = average thickness of hemisphere (given in Table 1)

α = half of the angle which is covered by explosive (given in Table 1)

After the total impulse imparted to the specimen and the loaded mass were found as mentioned above, the velocity imparted to the specimen V_{os} could be found as follows:

$$V_{os} = I_t / m_s$$

The nondimensional impulse parameter λ could then be found with the existing data.

$$\lambda = \frac{\rho_s (V_{os})^2 R_s^2}{M_{os}}$$

where

M_{os} = static yield moment of hemispherical specimen

$$M_{os} = \frac{\sigma_{os} H^2}{4}$$

where

σ_{os} = average static yield stress of the hemispherical specimen.

Hence, substituting this value of M_{os} in equation giving λ we get:

$$\lambda = \frac{4\rho_s (V_{os})^2 R_s^2}{\sigma_{os} H^2}$$

For mild steel specimens $\sigma_{os} = 44,967$ psi, and for aluminum 6061-T6, $\sigma_{os} = 40,828$; these values are averages of the values obtained in tensile tests and reported in detail in Appendix III. The densities of the materials used are also reported in Appendix III.

The calculations used to obtain the results for test 2 will be shown. For specimen 2 we have the following data:

$$R_s = 2.575 \text{ inches}$$
$$H = 0.07086 \text{ inches}$$
$$\alpha = 83 \text{ degrees}$$
$$\rho_s = 7.228 \times 10^{-4} \text{ lb}_f\text{-sec}^2/\text{in.}^4$$
$$W_e = 20.70 \text{ grams}$$
$$\sigma_{os} = 44,967 \text{ psi}$$

Thus,

$$m_s = 7.228 \times 10^{-4} \text{ lb}_f\text{-sec}^2/\text{in.}^4 \times 2\pi(2.575 \text{ in})^2$$
$$\times 0.07086 \text{ in.} \times (1 - \cos 83)$$
$$= 0.0018737 \text{ lb}_f\text{-sec}^2/\text{in.}$$

$$I_t = I_{sp} \times W_e = 0.4069 \; lb_f\text{-sec/(gram of explosive)}$$

$$\times \; 20.7 \; grams = 8.423 \; lb_f\text{-sec.}$$

$$V_{os} = I_t/m_s = 8.423 \; lb_f\text{-sec}/0.0018737 \; lb_f\text{-sec}^2/\text{in.}$$

$$= 4495.4 \; \text{in/sec.}$$

The non-dimensional parameter λ may now be found as follows:

$$\lambda = \frac{4 \times (7.228 \times 10^{-4} \; lb_f\text{-sec}^2/\text{in}^4) \times (4495.4 \; \text{in/sec})^2}{44,967 \; lb_f/\text{in}^2 \times (0.07086 \; \text{in})^2}$$

$$\times \; (2.575 \; \text{in})^2 = 1.716$$

For the calculation of energy ratios E_r shown in Table 1 the following formula was used:

$$E_r = \frac{\text{initial kinetic energy}}{\substack{\text{maximum strain energy which} \\ \text{can be absorbed elastically}}} = \frac{\rho_s E \, V_{os}^2}{\sigma_{os}^2}$$

For example, the specimen 2, using a value for young modulus of $E = 30 \times 10^6$ psi, we get:

$$E_r = \frac{(7.228 \times 10^{-4} \times lb_f\text{-sec}^2/\text{in}^4) \times 30 \times 10^6 \; lb_f/\text{in}^2}{(44,967 \; lb_f/\text{in}^2)^2}$$

$$\times \; (4495.4 \; \text{in/sec})^2 = 217$$

For tests 26 and 28 for which partial loading of the aluminum specimens was used a theory which was developed in Reference 9 is used in order to check the experimental results of the hemispherical specimen to its average thickness as follows:

$$\frac{W}{H} = \frac{\nu^2 \lambda H}{48 \, R_s a_7}$$

where

W = maximum deflection

H = average thickness of specimen

$\nu = 1.5(1 - \cos^2 \alpha)$

α = half of the angle covered by explosive

λ = the same non-dimensional parameter as mentioned above

R_s = mean radius of hemisphere

$a_7 = \frac{1}{2} + \frac{H}{8R_s}$

For example, using the data of test 26 we get:

$\nu = 1.5(1 - \cos^2 \alpha) = 1.5(1 - \cos^2 45) = 0.75$

$\lambda = 767$, $R_s = 2.5596$ in., $H = 0.09068$ in.

$a_7 = \frac{1}{2} + \frac{H}{8R_s} = \frac{1}{2} + \frac{0.09066}{8 \times 2.5596} = 0.5044$

-59-

$$\frac{W}{H} = \frac{0.75^2 \times 767 \times 0.09066 \text{ in}}{48 \times 2.5596 \text{ in} \times 0.5044} = 0.6311$$

In the same way for test 28 we find:

$$\frac{W}{H} = 1.68 \ .$$
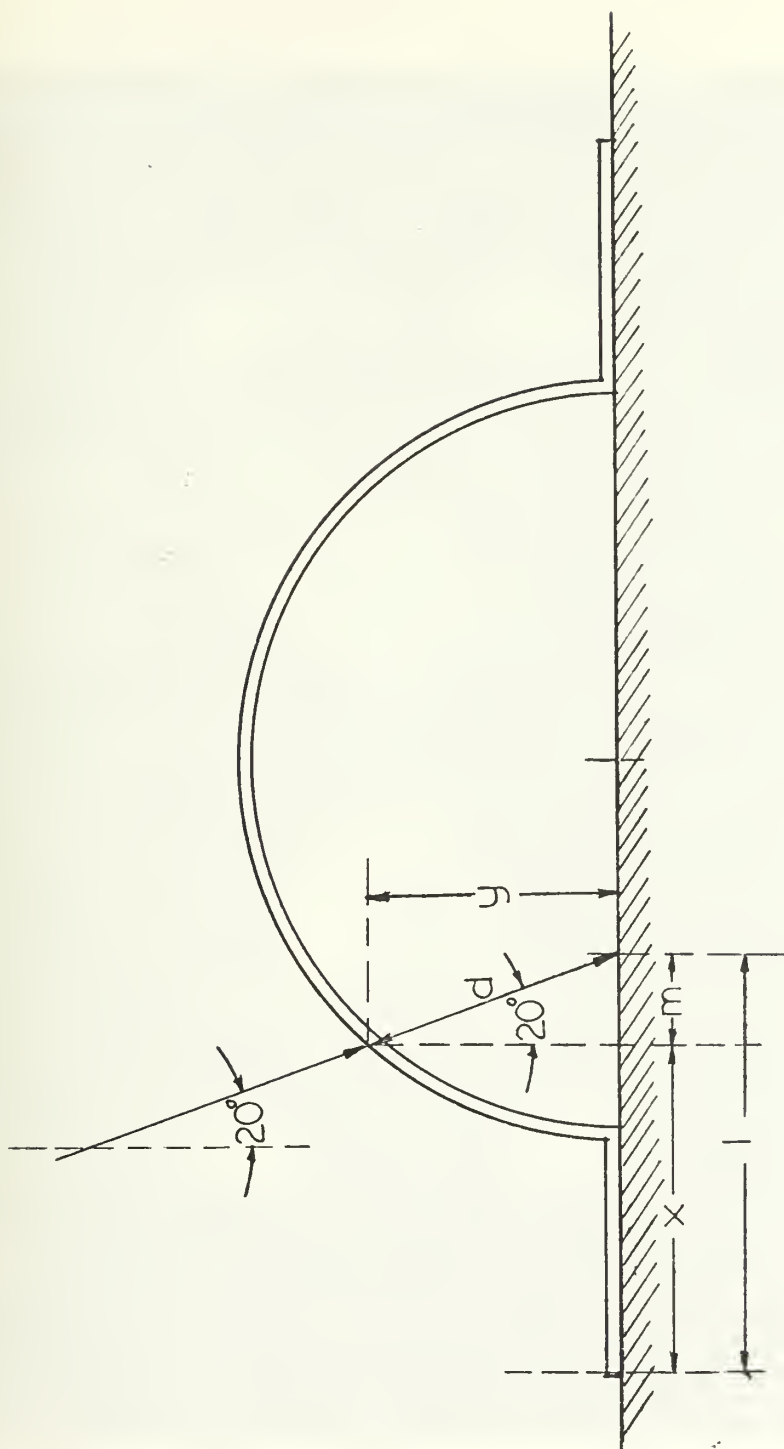
Figure I-I
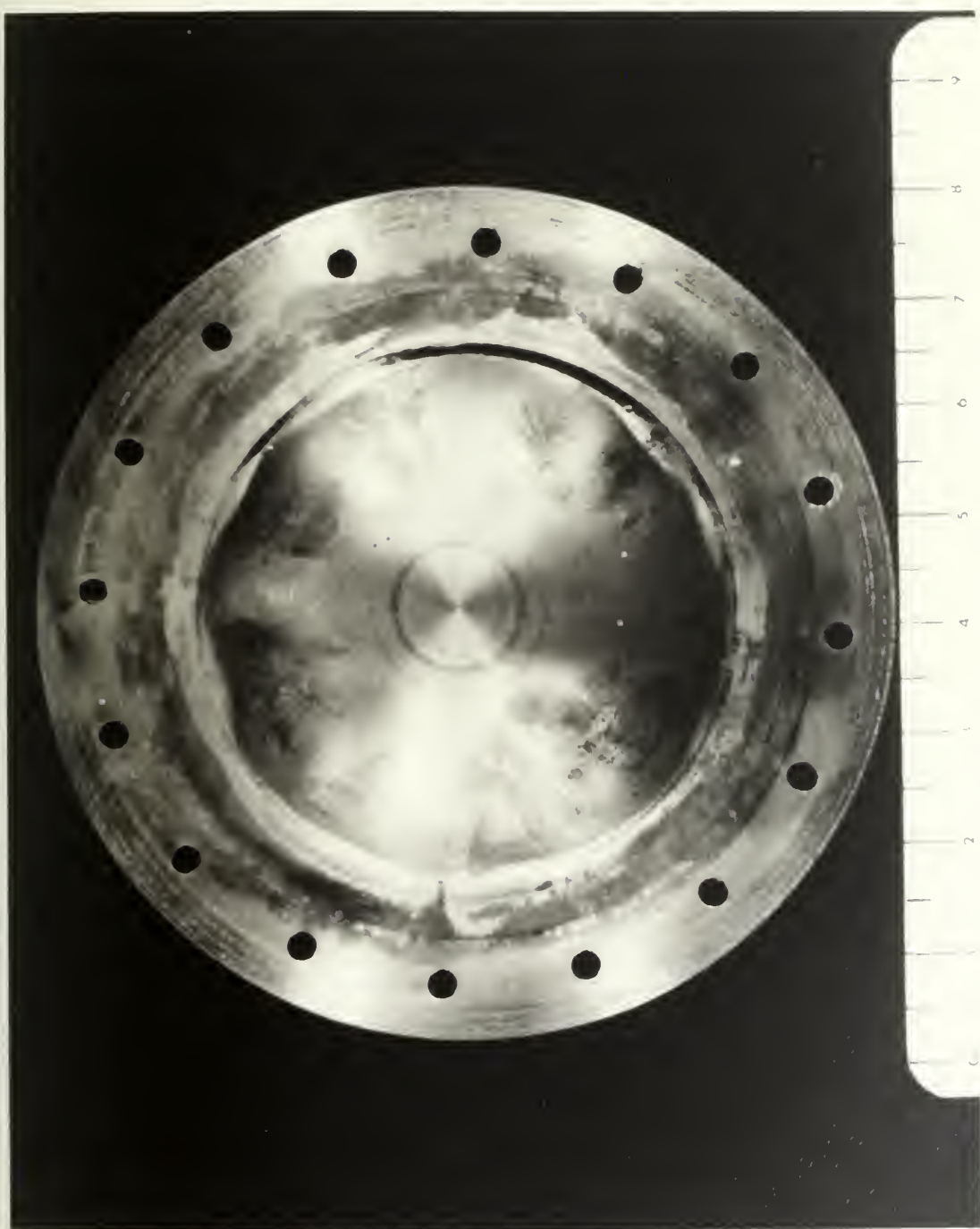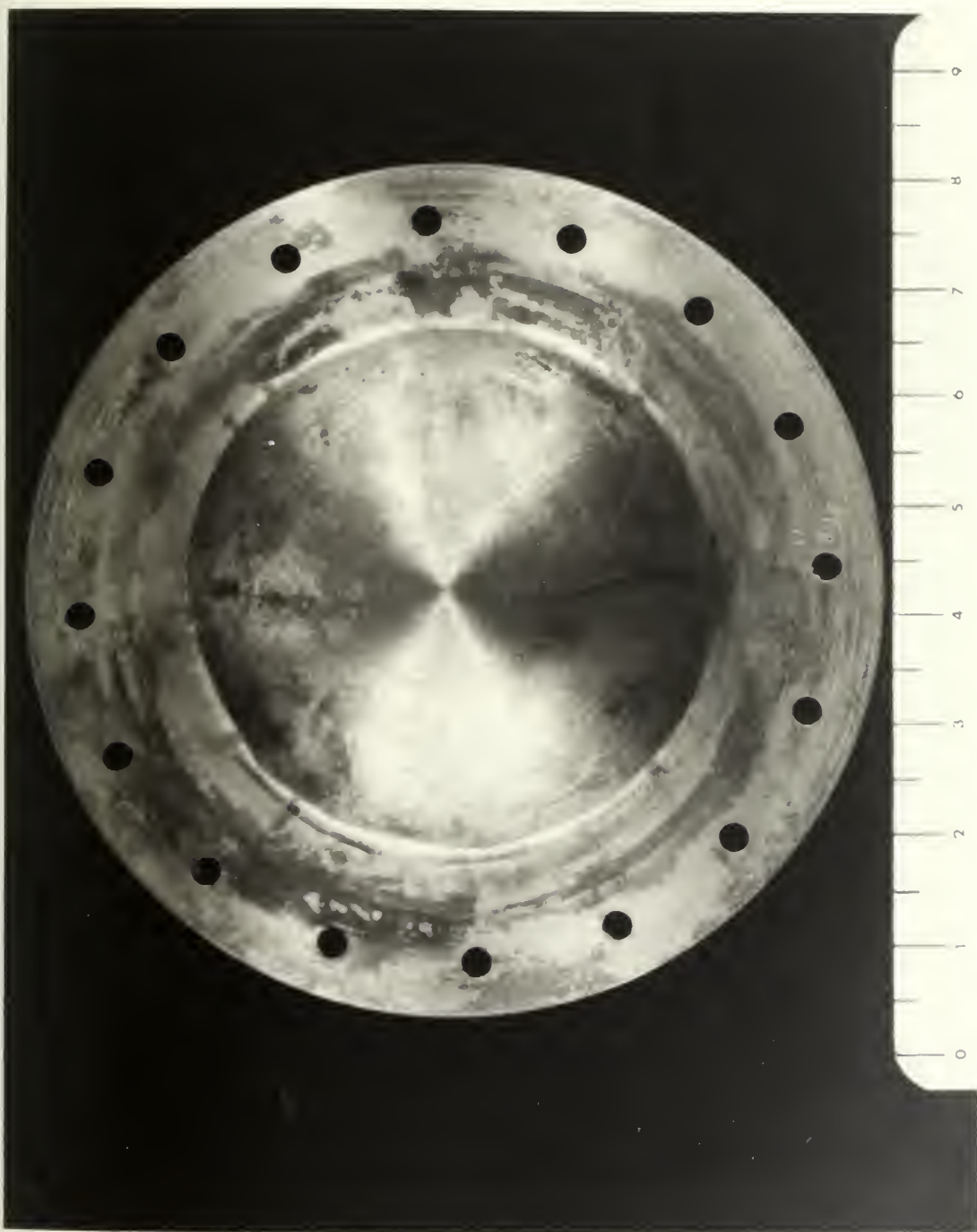
Figure I-2

Figure I -3

-63-

TABLE I-1

SPECIMEN NO. 2

RADIAL DEFLECTION MEASUREMENTS ON

SEMICIRCLE 330°-150°

Angle of Measurement From Left Side Measured From Bottom of Flange (Degrees)	Radial Deflection (inches)
10	0.129
20	0.1275
30	0.121
40	0.129
50	0.140
60	0.129
70	0.111
80	0.118
90	0.142
100	0.173
110	0.176
120	0.164
130	0.148
140	0.135
150	0.124
160	0.125
170	0.131

150°

90°

30°

---- Deformation profile

Scale : 1" ≅ 1"

Figure I-4

------ Deformation profiles
Scale : 5"≙1"
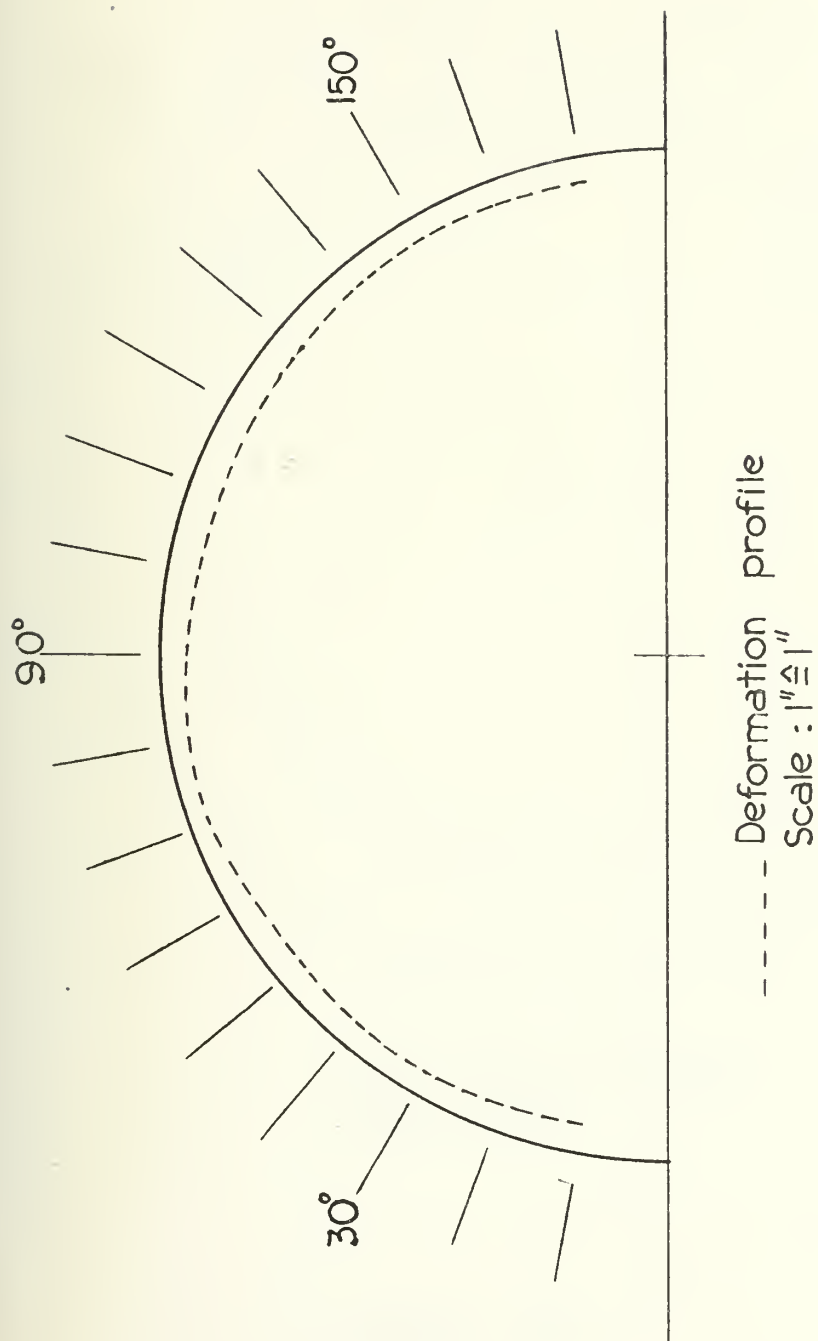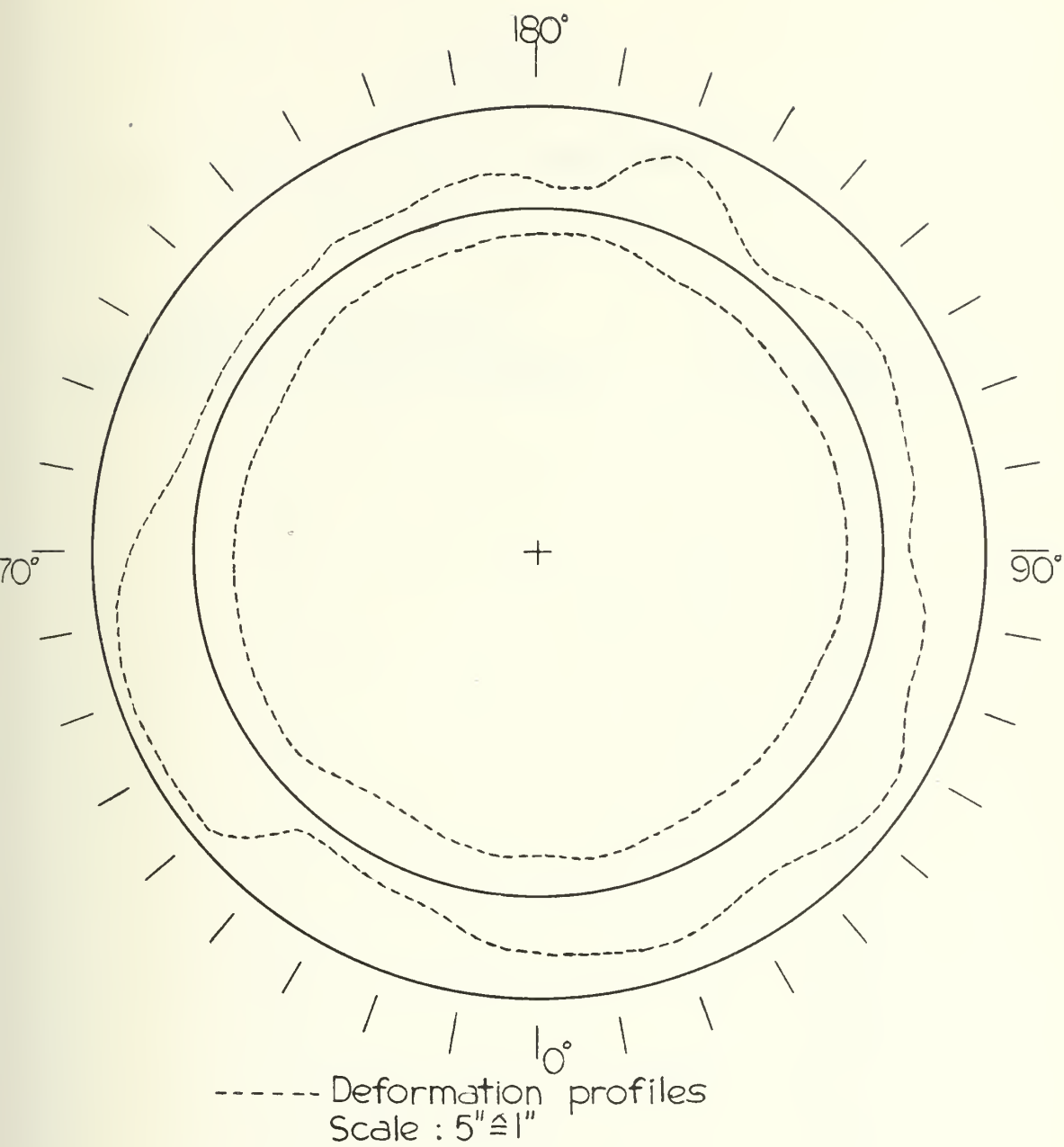
Figure I-5

TABLE I-2

SPECIMEN No. 4

RADIAL DEFLECTION MEASUREMENTS ON

SEMICIRCLE 270° - 90°

Angle of Measurement From Left Side, Measured From Bottom of Flange (Degrees)	Radial Deflection (inches
10	0.246
20	0.193
30	0.213
40	0.265
50	0.287
60	0.310
70	0.334
80	0.335
90	0.290
100	0.363
110	0.373
120	0.355
130	0.288
140	0.223
150	0.168
160	0.130
170	0.112

150°

90°

30°

Deformation profile
Scale : 1" = 1"

Figure I-6

Deformation profiles
Scale : 2" ≙ 1"

Figure I-7

TABLE I-3

SPECIMEN NO. 6

RADIAL DEFLECTION MEASUREMENTS ON

SEMICIRCLE 270° - 90°

Angle of Measurement From Left Side, Measured From Bottom of Flange (Degrees)	Radial Deflection (inches)
10	0.178
20	0.170
30	0.133
40	0.148
50	0.179
60	0.185
70	0.187
80	0.204
90	0.222
100	0.192
110	0.196
120	0.178
130	0.162
140	0.135
150	0.116
160	0.109
170	0.120

Deformation profile

Scale : 1" ≙ 1"

Figure I-8

180°

270°   90°

0°
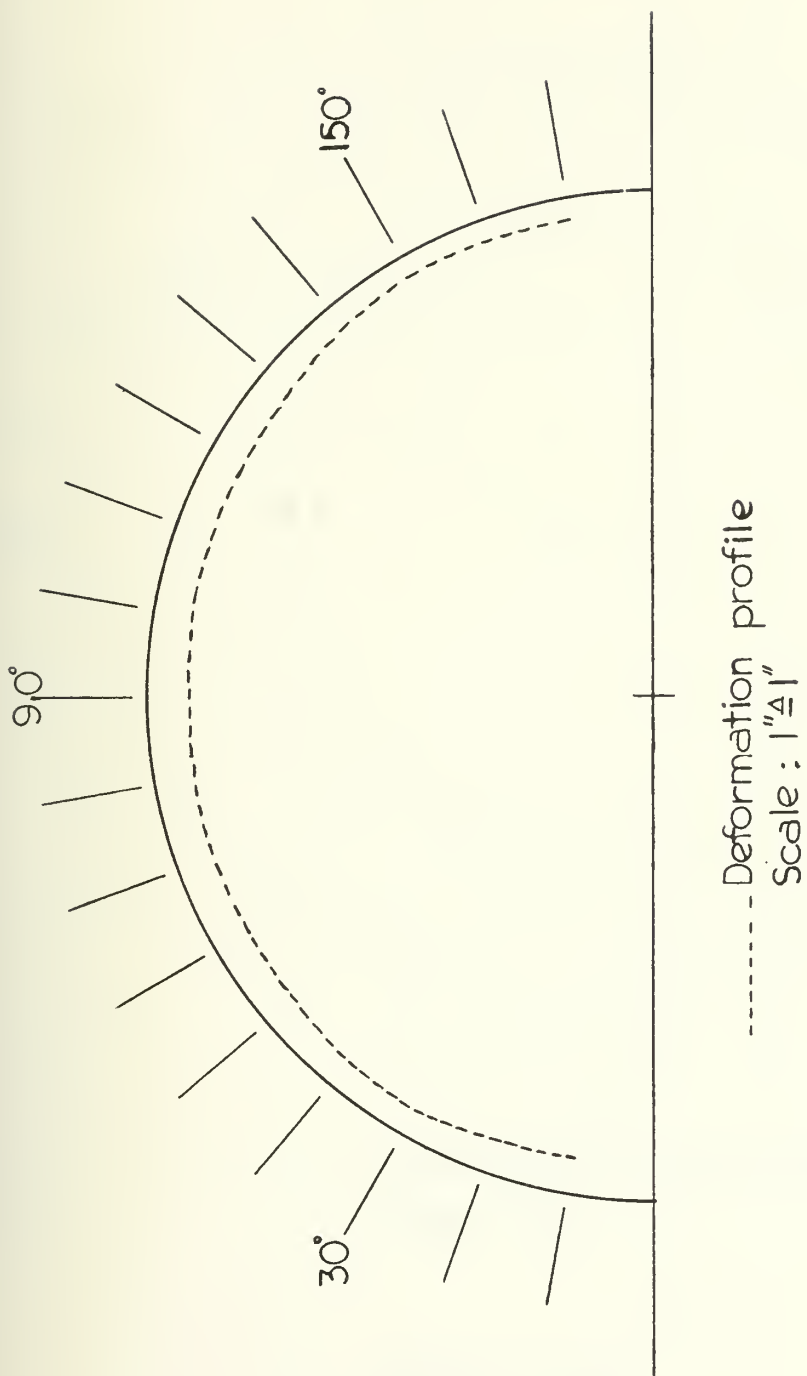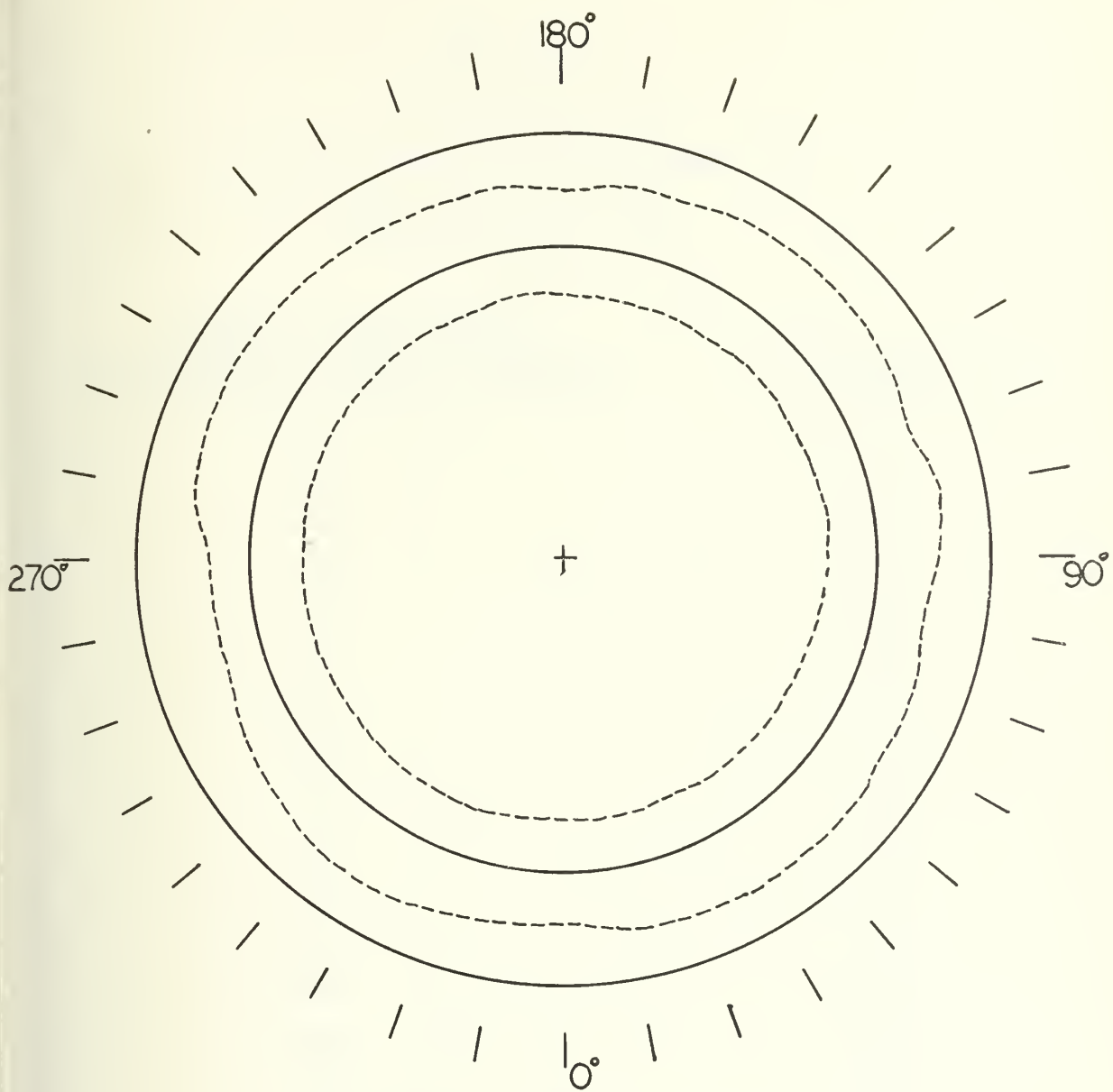
- - - - -Deformation profiles
Scale : 5"≙1"

Figure I-9

-72-

TABLE I-4

SPECIMEN NO. 7

RADIAL DEFLECTION MEASUREMENTS ON

SEMICIRCLE 270° - 90°

Angle of Measurement From Left Side, Measured From Bottom of Flange (Degrees)	Radial Deflection (inches)
10	0.040
20	0.028
30	0.0251
40	0.026
50	0.032
60	0.0425
70	0.0515
80	0.061
90	0.071
100	0.0625
110	0.0535
120	0.0475
130	0.039
140	0.034
150	0.032
160	0.033
170	0.040

Deformation profile
Scale :5"≌1"

Figure I-10

-74-

TABLE I-5

SPECIMEN NO. 9

RADIAL DEFLECTION MEASUREMENTS ON

SEMICIRCLE 0° - 180°

Angle of Measurement From Left Side, Measured From Bottom of Flange (Degrees)	Radial Deflection (inches)
10	0.117
20	0.085
30	0.073
40	0.069
50	0.080
60	0.087
70	0.093
80	0.097
90	0.108
100	0.098
110	0.083
120	0.071
130	0.055
140	0.045
150	0.0475
160	0.063
170	0.081

— — — Deformation profile
Scale : 5"≅1"

Figure I–11

150°

90°

30°

TABLE I-6

SPECIMEN NO. 11

RADIAL DEFLECTION MEASUREMENTS ON

SEMICIRCLE $0^{\circ} - 180^{\circ}$

Angle of Measurement From Left Side, Measured From Bottom of Flange (Degrees)	Radial Deflection (inches)
10	0.205
20	0.1525
30	0.1575
40	0.198
50	0.238
60	0.276
70	0.305
80	0.283
90	0.273
100	0.282
110	0.308
120	0.287
130	0.258
140	0.228
150	0.215
160	0.228
170	0.270

150°

90°

30°

----- Deformation profile
Scale : 1"≅1
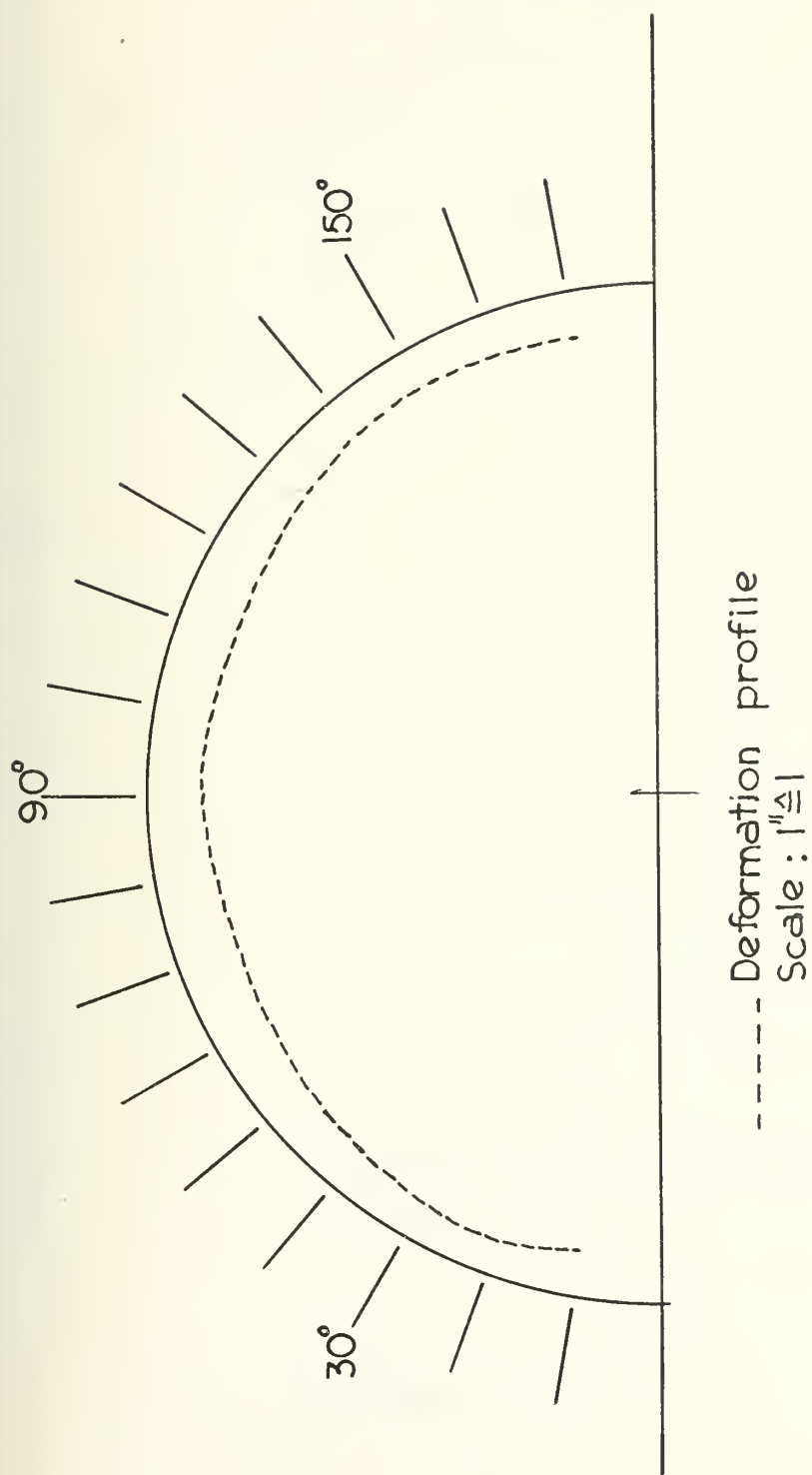
Figure I-12

------ Deformation profiles
Scale : $5'' \hat{=} 1''$

Figure I–13

TABLE I-7

SPECIMEN NO. 12

RADIAL DEFLECTION MEASUREMENTS NO

SEMICIRCLE $0^{\circ} - 180^{\circ}$

Angle of Measurement From Left Side, Measured From Bottom Flange of (Degrees)	Radial Deflection (inches)
10	0.060
20	0.058
30	0.053
40	0.063
50	0.077
60	0.083
70	0.091
80	0.087
90	0.093
100	0.095
110	0.090
120	0.086
130	0.0825
140	0.068
150	0.063
160	0.081
170	0.095

150°

90°

30°

---- Deformation profile
Scale : $2'' \hat{=} 1$
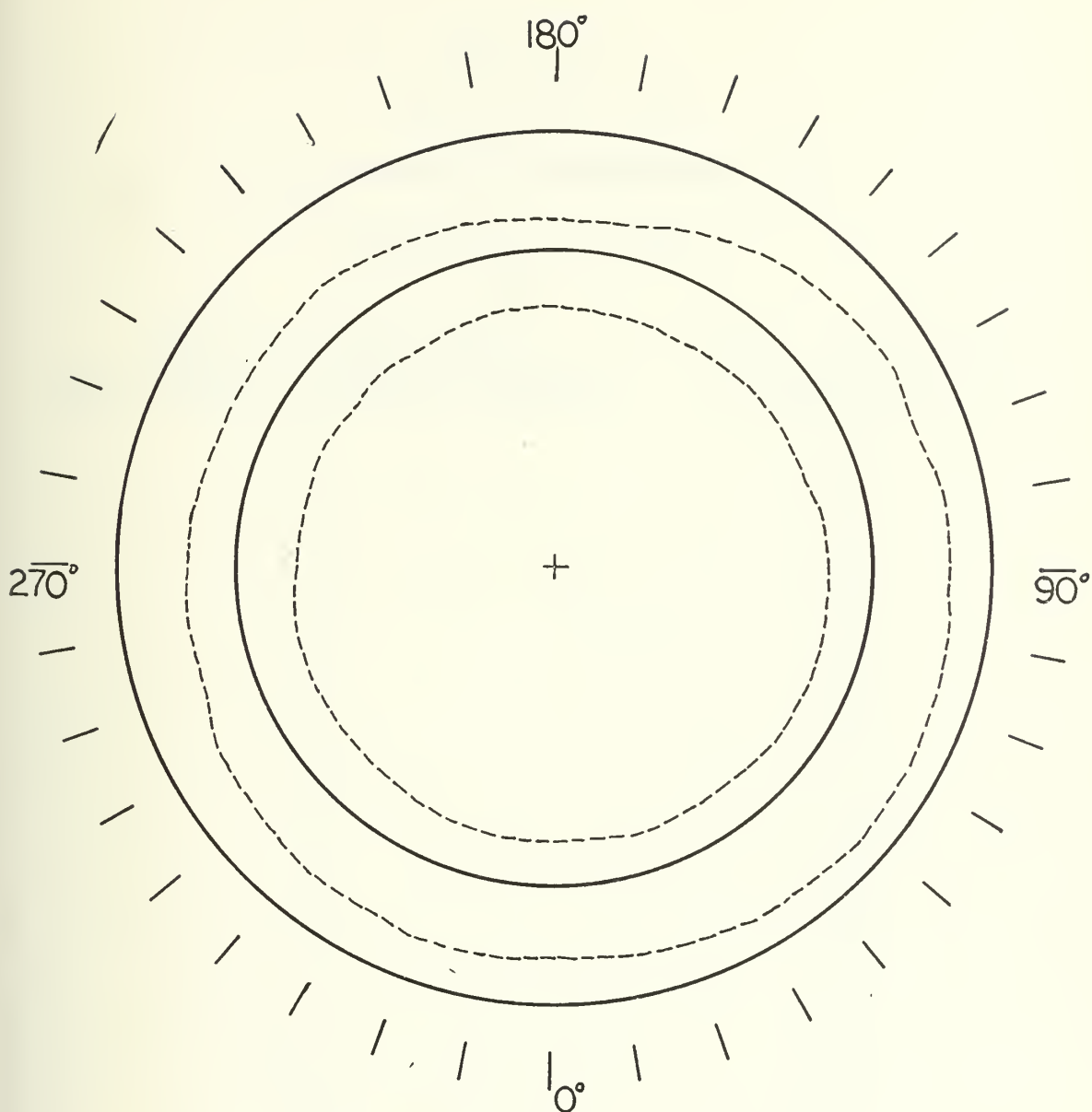
Figure I-14

- - - - - Deformation profiles
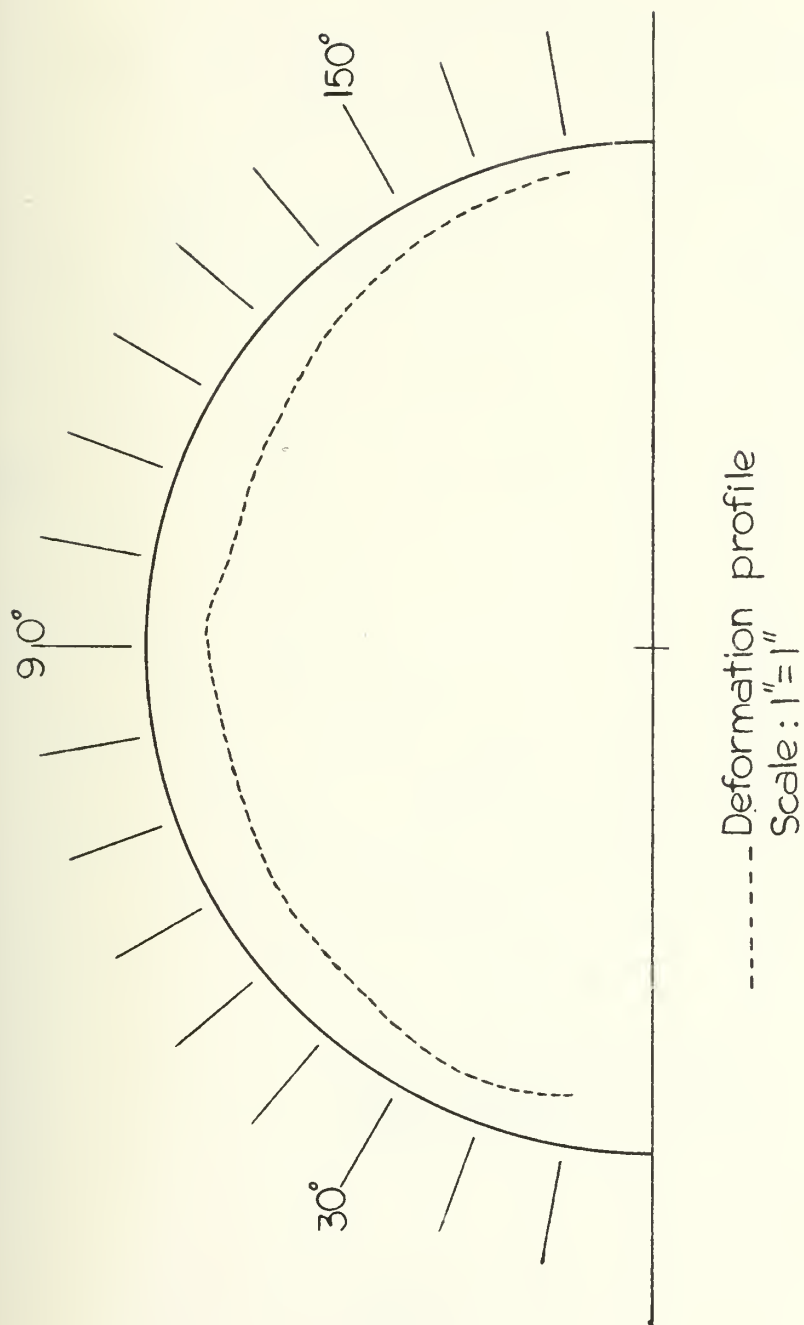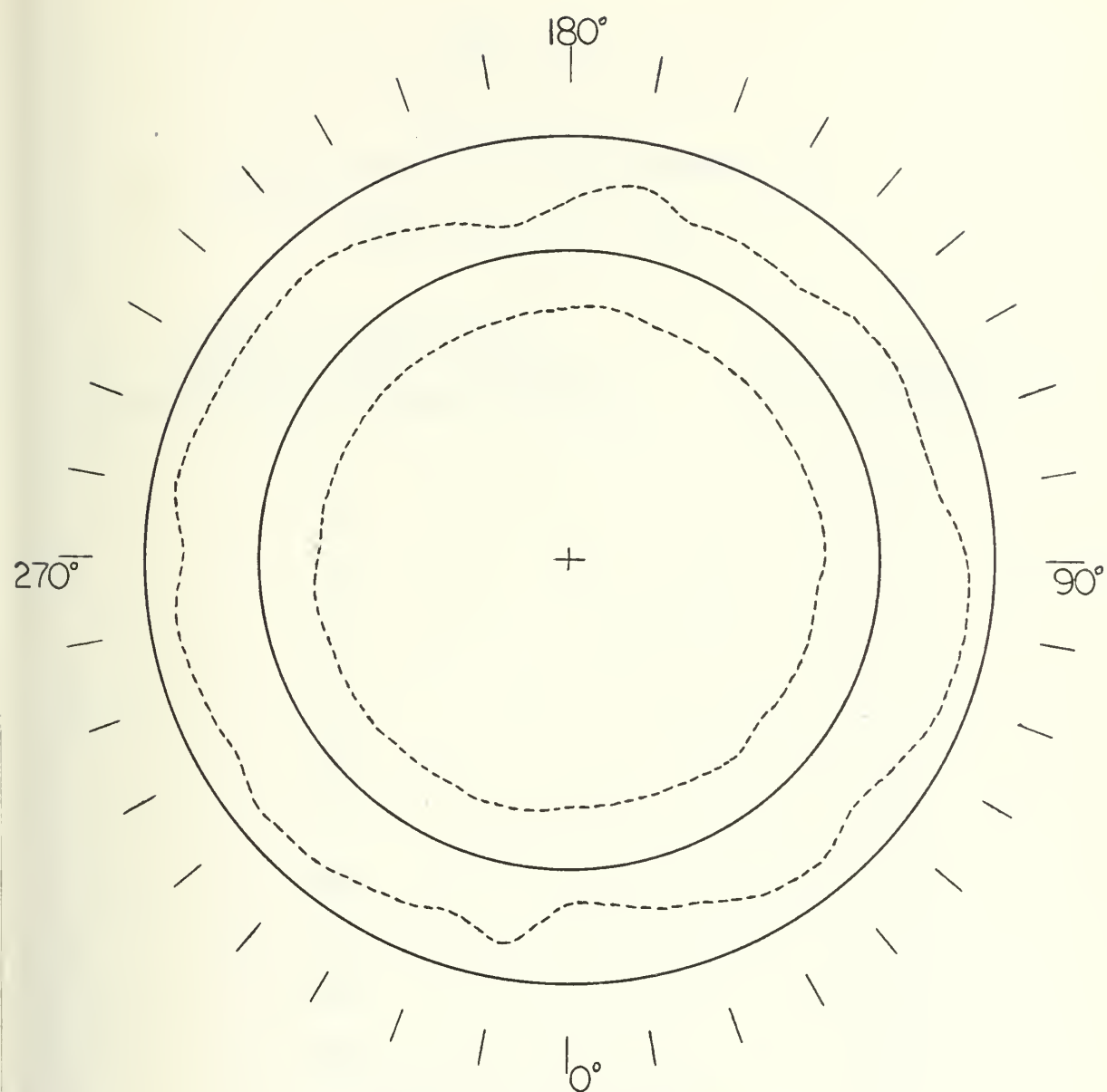
Scale : 10" ≙ 1"

Figure I-15

TABLE I-8

SPECIMEN NO. 13

RADIAL DEFLECTION MEASUREMENTS ON

SEMICIRCLE 0° - 180°

Angle of Measurement From Left Side, Measured From Bottom of Flange (Degrees)	Radial Deflection (inches)
10	0.084
20	0.0725
30	0.0975
40	0.132
50	0.162
60	0.175
70	0.1815
80	0.203
90	0.206
100	0.189
110	0.197
120	0.197
130	0.184
140	0.1625
150	0.146
160	0.150
170	0.178

150°

90°

30°

---- Deformation profile
Scale: 1" ≙ 1

Figure I-16

-84-

180°

270°

90°

0°
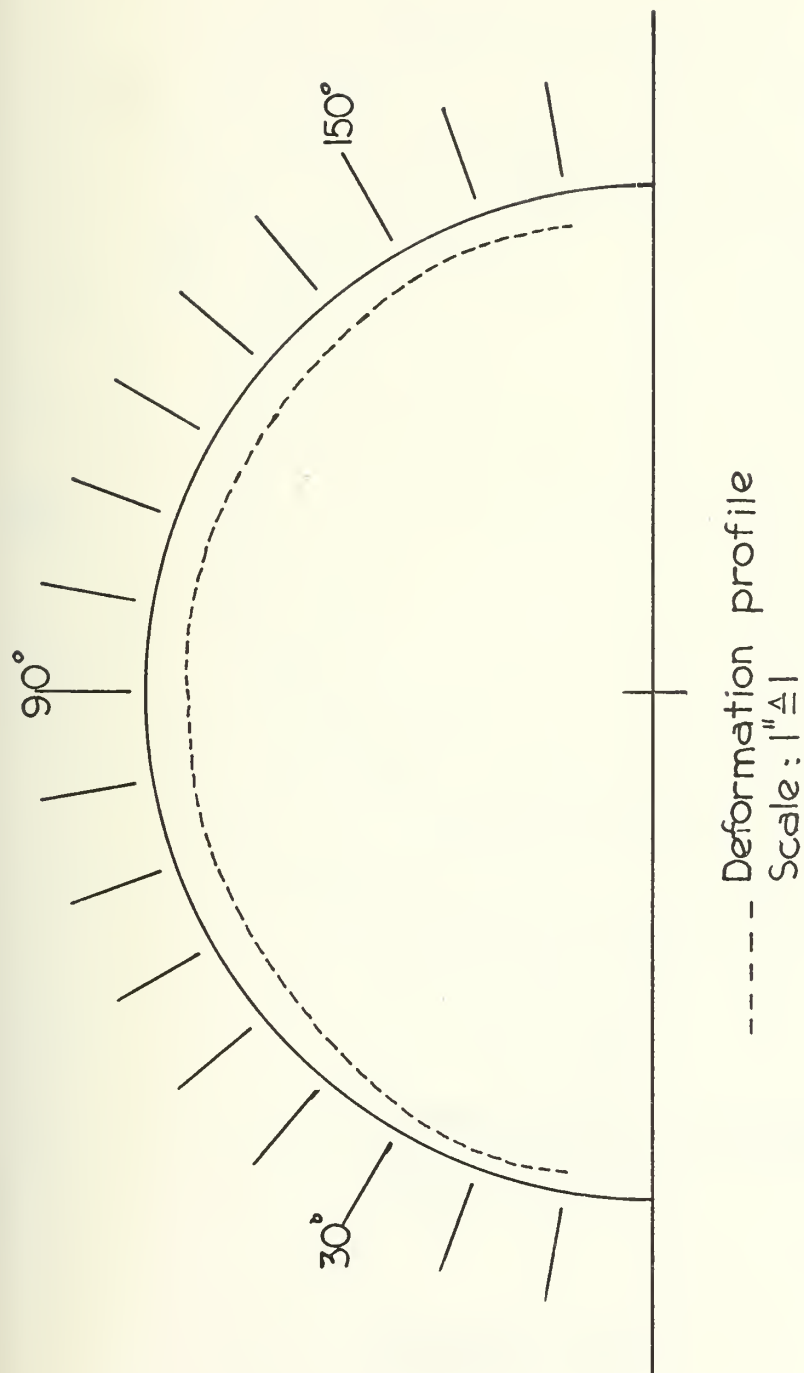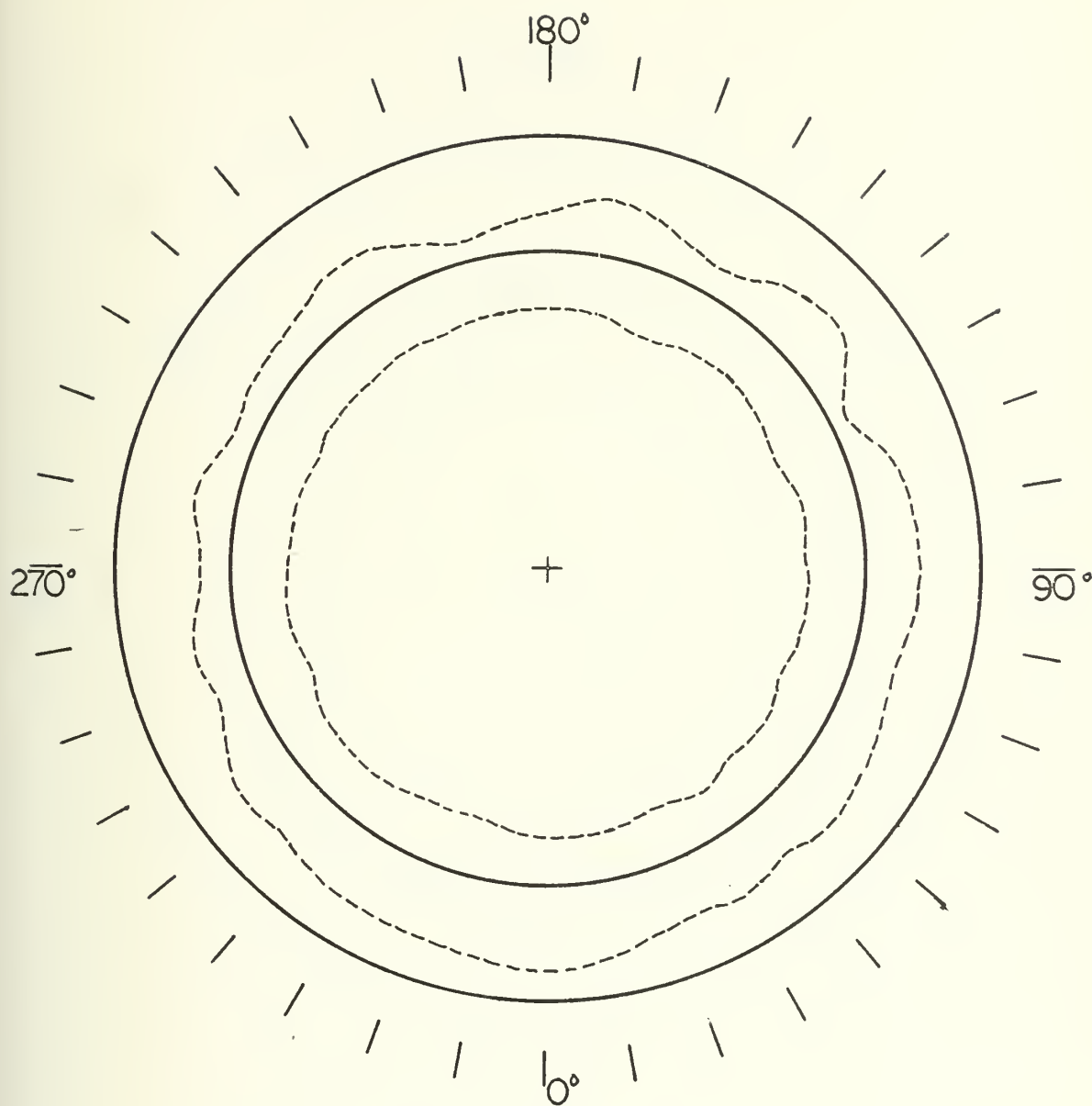
_ _ _ _ _Deformation profiles
Scale : 5"≙1"

Figure I-17

180°

270°

90°

0°
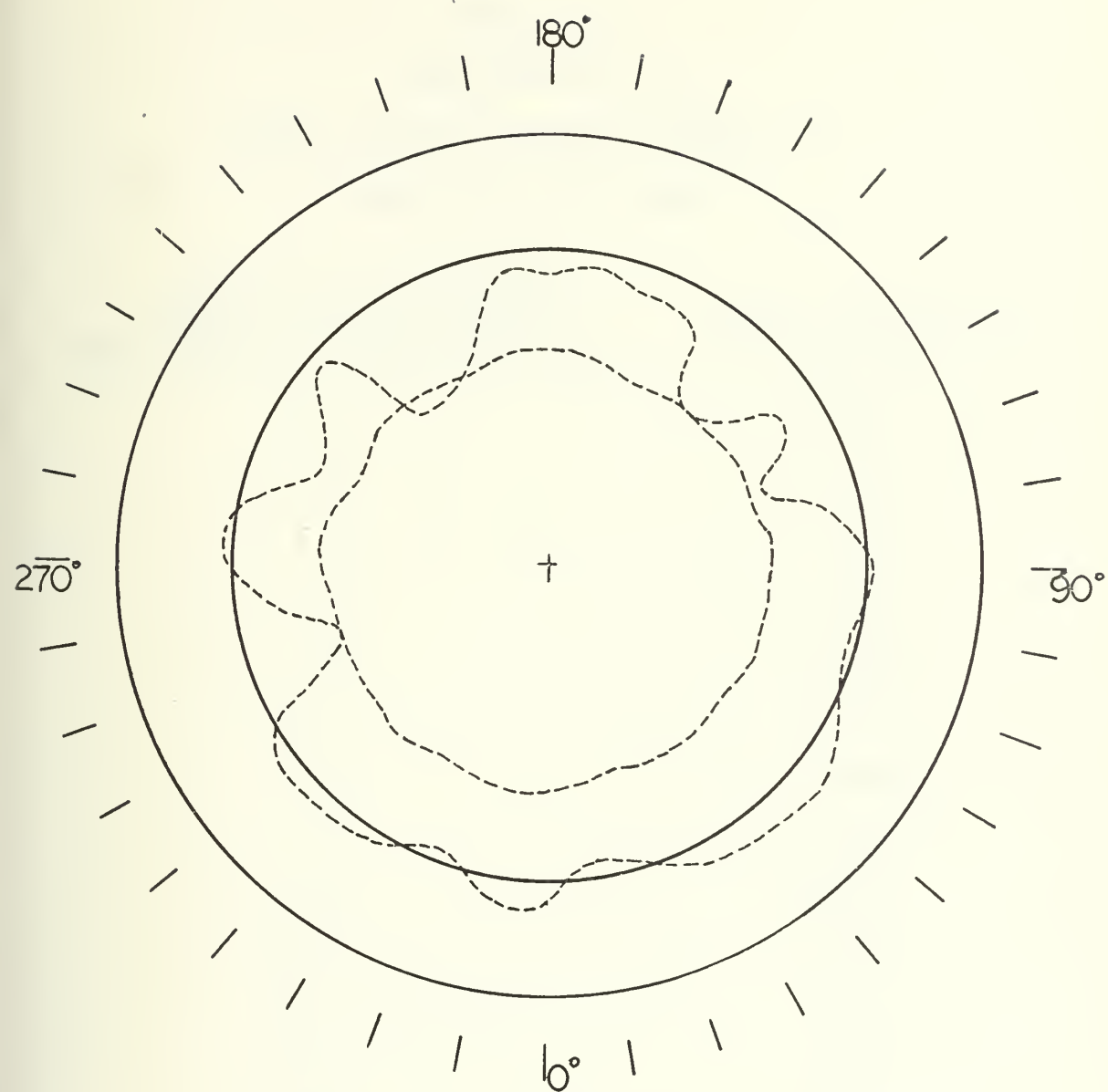
- - - - - Deformation profiles
Scale : 5"≙1"

Figure I-18

TABLE I-9

SPECIMEN NO. 15

RADIAL DEFLECTION MEASUREMENTS ON

SEMICIRCLE 0° - 180°

Angle of Measurement From Left Side, Measured From Bottom of Flange (Degrees)	Radial Deflection (inches)
10	0.034
20	0.0275
30	0.0278
40	0.0285
50	0.0325
60	0.0328
70	0.0318
80	0.0285
90	0.025
100	0.0255
110	0.0152
120	0.008
130	0.007
140	0.008
150	0.0065
160	0.00
170	0.012

Deformation profile
Scale : 5" ≅ 1

Figure I-19

-88-
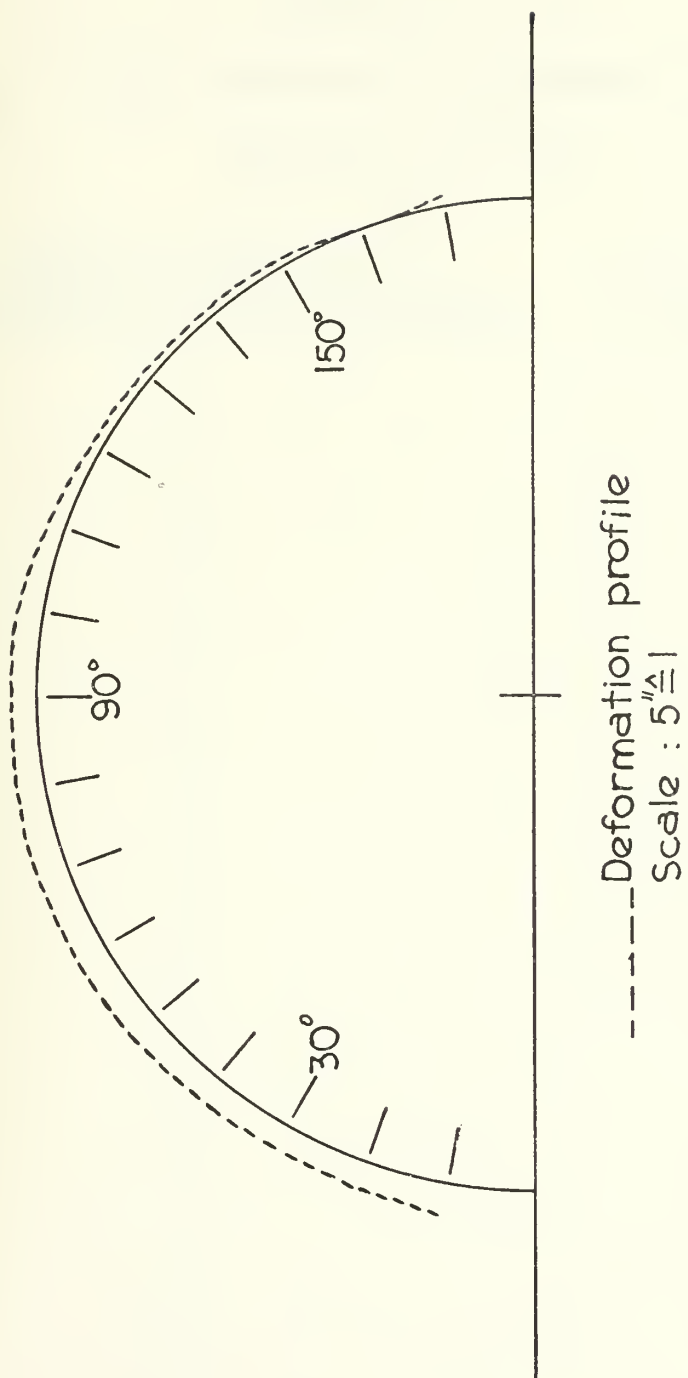
TABLE I-10

SPECIMEN NO. 16

RADIAL DEFLECTION MEASUREMENTS ON

SEMICIRCLE 270°-90°

Angle of Measurement From Left Side, Measured From Bottom of Flange (Degrees)	Radial Deflection (inches)
10	0.074
20	0.073
30	0.066
40	0.071
50	0.074
60	0.082
70	0.0925
80	0.101
90	0.108
100	0.104
110	0.106
120	0.093
130	0.082
140	0.078
150	0.080
160	0.090
170	0.088

Deformation profile
Scale : $2'' \hat{=} 1''$
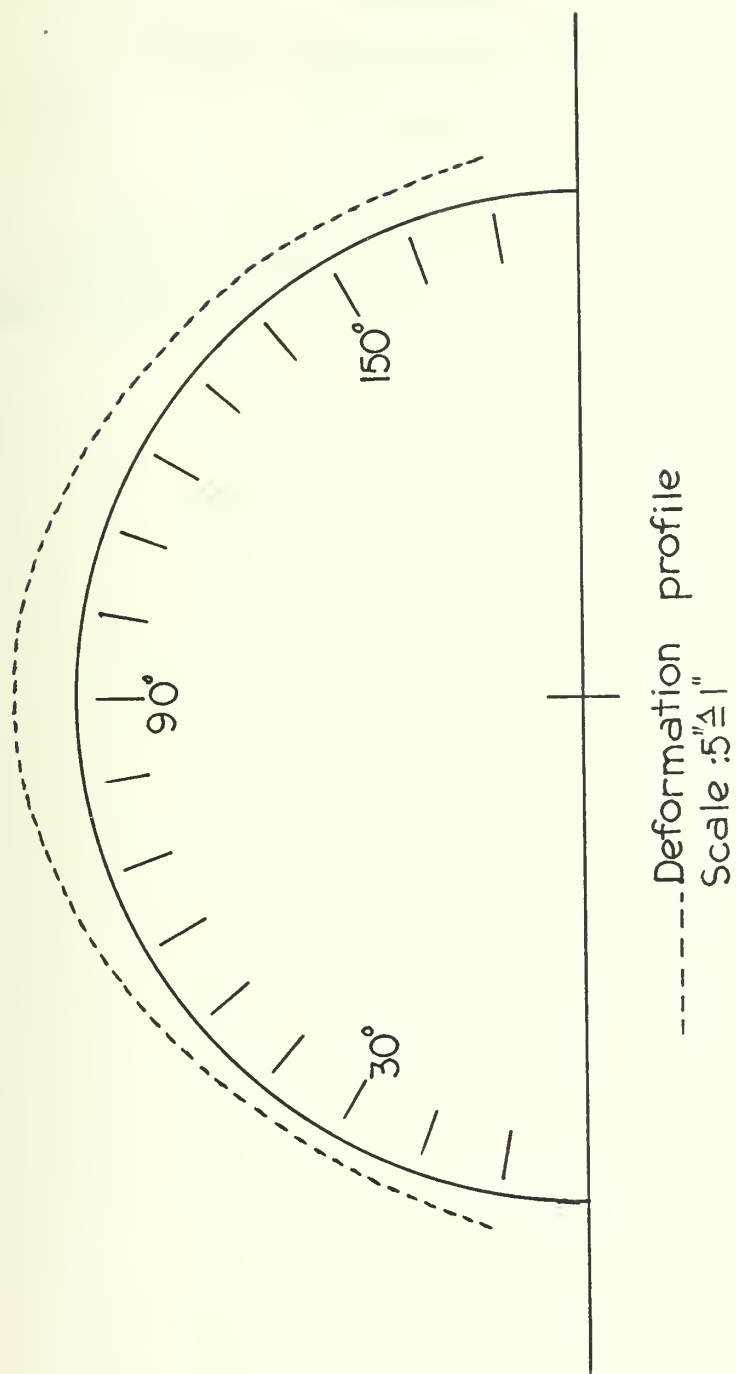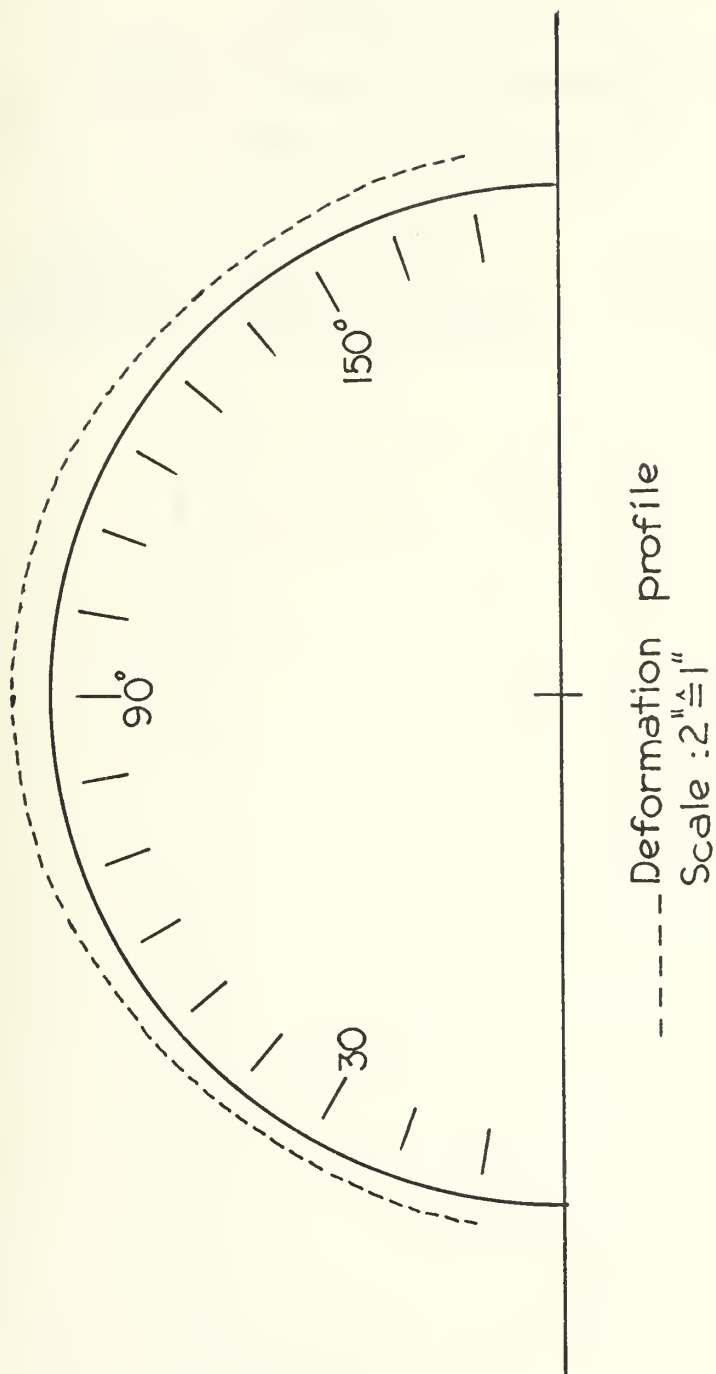
Figure I-20

TABLE I-11
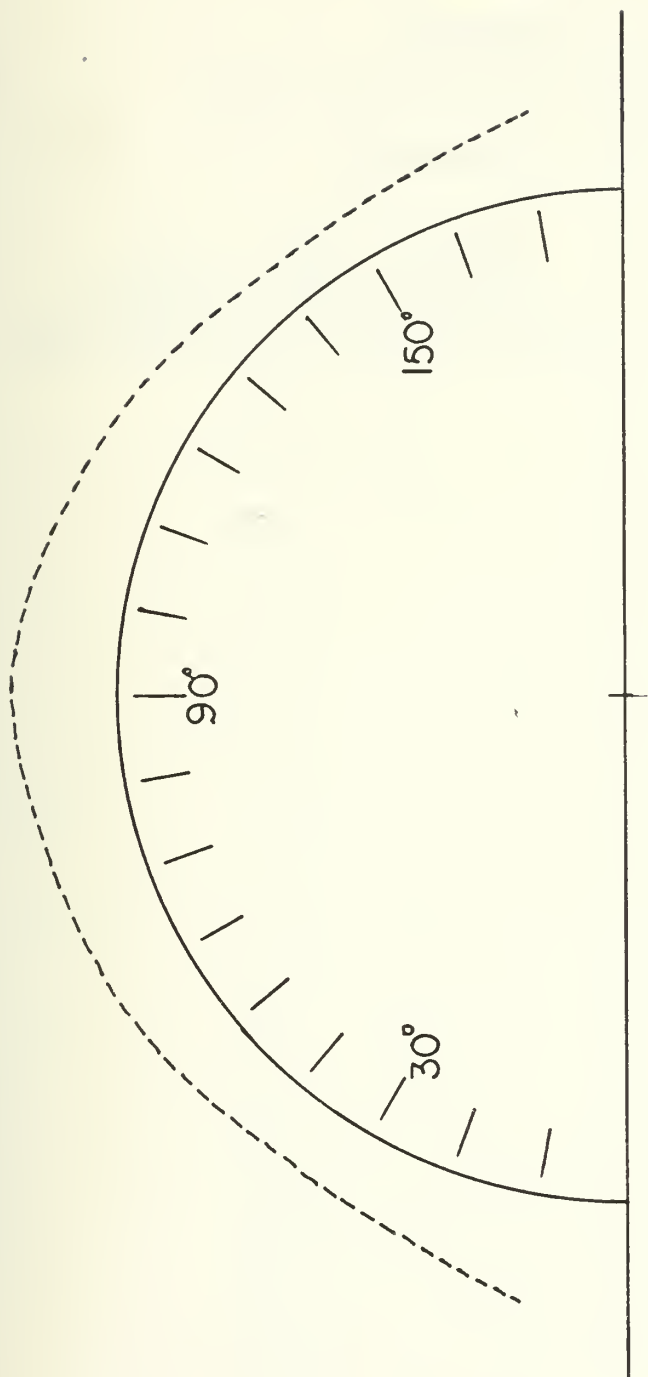
SPECIMEN NO. 17

RADIAL DEFLECTION MEASUREMENTS ON

SEMICIRCLE 0° - 180°

Angle of Measurement From Left Side, Measured From Bottom of Flange (Degrees)	Radial Deflection (inches)
10	0.077
20	0.067
30	0.059
40	0.060
50	0.069
60	0.077
70	0.083
80	0.080
90	0.075
100	0.065
110	0.058
120	0.050
130	0.043
140	0.038
150	0.037
160	0.047
170	0.0575

150°

90°

30°

-----Deformation profile
Scale : 2"≟1"

Figure I–21

-92-
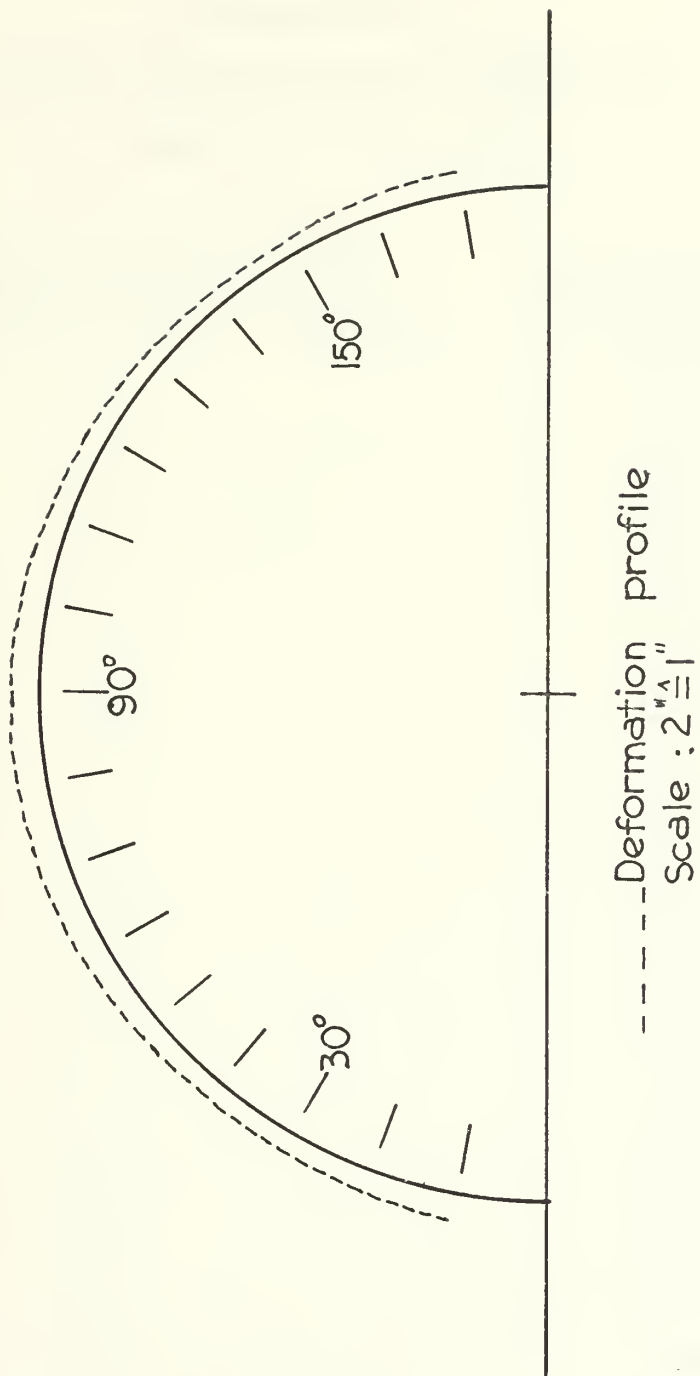
TABLE I-12

SPECIMEN NO. 18

RADIAL DEFLECTION MEASUREMENTS ON

SEMICIRCLE 45° - 225°

Angle of Measurement From Left Side, Measured From Bottom of Flange (Degrees)	Radial Deflection (inches)
10	0.101
20	0.102
30	0.092
40	0.093
50	0.106
60	0.108
70	0.1165
80	0.115
90	0.116
100	0.112
110	0.106
120	0.096
130	0.088
140	0.085
150	0.081
160	0.087
170	0.093

Deformation profile
Scale : $2'' \cong 1''$
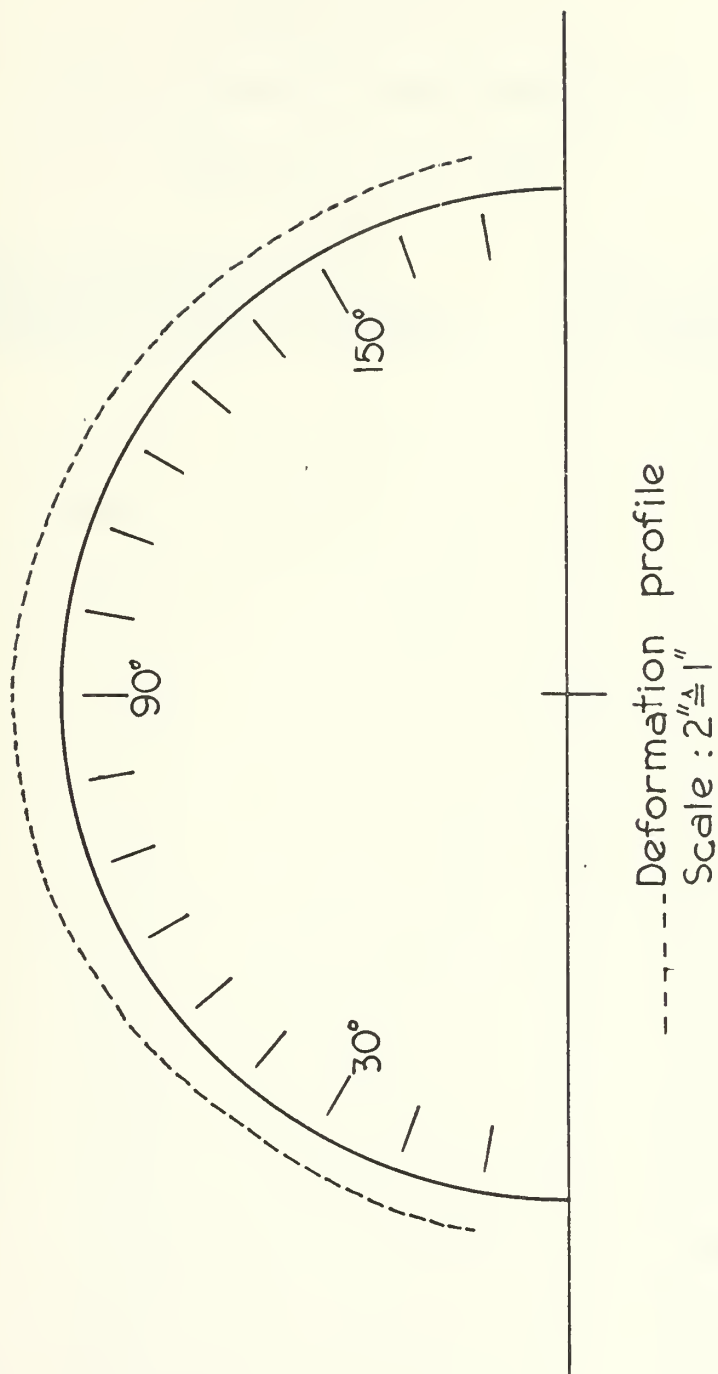
Figure I-22

TABLE I-13

SPECIMEN NO. 19

RADIAL DEFLECTION MEASUREMENTS ON

SEMICIRCLE 0° - 180°

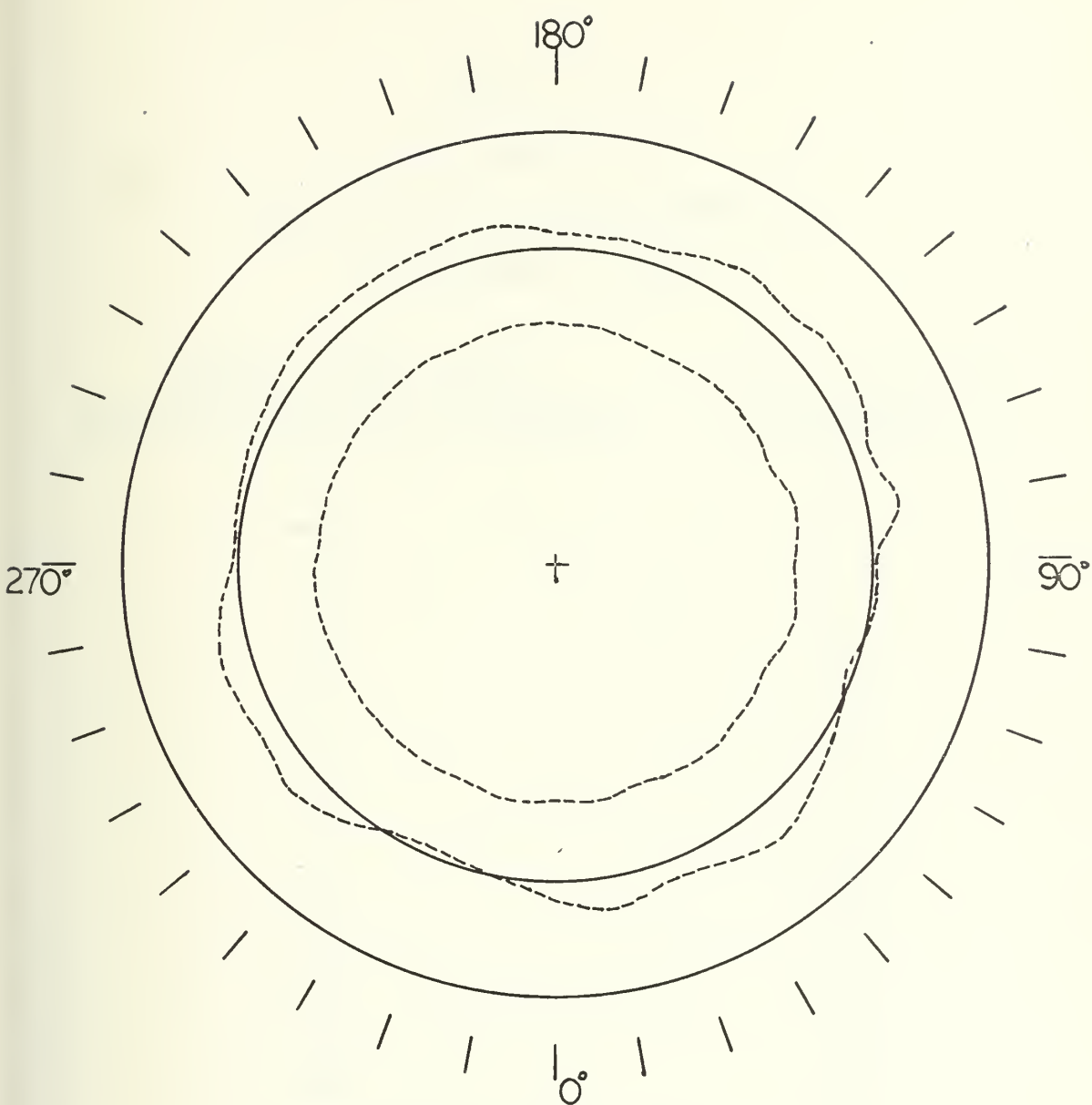| Angle of Measurement From Left Side, Measured From Bottom of Flange (Degrees)	Radial Deflection (inches)
10	0.0925
20	0.058
30	0.0565
40	0.071
50	0.082
60	0.103
70	0.112
80	0.125
90	0.119
100	0.097
110	0.105
120	0.108
130	0.104
140	0.088
150	0.078
160	0.077
170	0.091

150°

90°

30°

----- Deformation profile
Scale : 2″≙1″
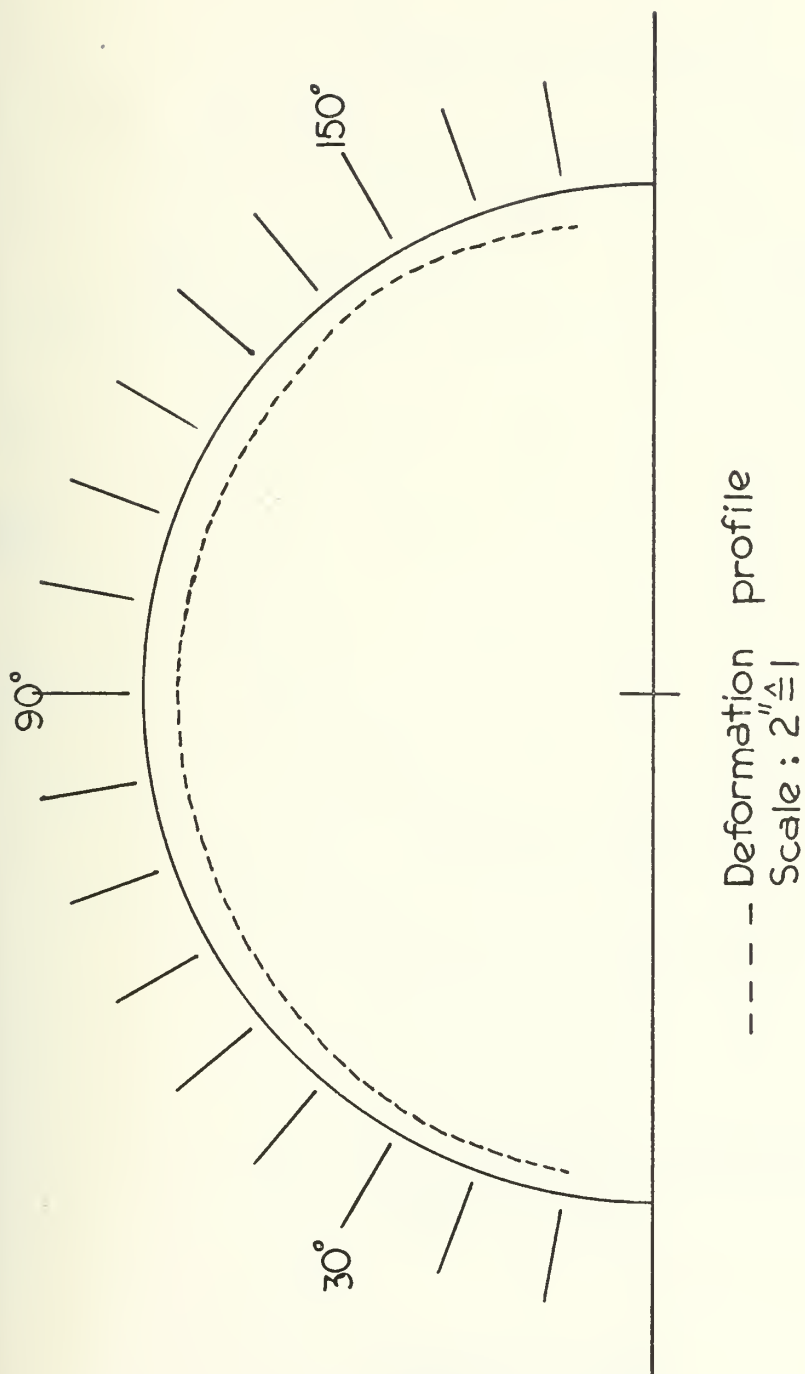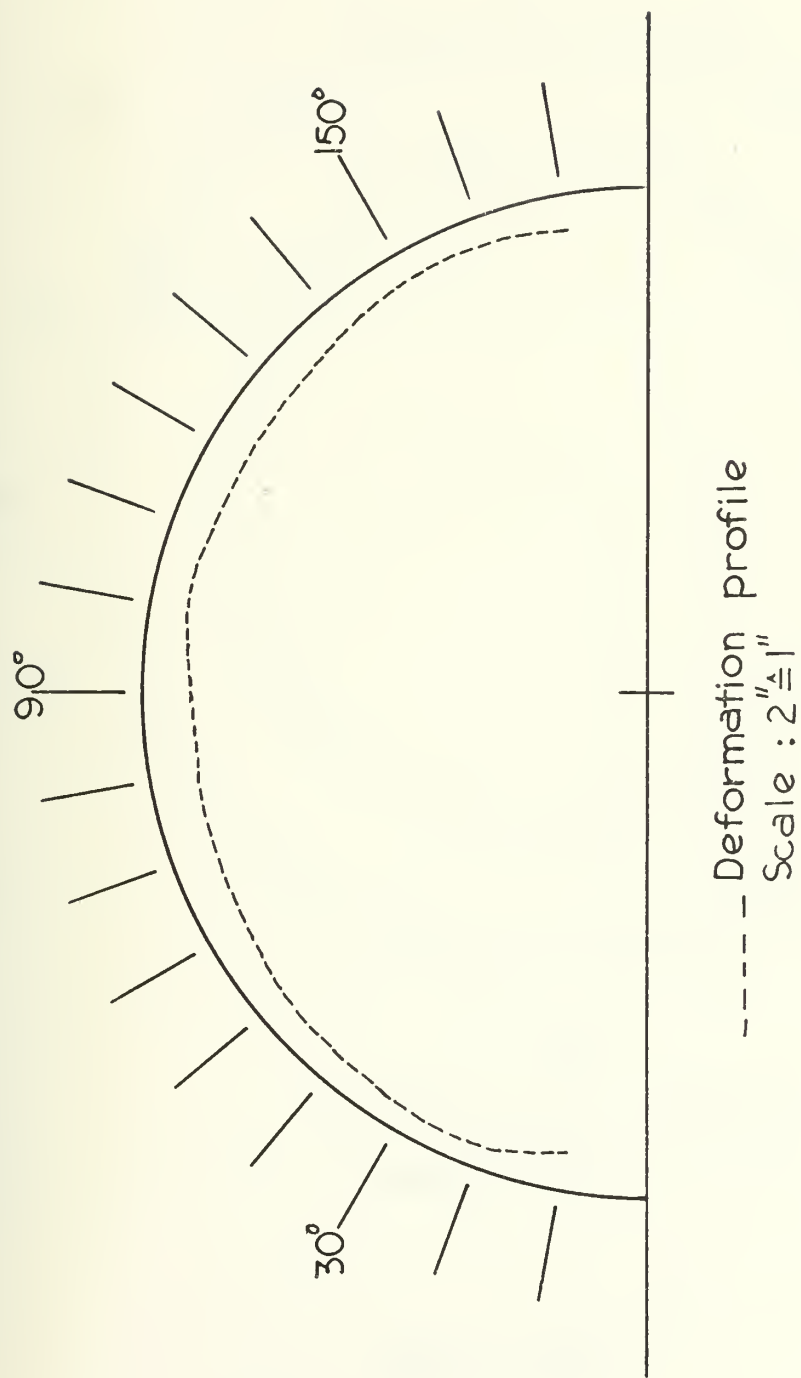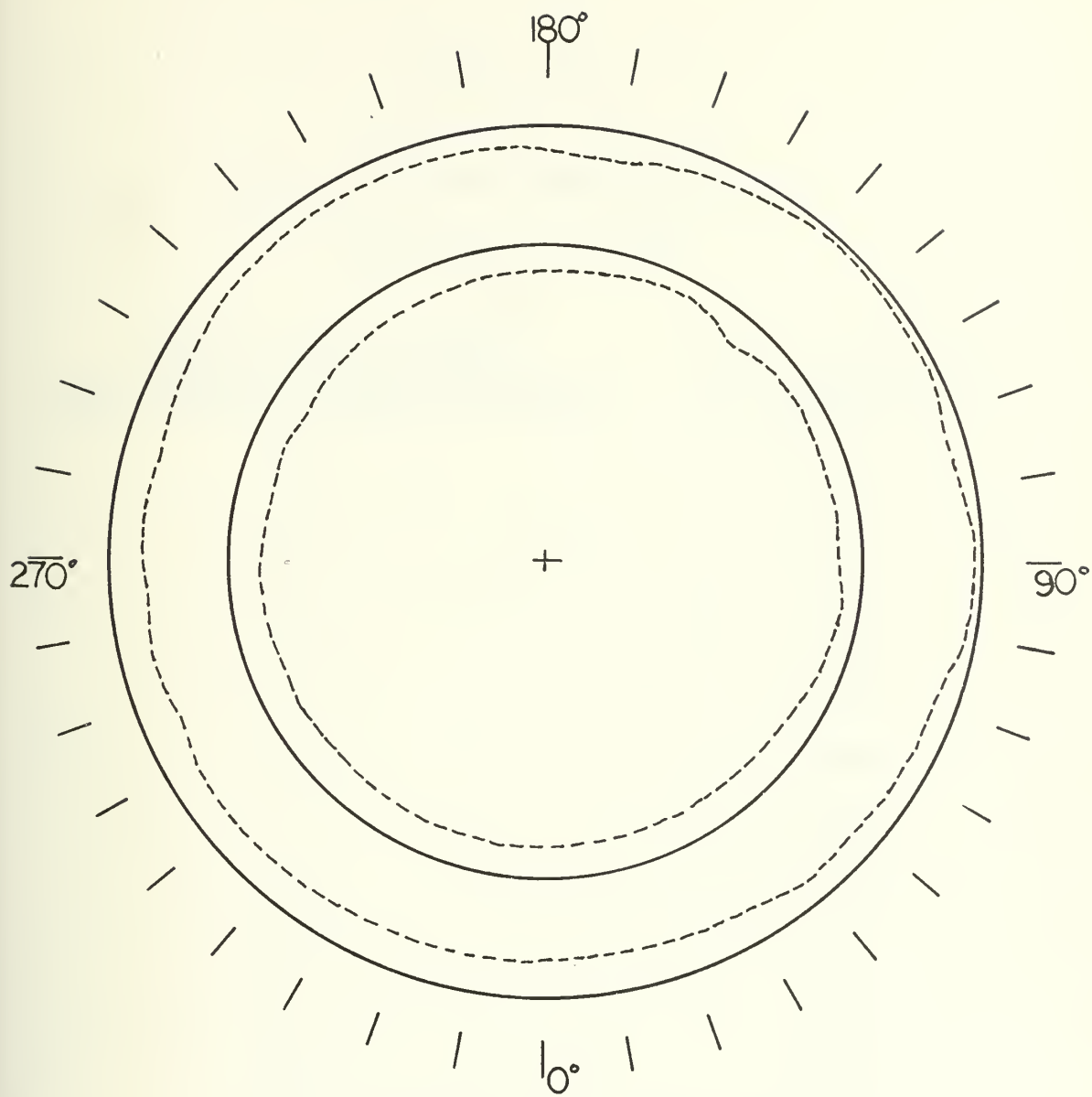
Figure I-23

- - - - - Deformation profiles
Scale : 5"≙1"

Figure I–24

TABLE I-14

SPECIMEN NO. 21

RADIAL DEFLECTION MEASUREMENTS ON

SEMICIRCLE 0° - 180°

Angle of Measurement From Left Side, Measured From Bottom of Flange (Degrees)	Radial Deflection (inches)
10	0.181
20	0.146
30	0.156
40	0.202
50	0.248
60	0.266
70	0.291
80	0.312
90	0.306
100	0.298
110	0.308
120	0.298
130	0.276
140	0.234
150	0.204
·160	0.214
170	0.302

150°

90°

30°

- - - - Deformation profile
Scale : $1'' \hat{=} 1''$
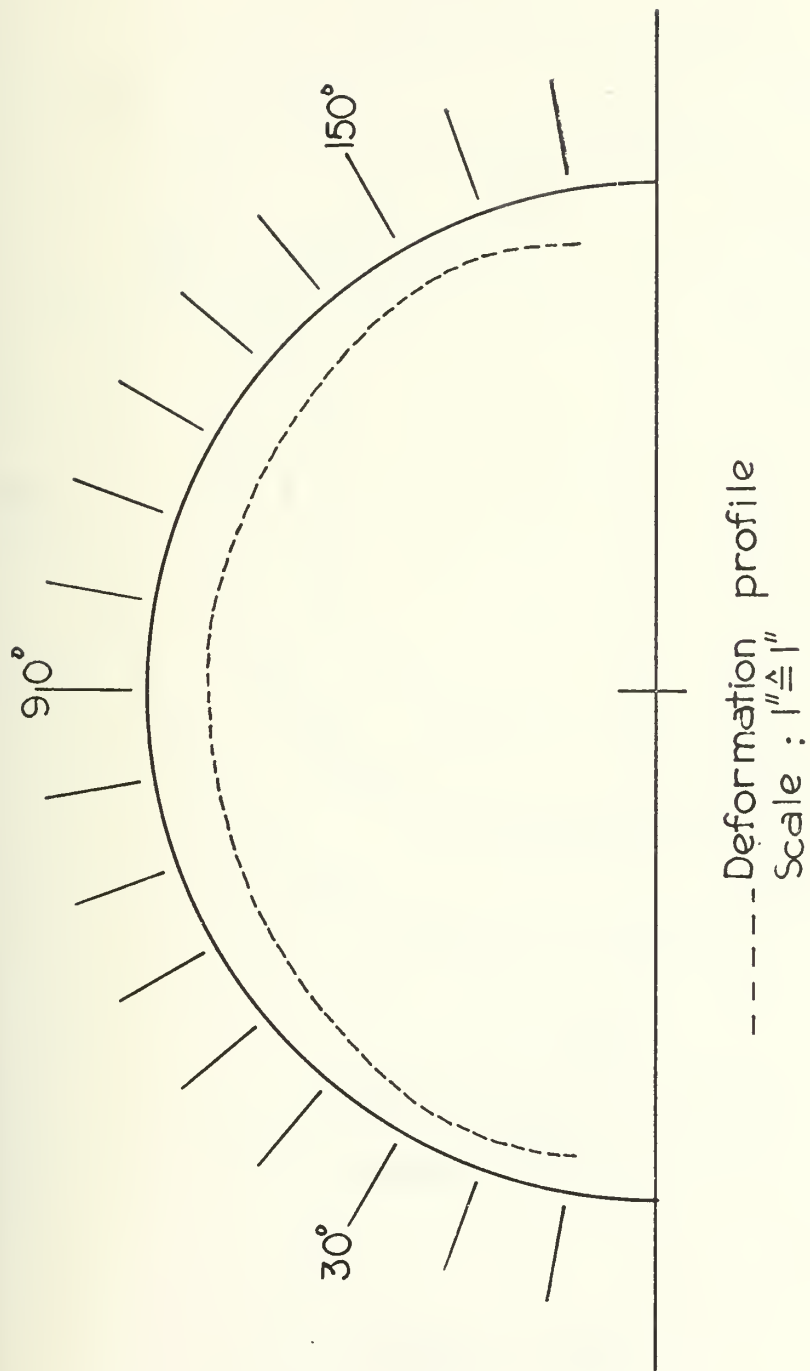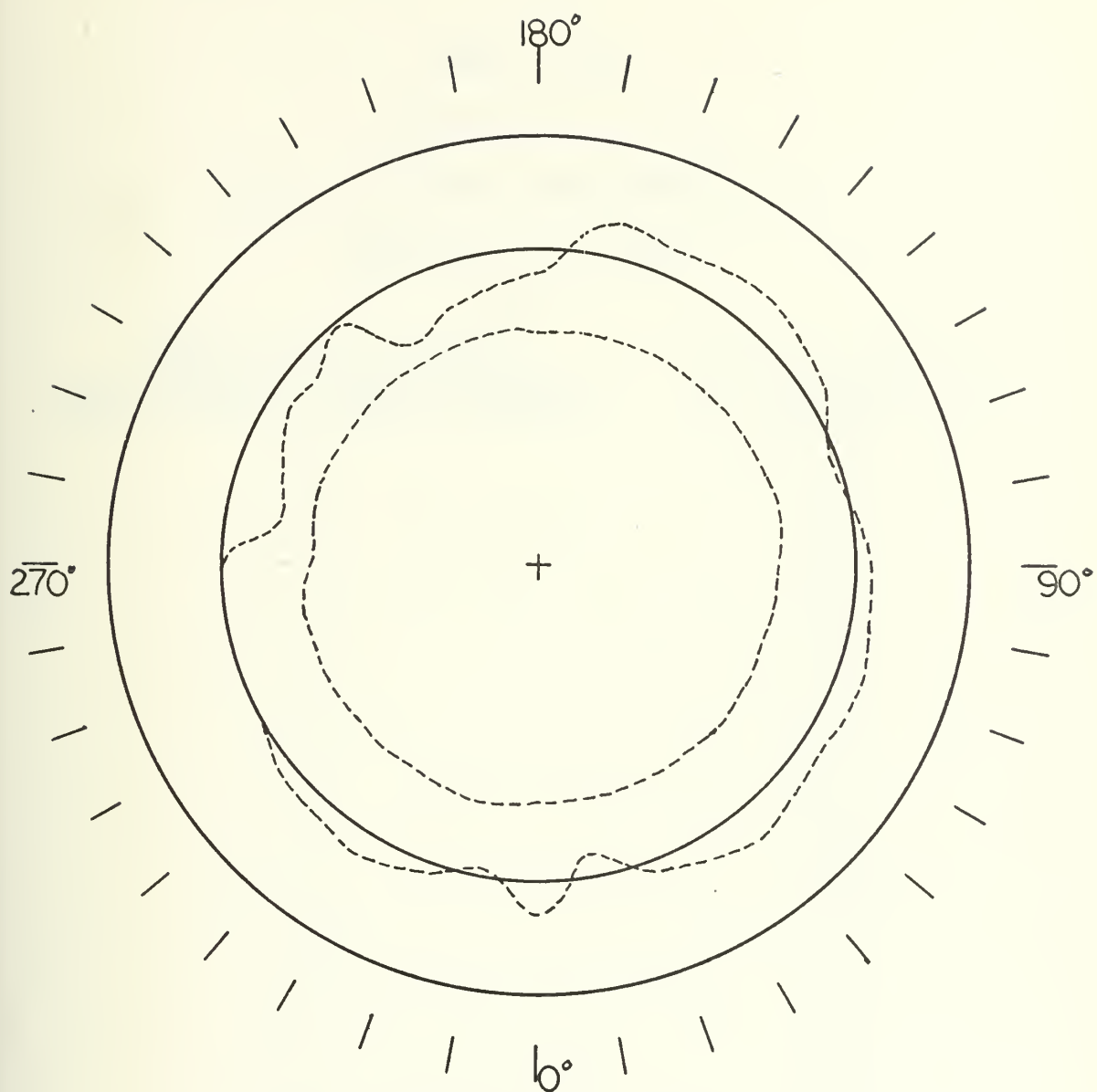
Figure I-25

Deformation profiles

Scale : $5'' \stackrel{\wedge}{=} 1''$

Figure I-26

TABLE I-15

SPECIMEN NO. 26

RADIAL DEFLECTION MEASUREMENTS ON

SEMICIRCLE 0° - 180°

Angle of Measurement From Left Side, Measured From Bottom of Flange (Degrees)	Radial Deflection (inches)
10	0.062
20	0.048
30	0.042
40	0.067
50	0.123
60	0.148
70	0.153
80	0.1535
90	0.1575
100	0.142
110	0.127
120	0.1175
130	0.108
140	0.053
150	0.012
160	0.010
170	0.0225

Deformation profile
Scale : $2'' = 1''$
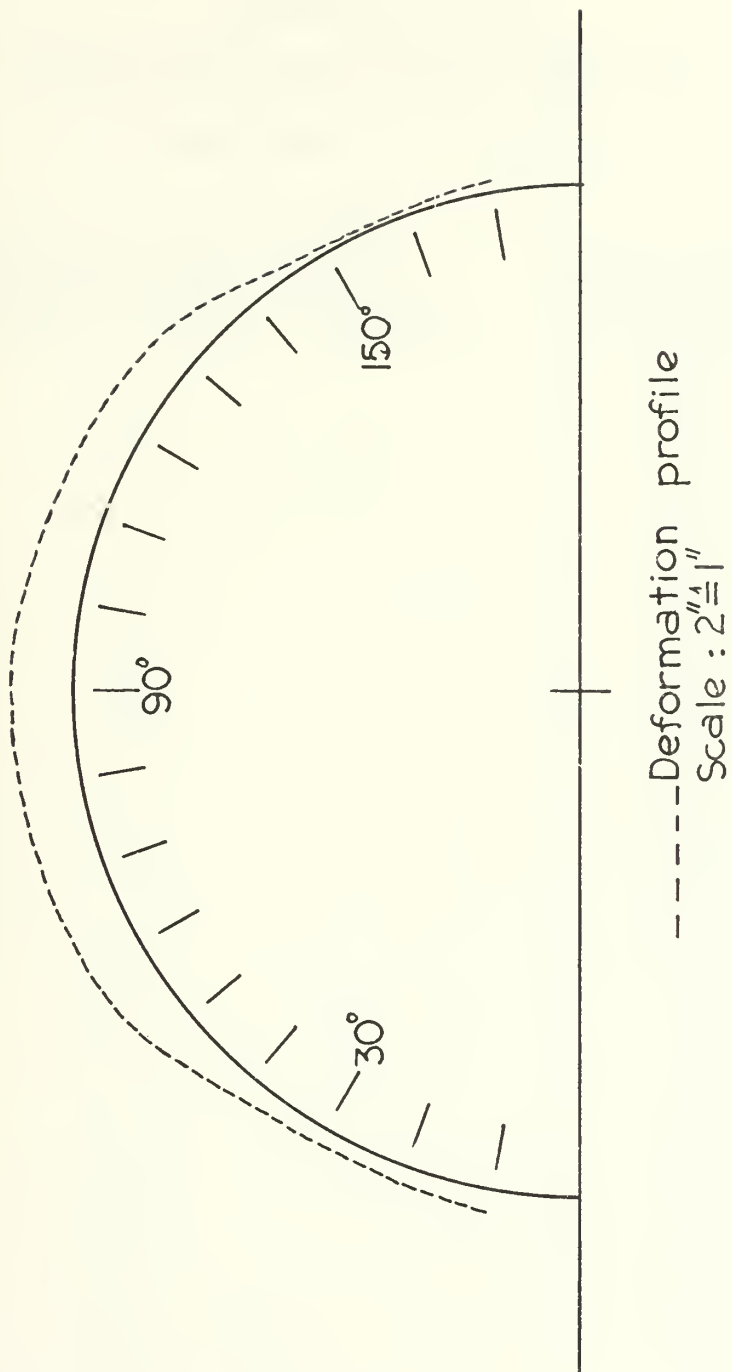
Figure I-27

TABLE I-16

SPECIMEN NO. 28

RADIAL DEFLECTION MEASUREMENTS ON

SEMICIRCLE 315°-135°

Angle of Measurements From Left Side, Measured From Bottom of Flange (Degrees)	Radial Deflection (inches)
10	0.072
20	0.061
30	0.108
40	0.157
50	0.156
60	0.148
70	0.147
80	0.1665
90	0.175
100	0.166
110	0.1475
120	0.137
130	0.133
140	0.125
150	0.088
160	0.046
170	0.053

----- Deformation profile
Scale : 2"=1"
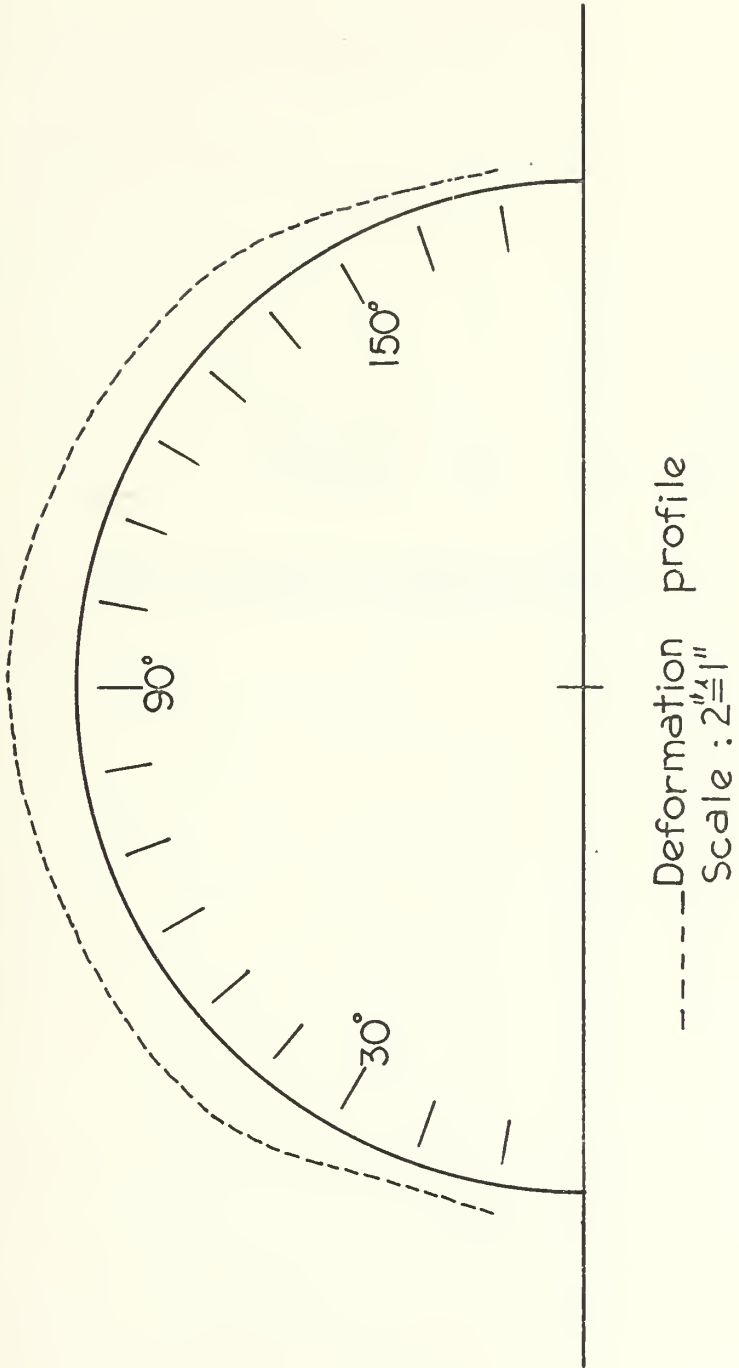
Figure I-28

APPENDIX II

CALIBRATION OF THE EXPLOSIVE

Calibration of the Explosive

Notation Used

I_{sp} = specific impulse imparted to specimen by the explosive

V_{avg} = average velocity of disc for a given test

x = displacement of disc from its rest position

Δx = distance between positions of the disc

Δt = time interval between positions of the disc

h = nominal thickness of explosive used

t = thickness of calibration specimen

W_e = weight of explosive

W_s = weight of disc specimen

I_t = total impulse imparted to specimen by explosive

Procedure

An important part of this work is to determine the impulse imparted to the test specimen by the explosive. To this end, the velocity of a flat circular plate accelerated upwards by the explosive was measured. Since the mass of the circular plate and that of the explosive were known, the specific impulse was calculated as a product of the mass of the specimen times the average velocity, divided by the mass of the explosive. Hence, the units of the specific impulse are dyne-sec per gram of explosive.

The specimens used for the calibration of the explosive were steel and aluminum discs at 3 inches diameter and thicknesses 1/8 inch or 1/4 inch. A Fastax (Wollensak WF-2) framing camera (approximately 12,000 pictures per second) equipped with a standard Fastax 1,000 cycles per second glow tube was used to record the motion of the specimens on 100 feet rolls of Eastman 4-x Negative Type 7224 film. The set-up used for the calibration tests is shown in Figures II-1, II-2 and II-3. A 1/4 inch thick foam attenuator (polyeurethene form of polyester type, with a density of 0.032 gram/cm^3), cut to the specimen size was attached on the specimen with Dupont No. 4684 cement and the explosive cut in the same shape was attached on the form using the same cement.

-107-

A steel plate with a 3.5 inches diameter hole in
its middle was bolted to the table of the blasting cham-
ber and used as a base. A steel rule with one inch
intervals marked was erected perpendicular to the plate
surface at the edge of the hole and was held in place
by clamps attached on a vertical bar which in turn was
bolted on the plate. The hole in the plate was just
large enough for the specimen to go through, thus keep-
ina a great amount of smoke out of the field of view of
the camera. In order to hold the disc in position, a
piece of cardboard with a circular hole in its center of
diameter slightly smaller than that of the disc was at-
tached to the steel plate by masking tape. The disc
rested on this cardboard piece as shown in Figure II-3.
In all tests made for the calibration the specimens were
directed upwards.

The detonation procedure was kept the same as that
of the tests with the actual specimens. A Detasheet
leader of dimensions 1/4" x 40" x 0.015" was folded over
1/4" at one end and was attached in the center of the
explosive on the disc. The other end was folded over a
length of 1.5 inches and then placed in contact with a
number 6 blasting cap, whose leads were connected to the
blasting control circuit.

The camera was set so that when the circuit was actuated it would run for 0.7 seconds in order to reach its maximum speed before the blasting cap was detonated. A previously calibrated 1,000 cps. timing device recorded equally spaced markers on the edge of the film. Two 1,000 watt spot lights were aimed at the flight path of the specimen in order to provide the required illumination. All the specimens were painted with white enamel, so that their images would be more easily distinguished in the film. The speed of the camera in the different tests was measured from the films and it was found to vary between 11,300 and 14,000 pictures per second.

The next step was to measure the velocity of the specimens using the data taken from the films. Each film was first measured to find out the time elapsed between two successive frames. This time was based on the 1,000 cps. timing marks which had previously been checked for accuracy with an oscilloscope. The time between successive frames was assumed to be constant over the length of the film after the explosion. Next each frame was projected on a screen placed at such distance from the projector so that the images came out in full size. Then the images of the specimen as shown in each frame were drawn on a sheet of paper which was graduated in inches and tenths of an inch and which was attached on

the screen. The subdivisions of the measuring rule were
made to coincide with the subdivisions of the graduated
sheet. In some tests every image of successive frames
was drawn while in others every other, every third or
every fourth image was drawn. A typical graduated sheet
with the specimen images drawn is shown in Figure II-4
(from test No. 20).

Next, the distance of the apparent center of gravity
of the disc (as shown by its image) from the base was
measured. The differences in distance from the base be-
tween each pair of successive images was then found and
all the differences were averaged. The average velocity
could then be found by dividing the average distance be-
tween frames by the time between frames which was already
calculated from the film. In Figure II-5, a photograph
of a specimen during a test (test No. 15) is shown; the
specimen can be seen clearly at the top of the smoke
which covers the lower part of the graduated steel rule.

Once the average velocity had been found, the spec-
ific impulse was found by using the equation:

$$I_{sp} = \frac{W_s V_{avg}}{W_e}$$

-110-

Results

Twenty-six tests were conducted with circular discs of which twenty-one gave results and were taken into account in the calculation of the average specific impulse. The average specific impulse is:

$$I_{sp} = 18.172 \times 10^4 \text{ dyne-sec/(gram of explosive)}$$

or

$$I_{sp} = 0.4069 \qquad \text{lb-sec/(gram of explosive)}$$

Four additional tests were made in order to assess the effect of the explosive leader on the specific impulse. In these tests only the leader was attached on the foam attenuator by Dupont No. 4684 cement. In two of these tests only an area of 1/4" x 1/4" of the explosive way in contact with the foam, while in the other two the leader was folded over a length of 1/4" and then the folded part was attached on the foam of the specimen (the second case representing the actual way in which the leader was attached on the specimen in all the calibration tests). In the calculation of the average specific impulse mentioned above, the effect of the leader was taken into account.

-111-

As a check with previous calculations of specific impulse, in Reference (5), a value of Is = 17.09×10^4 dyne-sec/gram of explosive is reported, in Reference (6), a value of 17.69×10^4 dyne-sec/gram, while in Reference (7), values of 19.2×10^4 dyne-sec/gram and 18.42×10^4 dyne-sec/gram are reported. Thus, it is seen that the value of specific impulse obtained herein, lies in the range of results obtained previously.

Table II-1 shows the data used in obtaining the average velocity in each test. Table II-2 shows the data used for the calculation of specific impulse or total impulse for all tests made and Table III-3 shows the specific impulses of the different tests used in the calculation of the average specific impulse.

In Figure II-6, a graph is presented of the total impulse of each test as function of the explosive weight. The straight line drawn through the origin has a slope equal to the specific impulse referred to above. Thus, it is seen that the variation of total impulse with explosive weight is linear. In Figure II-7 the calibration results are shown with specific impulses plotted as functions of nominal thickness of the explosive used.

Sample Calculations

For the sample calculations made below the results
found for test No. 5 were considered. Table II-1 shows
the heights of the successive positions of the specimen
from the base. It should be mentioned here that these
heights measurements taken from the motion pictures
taken during the calibration tests are not exact because
they neglect the thicknesses of the cardboard (used to
support the specimens as mentioned above), the attenuator,
the explosive and the specimen itself. This inaccuracy
doesn't have any effect on the results however, since
the average velocity was calculated on the basis of dif-
ferences in distance between positions of the specimen,
and not on the basis of distances from the base. The
average distance between positions of the image of the
specimen for test No. 5 was found to be 0.377 in as
shown in Table II-1. The speed of the camera was found
as 11,500 pictures per second. The positions of the
specimen were measured every 4 frames and hence the time
between two positions of the specimen is

$$\frac{4}{11,500} = \frac{1}{2,875} \text{ seconds}$$

Therefore, the average velocity in this case will be:

-113-

$$V_{avg} = \frac{0.377 \text{ in.}}{(1/2,875) \text{ sec.}} = 1,084 \text{ inches/second}$$

After finding the average velocity, a calculation of the specific impulse can be made, since we know also the weight of the specimen and the weight of the explosive which are given in Table II-2. From Table II-2, we have:

$$W_s = 108.35 \text{ grams (weight of specimen)}$$

$$W_e = 1.6 \text{ grams (weight of explosive)}$$

Converting the above found average velocity in centimeter per second we have:

$$V_{avg} = 1,084 \text{ inches/second} = 2,753 \text{ cm/sec.}$$

Finally, with the above data the value of specific impulse for test No. 5 is calculated as follows:

$$I_{sp} = \frac{W_e \times V_{avg}}{W_e} = \frac{108.35 \text{ grams} \times 2,753 \text{ cm/sec}}{1.6 \text{ grams}}$$

$$= 18.64 \times 10^4 \text{ dyne-sec/(gram of explosive)}$$

The values for specific impulse calculated in a similar way for all tests made are given in the seventh column of Table II-2.

-114-

Calculations of Effect of Gravity and Air Drag
on Specific Impulse

It is our purpose here to find out how much the velocity calculated from the films taken during the calibration tests must be changed in order to take into account the effects of gravity and air drag.

The following nomenclature is used:

V_o = velocity measured from calibration film

V_g = velocity which must be added to V_o because of gravity effects

V_a = velocity which must be added to V_o because of air drag effects

m = mass of calibration specimen

h = average height of different positions of calibration specimen, used in the calculation of V_o

g = acceleration of gravity

D = air drag

Considering gravity effects first and equating the total energy of the calibration specimen in height zero and h , we have:

$$\frac{1}{2} m \left(V_o + V_g\right)^2 = \frac{1}{2} m V_o^2 + mgh .$$

Disregarding the second order term (V_g^2) and solving for V_g, we get:

$$V_g = \frac{gh}{V_o}$$

Next considering air drag effects alone, and equating again the energy at zero height to the energy at height h, we get:

$$\frac{1}{2} m (V_o + V_a)^2 = \frac{1}{2} m V_o^2 + D \cdot h$$

Disregarding again the second order term V_a^2 and solving for V_a, we get

$$V_a = \frac{D \cdot h}{m V_o}$$

As an example, for test No. 18 with V_o = 4,810 in/sec. h = 7.3 in, m = 40.35 grams = 0.0889 lb_m we have:

$$V_g = \frac{32.2 \text{ ft/sec}^2 \times 7.3 \text{ in} \times 12 \text{ in/ft}}{4,810 \text{ in/sec}} = 0.586 \text{ in/sec}$$

which corresponds to 0.012% increase of V_o. For the air drag effects we used the following formula:

$$D = C_D \times \frac{\rho}{2} V^2 A$$

where

C_D = drag coefficient, which for Reynolds numbers
higher than 10^3 for a disc normal to the
flow is 1.12 according to reference 8.

ρ = air density

A = area of calibration specimen

In the case of test No. 18 we have:

$$\text{Reynolds No.} \quad Re = \frac{V_o d}{\nu}$$

where

V_o = average speed of specimen

d = diameter of specimen

ν = kinematic viscosity of air

$$Re = \frac{4{,}810 \text{ in/sec} \times 3 \text{ in.}}{1.69 \times 10^{-4} \text{ft}^2/\text{sec} \times 12 \text{ in/ft} \times 12 \text{ in/ft}} = 5.929 \times 10^5$$

Hence, $C_D = 1.12$ according to Reference 8.

$$\rho = 0.0683 \text{ lb}_m/\text{ft}^3$$

$$A = \frac{\pi d^2}{4} = \frac{\pi}{4}(3)^2 = 7.065 \text{ in}^2$$

$$D = \frac{1.12 \times 0.0683 \text{ lb}_m/\text{ft}^3 \times \left(\frac{4{,}810}{12} \text{ ft/sec}\right) \times 7.065 \text{ in}^2}{2 \times 32.2 \text{ lb}_m \text{ ft/lb}_f \text{ sec} \times 144 \text{ in}^2/\text{ft}^2}$$

$$= 9.36 \text{ lb}_f$$

and therefore:

$$V_a = \frac{D \cdot h}{m V_o} = \frac{9.36 \text{ lb}_f \times 7.3 \text{ in} \times 12 \text{ in/ft} \times 32.2 \text{ lb}_m \text{ ft/lb}_f \text{ sec}}{0.0889 \text{ lb}_m \times 4{,}810 \text{ in/sec}}$$

$$= 61.743 \text{ in/sec}$$

This corresponds to 1.279% increase of V_o. In test No. 18 and 16, the air drag effects were found 1.279% (as above) and 0.986% respectively and they were taken into account in the calculation of the corresponding specific impulses. In all other cases, both gravity and air drag effects were found varying from 0.01% to 0.4% and they were neglected.

The Effect of Specimen Rotation On Specific Impulse

The total kinetic energy (KE) of the disc used as specimen for the calibration, is equal to the sum of its translational energy and the energies of rotation about its x, y and z axes. x is the axis lying on the plane of the measurement rule, y is the axis normal to the plane of the measurement rule and z is the axis normal to the plane of the disc and parallel to the measurement rule, as shown in Figure II-2. The equation for the total kinetic energy is:

$$KE = m \frac{V_o^2}{2} + (I_x w_x^2 + I_y w_y^2 + I_z w_z^2)/2$$

where

m = mass of calibration specimen

V_o = average speed of specimen

I_x = moment of inertia about x axis

I_y = moment of inertia about y axis

I_z = moment of inertia about z axis

W_x = angular velocity about x axis

W_y = angular velocity about y axis

W_z = angular velocity about z axis

In all cases rotation about z axis was neglected ($W_z = 0$). Because of symmetry the moments of inertia

about x and y axes are equal $(I_x = I_y = I)$. This
moment of inertia with respect to axes x and y for
a disc of mass m and radius a is given by:

$$I = \frac{ma^2}{4} \text{ grams - cm}^2$$

if m is given in grams and a in centimeters.
Hence, the equation for the total kinetic energy becomes:

$$KE = m\frac{v_o^2}{2} + \frac{ma^2}{8} (w_x^2 + w_y^2)$$

As an example, let us consider test No. 9. In this
case, we have:

> m = 107.30 grams, V_o = 5,009 cm/sec   h = 7.5 in
>
> ϕ_x = 0 (rotation about x axis)
>
> ϕ_y = 22° = 0.384 radians (rotation about y axis)
>
> a = 1.5 in x 2.54 cm/in = 3.81 cm

$$I = \frac{ma^2}{4} = \frac{107.38 \times (3.81)^2}{4} = 389.68 \text{ grams-cm}^2$$

$$W_x^2 = 0 , \quad w_y^2 = \left(\frac{0.384 \times 5.009}{7.5 \times 2.54}\right)^2 = 10,195 \text{ sec}^2$$

$$KE = m\frac{v_o^2}{2} + I\frac{w_y^2}{2} = 107.38 \frac{(5.009)^2}{2} + 389.68 \frac{10.195}{2}$$

$$= (1.347 + 0.00198) \times 10^9 \text{ ergs} = 1.34898 \times 10^9 \text{ ergs}$$

If we call V_t the speed calculated after taking into account the rotation effect we will have:

$$\frac{1}{2} m V_t^2 = 1.34898 \times 10^9 \text{ ergs}$$

or

$$V_t^2 = \frac{134898 \times 10^9 \times 2}{10738} = 25125.349 \text{ cm}^2/\text{sec}^2$$

or

$$V_t = 5012.5 \text{ cm/sec}$$

Hence we see that the increase in speed due to rotation is 0.0698% and is therefore negligible. Similar results for rotation effects were also found in the other tests and therefore the effects of rotation on specific impulse were neglected.

Calculation of Effect of Explosive Leader On

Specific Impulse

As mentioned above two tests were performed in
which the leader was folded over a length of 1/4" and
then attached to the center of the specimen on the at-
tenuator. These tests are 27 and 28 of Table II-1.
The total impulse imparted to the specimens was cal-
culated by multiplying the average speed as shown in
Table II-1 by the weight of the specimen and is shown
in Table II-2. The average of the two thus obtained
total impulses is 2.405×10^4 dyne-sec.

In order to find the effect of the leader on the
specific impulse, the total impulse mentioned above was
subtracted from the total impulses I_t of all the tests
and the new total impulse is shown as I_t' in Table II-2
then these values I_t' so obtained were divided by the
weight of explosive used for each test and thus the
corrected value for the specific impulse given as I_{sp}'
in Table II-2 was obtained.

As an example, let us consider test No. 1. The
initial total impulse before the correction was
35.72×10^4 dyne-sec as given in Table II-2. The
corrected total impulse is:

$$I_t' = 35.72 \times 10^4 - 2.405 \times 10^4 = 33.315 \times 10^4 \text{ dyne-sec}$$

And since the weight of explosive used in test No. 1 was 2 grams, the corrected specific impulse is:

$$I_{sp}' = \frac{33.315 \times 10^4}{2} = 16.657 \times 10^4 \text{ dyne-sec/(gram of explosive)}$$

TABLE II-1

DATA USED IN OBTAINING THE AVERAGE VELOCITY OF

THE SPECIMEN IN EACH TEST MADE

Test Number	x (in)	Δx (in)	$(\Delta x)_{avg}$ (in)	Δt (sec)	V_{avg} (in/sec)	V_{avg} (corrected) (in/sec)
1	4.43					
	4.91	0.48				
	5.34	0.43				
	5.77	0.43				
	6.22	0.45				
	6.65	0.43				
	7.03	0.38	0.433	$\frac{1}{3,000}$	1,299	1,299
2	4.29					
	4.68	0.39				
	5.10	0.42				
	5.47	0.37				
	5.87	0.40				
	6.26	0.39				
	6.68	0.42	0.3983	$\frac{1}{6,000}$	2,390	2,390
3	Film came out very dark, probably due to insufficient illumination.					

TABLE II-1 (continued)

Test Number	x	Δx	$(\Delta x)_{avg}$	Δt	V_{avg}	V_{avg} (corrected)
4	3.29					
	3.67	0.38				
	4.01	0.34				
	4.38	0.37				
	4.73	0.35				
	5.06	0.33				
	5.41	0.35	0.353	$\frac{1}{6,000}$	2,118	2,118
5	4.08					
	4.42	0.34				
	4.80	0.38				
	5.16	0.36				
	5.54	0.38				
	5.92	0.38				
	6.30	0.38				
	6.72	0.42	0.377	$\frac{1}{2,875}$	1,084	1,084
6	3.39					
	4.08	0.69				
	4.76	0.68				
	5.41	0.65				
	6.09	0.68				
	6.83	0.74				
	7.54	0.71	0.691	$\frac{1}{3,000}$	2,075	2,075

TABLE II-1 (continued)

Test Number	x	Δx	$(\Delta x)_{avg}$	Δt	V_{avg}	V_{avg} (corrected)
7	4.0					
	4.32	0.32				
	4.70	0.38				
	5.07	0.37				
	5.46	0.39				
	5.83	0.37				
	6.20	0.37	0.366	$\frac{1}{5,650}$	2,068	2,068
8	5.28					
	5.57	0.29				
	5.88	0.31				
	6.18	0.30				
	6.46	0.28				
	6.76	0.30				
	7.08	0.32	0.30	$\frac{1}{5,900}$	1,770	1,770
9	5.38					
	6.02	0.64				
	6.68	0.66				
	7.36	0.68				
	8.04	0.68				
	8.80	0.76				
	9.50	0.70	0.686	$\frac{1}{2,875}$	1,972	1,972

TABLE II-1 (continued)

Test Number	x	Δx	$(\Delta x)_{avg}$	Δt	V_{avg}	V_{avg} (corrected)
10	5.90					
	6.44	0.54				
	6.96	0.52				
	7.45	0.49				
	7.98	0.53				
	8.48	0.50				
	8.95	0.47	0.508	$\dfrac{1}{5,900}$	2,997	2,997
11	5.78					
	6.12	0.34				
	6.50	0.38				
	6.88	0.38				
	7.31	0.43				
	7.77	0.44	0.394	$\dfrac{1}{6,000}$	2,364	2,364
12	6.12					
	6.54	0.42				
	6.93	0.39				
	7.27	0.34				
	7.57	0.30				
	7.88	0.31	0.352	$\dfrac{1}{6,500}$	2,288	2,288

TABLE II-1 (continued)

Test Number	x	Δx	$(\Delta x)_{avg}$	Δt	V_{avg}	V_{avg} (corrected)
13	4.53					
	5.10	0.57				
	5.68	0.58				
	6.20	0.52				
	6.74	0.54				
	7.30	0.56	0.554	$\frac{1}{6,750}$	3,740	3,740
14	4.89					
	5.32	0.43				
	5.76	0.44				
	6.23	0.47	0.446	$\frac{1}{6,750}$	3,010	3,010
15	6.98					
	7.37	0.39				
	7.73	0.36				
	8.12	0.39				
	8.49	0.38				
	8.83	0.34				
	9.20	0.37	0.3716	$\frac{1}{7,000}$	2,601	2,601

TABLE II-1 (continued)

Test Number	x	Δx	$(\Delta x)_{avg}$	Δt	V_{avg}	V_{avg} (corrected)
16	5.69					
	6.57	0.88				
	7.29	0.72				
	8.08	0.79				
	8.77	0.69	0.77	$\frac{1}{6,250}$	4,812	4,872
17	Field of view of camera was blocked by smoke.					
18	4.03					
	4.53	0.50				
	4.94	0.41				
	5.38	0.44				
	5.83	0.45				
	6.30	0.47				
	6.72	0.42				
	7.16	0.44	0.447	$\frac{1}{12,500}$	5,587	5,646
19	Position of specimen was not clear.					
20	4.58					
	5.04	0.46				
	5.52	0.48				
	6.00	0.48				
	6.48	0.48				
	6.99	0.51				
	7.48	0.49	0.483	$\frac{1}{6,150}$	2,975	2,975

TABLE II-1 (continued)

Test Number	x	Δx	$(\Delta x)_{avg}$	Δt	V_{avg}	V_{avg} (corrected)
21	Specimen exhibited a large amount of rotation.					
22	6.83					
	7.34	0.51				
	7.78	0.44				
	8.25	0.47				
	8.74	0.49				
	9.21	0.47	0.476	$\frac{1}{6,350}$	3,020	3,020
23	5.97					
	6.49	0.52				
	6.99	0.50				
	7.47	0.48				
	7.90	0.43				
	8.32	0.42	0.47	$\frac{1}{6,350}$	2,985	2,985
24	7.96					
	8.90	1.64	1.64	$\frac{1}{2,133}$	3,500	3,500
25	8.09					
	8.67	0.58				
	9.19	0.52				
	9.69	0.50	0.533	$\frac{1}{6,500}$	3,470	3,470
26	Specimen exhibited a large amount of rotation.					

TABLE II-1 (continued)

Test Number	x	Δx	$(\Delta x)_{avg}$	Δt	V_{avg}	V_{avg} (corrected)
27	4.45					
	4.54	0.09				
	4.63	0.09				
	4.73	0.10				
	4.84	0.11				
	4.93	0.09	0.096	$\frac{1}{867}$	83.2	83.2
28	5.0					
	5.11	0.11				
	5.23	0.12				
	5.33	0.10				
	5.45	0.12				
	5.54	0.09	0.108	$\frac{1}{867}$	93.7	93.7
29	4.41					
	4.48	0.07				
	4.56	0.08				
	4.63	0.07				
	4.70	0.07	0.0725	$\frac{1}{700}$	50.7	50.7

TABLE II-1 (continued)

Test Number	x	Δx	$(\Delta x)_{avg}$	Δt	V_{avg}	V_{avg} (corrected)
30	4.03					
	4.12	0.09				
	4.20	0.08				
	4.29	0.09				
	4.38	0.08				
	4.46	0.08	0.084	$\dfrac{1}{650}$	54.6	54.6

Remarks on TABLE II-1

1. In the above calculations of average velocity, only
   in the tests No. 16 and 18 the correction due to air
   drag was taken into account, since it was found to
   amount to about 1% of the initially calculated values.
   In all other tests the corrections due to air drag
   were negligible. In all tests the corrections due
   to gravity and rotation were found to be negligible.

2. In Table II-1 Δt refers to the time elasped between
   two successive measurements.

3. The last four tests are the ones made with the
   leader alone as mentioned above.

TABLE II-2

DATA USED IN COMPUTING THE AVERAGE SPECIFIC IMPULSE

OF THE DETASHEET EXPLOSIVE

Test No.	t (in)	W_s (gms)	W_e (gms)	h (in)	V_{avg} (cm/sec)	$I_{sp} \times 10^{-4}$ $\left(\frac{\text{dyne-sec}}{\text{grams}}\right)$	$I_t \times 10^{-4}$ (dyne-sec)	$I'_t \times 10^{-4}$ (dyne-sec)	$I'_{sp} \times 10^{-4}$ $\left(\frac{\text{dyne-sec}}{\text{grams}}\right)$
1	1/8	108.3	2.0	0.010	3,299	17.86	35.72	33.315	16.657
2	1/8	108.0	3.53	0.020	6,070	18.571	65.556	63.151	17.89
3	1/8	106.5	3.35	0.020	Film came out very dark				
4	1/8	107.4	2.81	0.015	5,380	20.56	57.78	55.375	19.70
5	1/8	108.35	1.6	0.010	2,753	18.64	29.83	27.425	17.14
6	1/8	106.35	2.79	0.015	5,260	20.05	55.939	53.534	19.18
7	1/8	106.51	2.83	0.015	5,252	19.76	55.94	53.535	18.92
8	1/4	221.1	5.42	0.030	4,496	18.34	99.40	96.995	17.89
9	1/8	107.38	2.77	0.015	5,009	19.42	53.79	51.385	18.55
10	1/8	107.88	4.35	0.025	7,613	18.88	82.13	79.725	18.32
11	1/4	221.25	6.8	0.040	6,005	19.54	132.86	130.455	19.184
12	1/4	221.3	6.62	0.040	5,812	19.43	128.61	126.205	19.06

TABLE II-2 (continued)

Test No.	t (in)	W_s (gms)	W_e (gms)	h (in)	V_{avg} (cm/sec)	$I_{sp} \times 10^{-4}$ $\left(\dfrac{\text{dyne-sec}}{\text{grams}}\right)$	$I_t \times 10^{-4}$ (dyne-sec)	$I'_t \times 10^{-4}$ (dyne-sec)	$I'_{sp} \times 10^{-4}$ $\left(\dfrac{\text{dyne-sec}}{\text{grams}}\right)$
13	1/8	107.3	5.6	0.030	9,498	18.20	101.92	99.515	17.77
14	1/8	106.77	4.14	0.025	7,645	19.72	81.63	79.225	19.136
15	1/4	221.45	7.95	0.045	6,607	18.40	146.30	143.895	18.10
16	1/8	40.35	2.75	0.015	12,376	18.158	49.93	47.525	17.28
17	1/4	213.96	7.98	0.045	Field of view of camera was blocked by smoke.				16.59
18	1/8	40.10	3.32	0.020	14,340	17.32	57.5	55.095	
19	1/4	221.74	5.67	0.030	Position of specimen was not clear.				
20	1/8	108.0	4.63	0.025	7,560	17.62	81.58	79.175	17.10
21	1/8	107.83	5.24	0.030	Specimen showed a large rotation.				
22	1/4	223.95	8.71	0.050	7,670	19.70	171.60	169.195	19.42
23	1/4	213.63	8.80	0.050	7,580	18.38	161.80	159.395	18.11
24	1/4	221.09	10.90	0.060	8,900	18.10	198.00	195.595	17.94
25	1/4	215.06	10.58	0.060	8,810	17.93	189.50	187.095	17.68

TABLE II-2 (continued)

Test No.	t (in)	W_s (gms)	W_e (gms)	h (in)	V_{avg} (cm/sec)	$I_{sp} \times 10^{-4}$ $\left(\dfrac{\text{dyne-sec}}{\text{grams}}\right)$	$I_t \times 10^{-4}$ (dyne-sec)	$I_t' \times 10^{-4}$ (dyne-sec)	$I_{sp}' \times 10^{-4}$ $\left(\dfrac{\text{dyne-sec}}{\text{grams}}\right)$
26	1/8	40.73	3.35	0.020	Specimen showed a large rotation.				
27	1/8	107.52	--	--	211.5	--	2.27	--	--
28	1/8	106.7	--	--	238.0	--	2.54	--	--
29	1/8	108.6	--	--	129.0	--	1.4	--	--
30	1/8	109.99	--	--	138.6	--	1.524	--	--

Remarks on TABLE II-2

1. In tests No. 16, 17 and 26 aluminum specimens where used, while in all the others steel specimens where used.

2. V_{avg} in this table was taken from the corrected average velocity from Table II-1.

3. I_t' in the above table represents the corrected total impulse obtained as explained above by taking into account the effect of the explosive leader. I_{sp}' is the corresponding corrected value of the specific impulse.

TABLE II-3

CALCULATION OF AVERAGE SPECIFIC IMPULSE

Test No.	$I'_{sp} \left(\dfrac{\text{dyne-sec}}{\text{gram}}\right) \times 10^4$
1	16.657
2	17.89
4 /	19.70
5	17.14
6	19.18
7	18.92
8	17.89
9	18.55
10	18.32
11	19.184
12	19.06
13	17.77
14	19.136
15	18.10
16	17.28
18	16.59
20	17.10
22	19.42
23	18.11
24	17.94
25	17.68

TABLE II-3 (continued)

The average of the above twenty-one values gives:

Average, specific impulse $= 18.172 \times 10^{4} \frac{\text{dyne-sec}}{\text{gram}}$

Remarks on TABLE II-3

1. In this table all tests that gave resuls are listed.

2. The specific impulse I'_{sp} is the corrected specific impulse as taken from TABLE II-2.
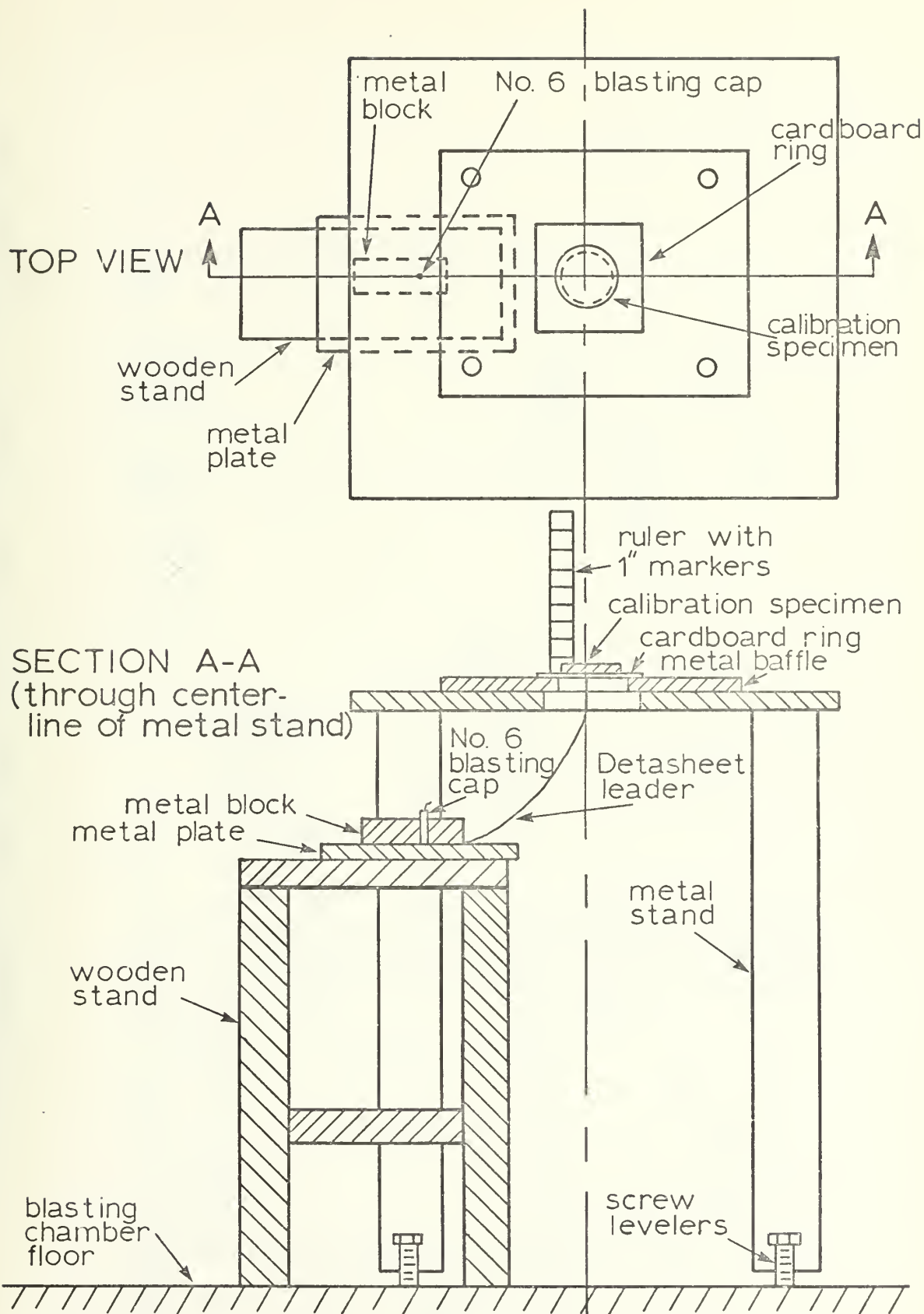
FIGURE II -1: Set-up for explosive calibration inside the blasting chamber
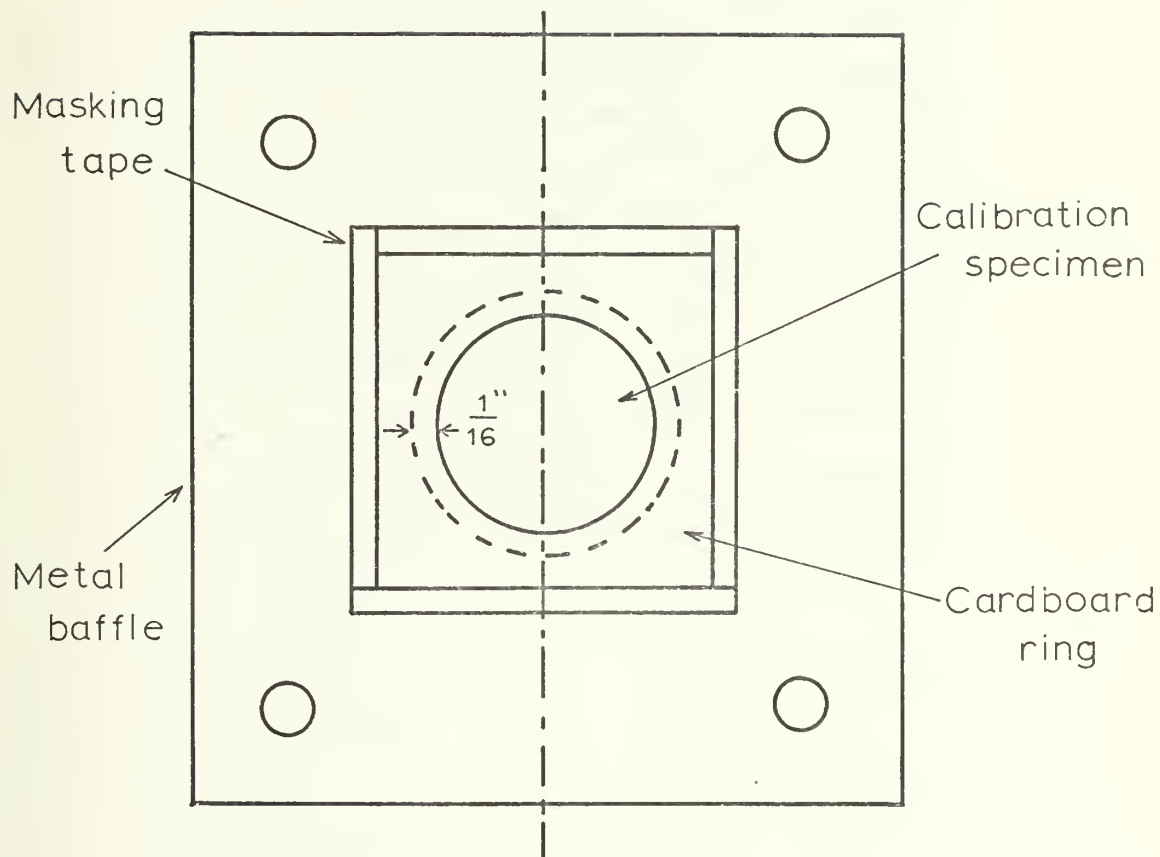
-138-
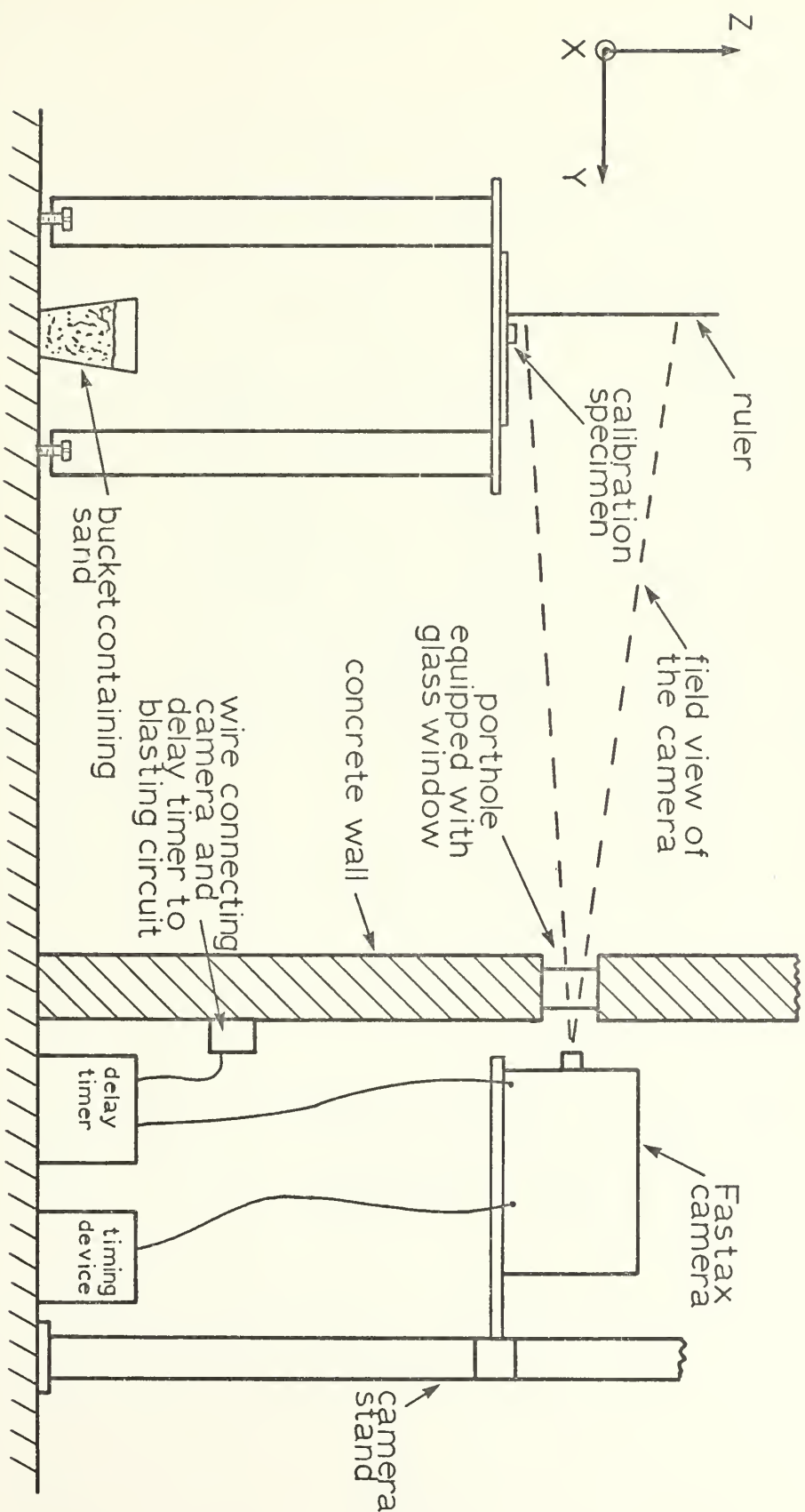
FIGURE II-2: Overall set-up for explosive calibration

Figure Ⅱ-3: Bottom view from metal
baffle of figure Ⅱ-1
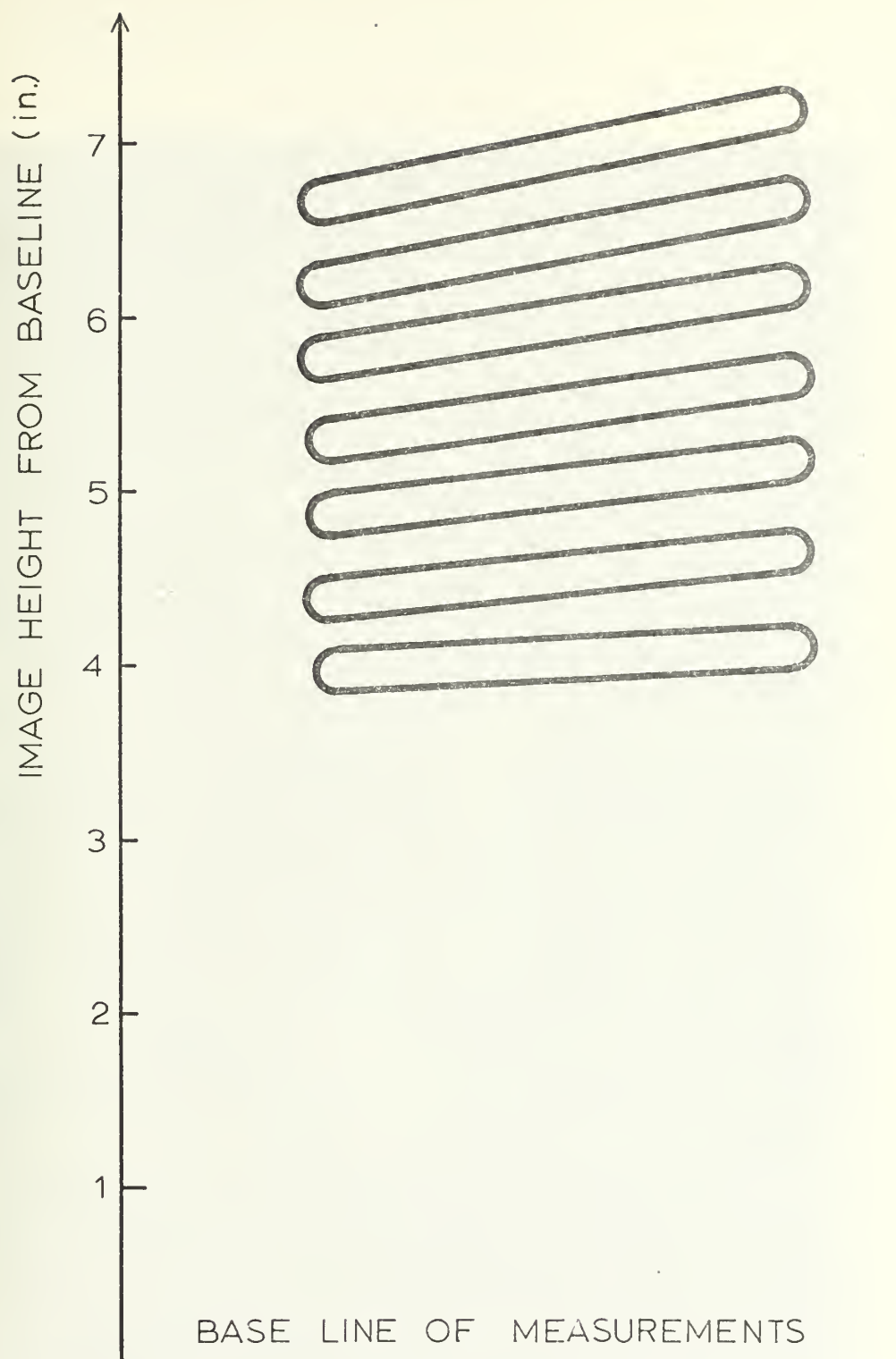
Figure II-4: Images of calibration specimen from test No. 20
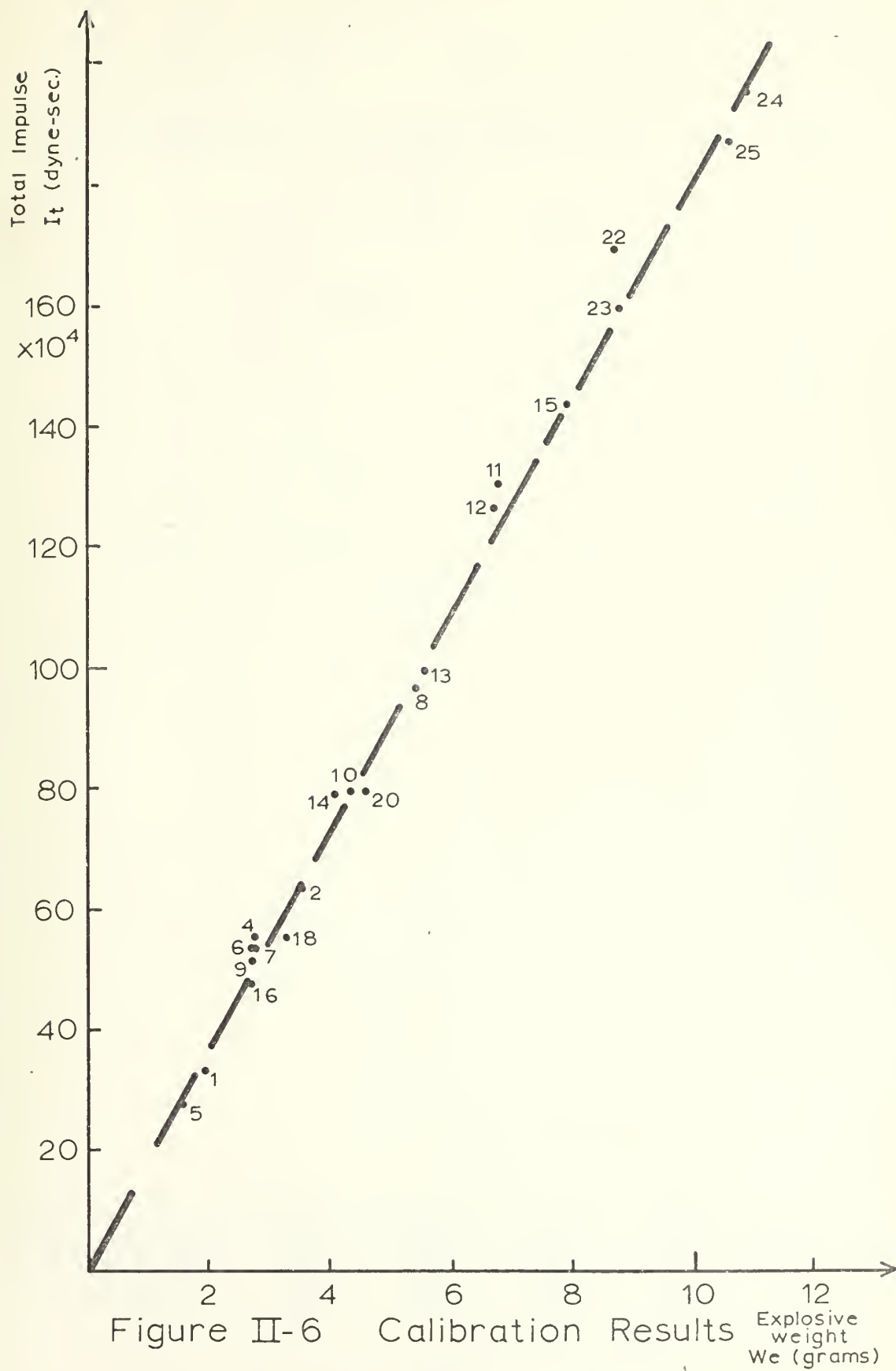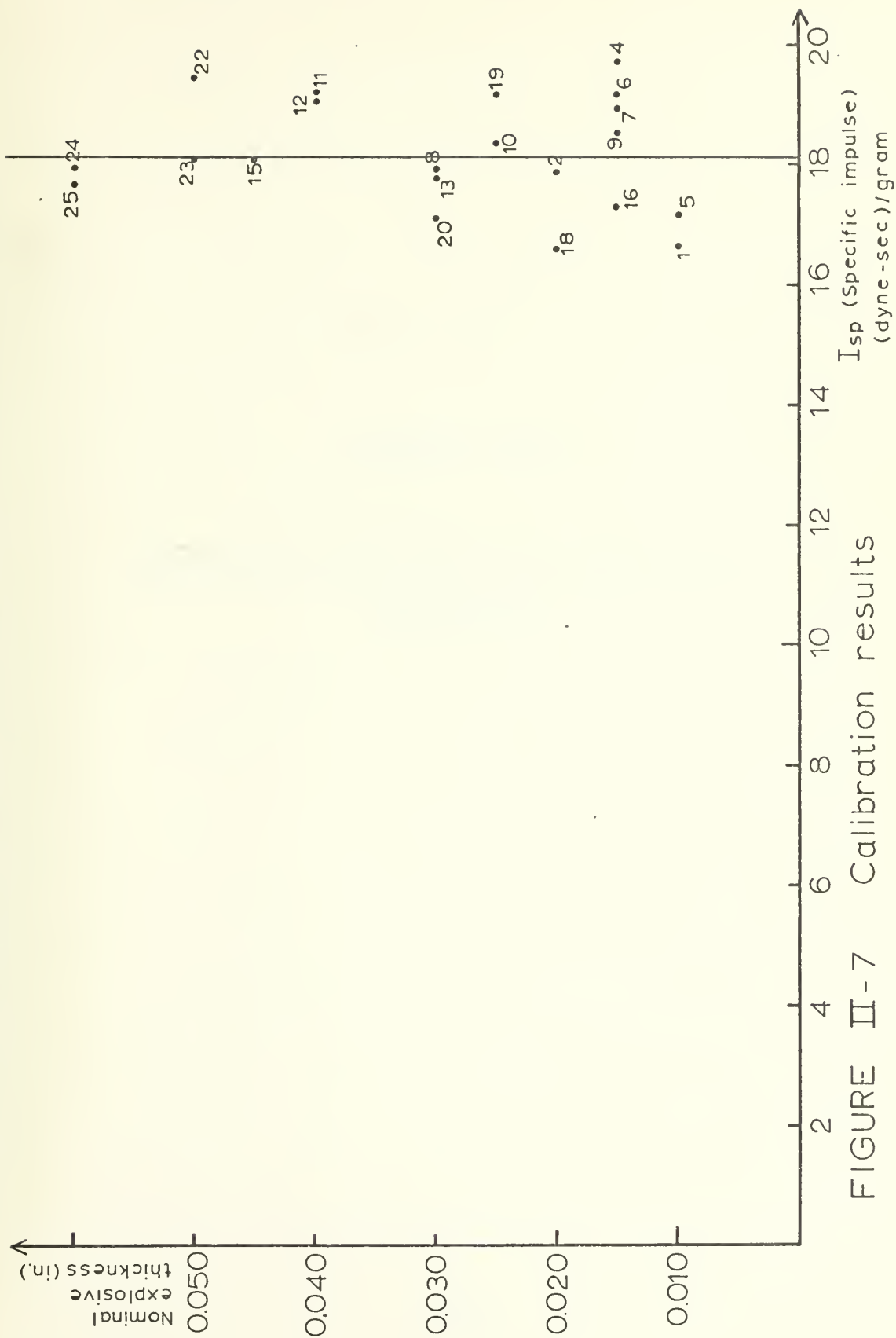
Figure II-5

Figure II-6   Calibration Results
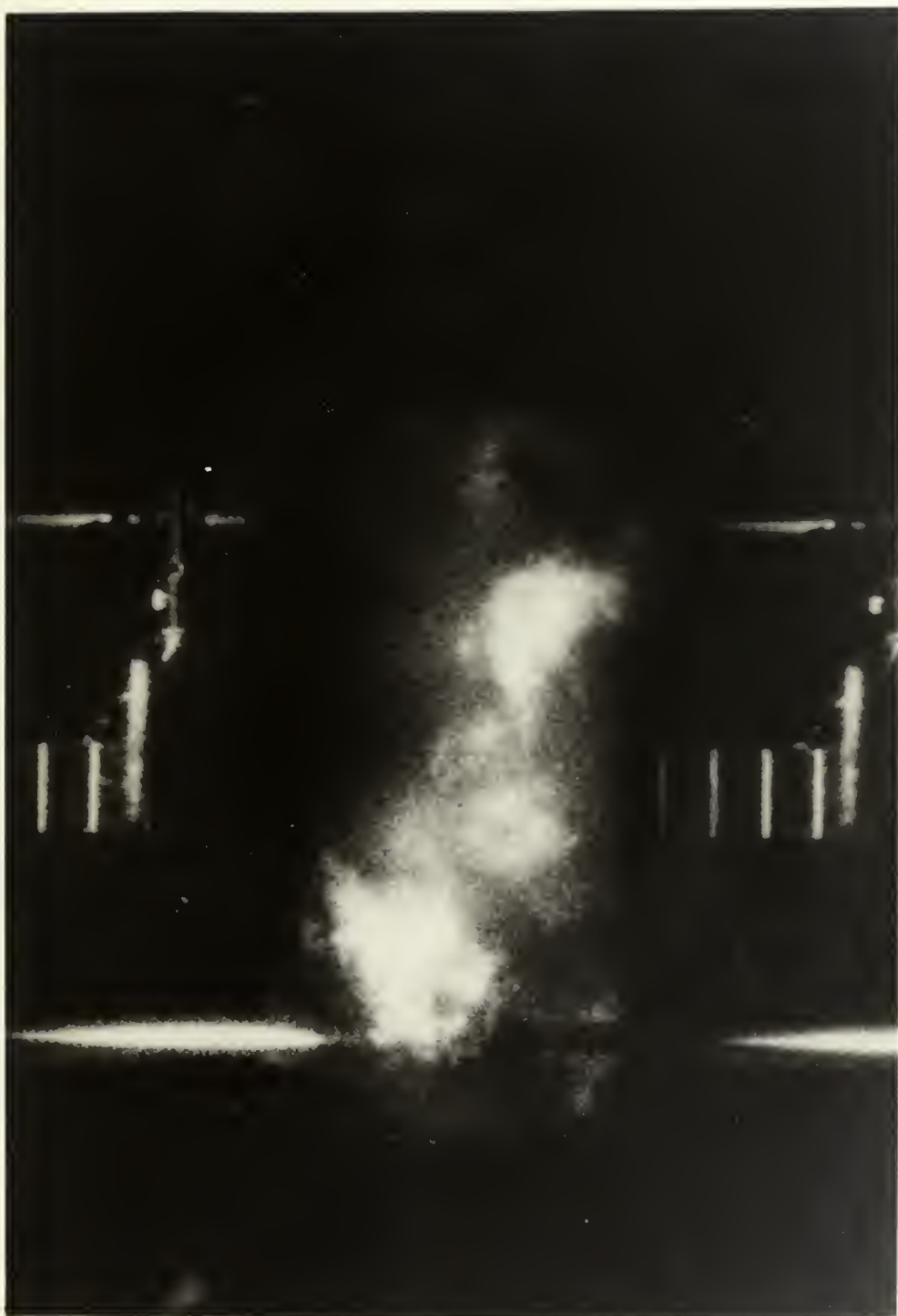
FIGURE II-7   Calibration results

APPENDIX -III-

PROPERTIES OF MATERIALS USED FOR SPECIMEN

FABRICATION

Properties of Materials Used
For Specimen Fabrication

Tensile tests were performed in order to find the strength characteristics of the materials used in the fabrication of the hemispherical test specimens. The tensile test specimens were cut from material left after the hydroforming of the hemispherical specimens. Since the aluminum hemispherical specimens were hydroformed in the zero condition of Aluminum 6061, and then heat treated to the T-6 condition, the material used in the fabrication of the tensile test specimens was also heat treated with the hemispherical specimens. The hemispherical specimens were hydroformed out of metal plates of area 1' x 1' and after the hydroformed hemispheres were cut, some of the remaining material was used for the fabrication of tensile test specimens. From each of the plates used for this purpose two tensile specimens were made with fiber direction perpendicular to each other; thus the name of the specimens has the same number but different letters. Four tensile tests with steel specimens and four with aluminum specimens were made. The steel specimens come all from the same order of material, while the aluminum specimens come from two different orders of material. From the tensile tests with aluminum specimens only three gave results.

An Instron testing machine which belongs to the Civil Engineering Department of M.I.T. and which has a total load carrying capability of 10,000 lbs. was used in conducting all the tensile tests. The machine setting used for all the steel specimens was 0.1 in/min. except for specimen L27 for which a machine setting of 0.05 in/min. was used. The machine setting used for all the aluminum specimens was 0.05 in/min., except for L13 for which a machine setting of 0.1 in/in/min. was used. The results of all these tests and the specimen characteristics are shown in Table III-1. The yield stress for the aluminum specimens was calculated on the basis of 0.2% offset method and is approximate because the scale of elongation in the graph produced in the Instron machine was not very large. The gauge lengths used were about 2 inches for all streel specimens, one inch for the aluminum specimens.

Two typical stress-strain diagrams of the tests made are shown in Figure III-1 for a steel specimen and in Figure III-2 for an aluminum specimen. These were obtained from load-elongation diagrams drawn during the the tests by the Instron machine, the initial cross sectional area of the specimen used in order to obtain the stress.

A chemical analysis for carbon content of the steel used for the fabrication of steel hemispherical specimens gave a carbon content of 0.21%.

Due to time shortage, the densities of the materials used were not determined experimentally, but on average of the values given in References 3, 5 and 6 is used. These average are 7.228×10^{-4} lb_f sec^2/in^4 for mild steel and 2.49×10^{-4} lb_f sec^2/in^4 for aluminum 6061-T6.

Finally, the Young's modulus used for steel is 30×10^6 psi and that for aluminum 10.5×10^6 psi. These values were not measured.

TABLE III-1

SPECIMEN CHARACTERISTICS AND RESULTS OF TENSILE TESTS

| Tensile Specimen Material	Specimen Number	Cross Sectional area (in^2)	G_y(psi) Lower Yield Stress	G_u(psi) Ultimate Stress	e Percentage Elongation
Aluminum 6061-T6	C13	0.109032	42,097	45,766	20.0
Aluminum 6061-T6	L13	0.106323	41,383	43,624	24.0
Aluminum 6061-T6	C14	0.105116	39,004	44,046	24.0
Mild Steel	C19	0.094116	44,201	65,451	34.1
Mild Steel	L19	0.093240	44,777	65,744	30.5
Mild Steel	C27	0.093957	45,872	65,775	26.6
Mild Steel	L27	0.093737	45,019	64,543	33.3
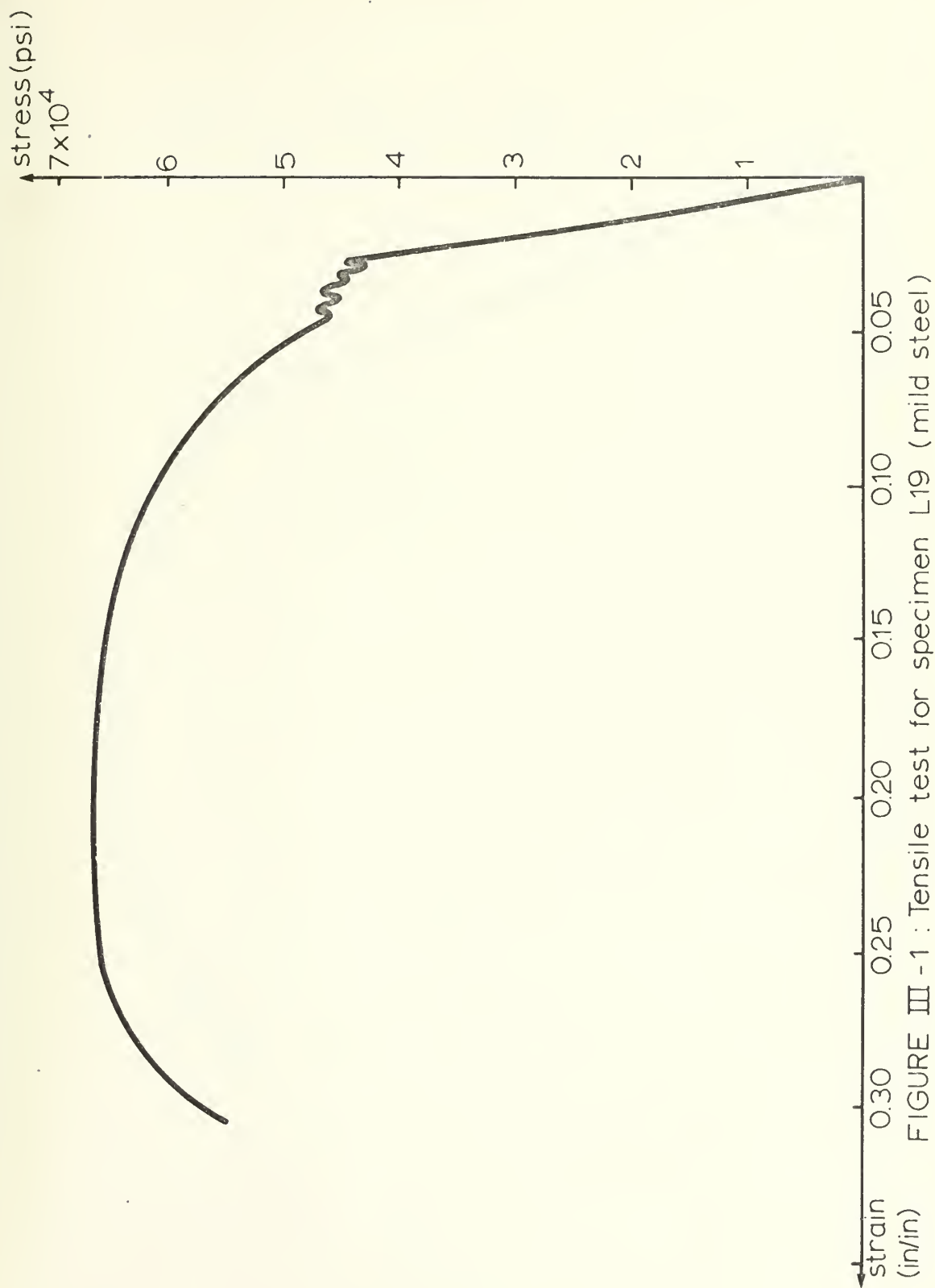
stress(psi)

FIGURE III-1: Tensile test for specimen L19 (mild steel)
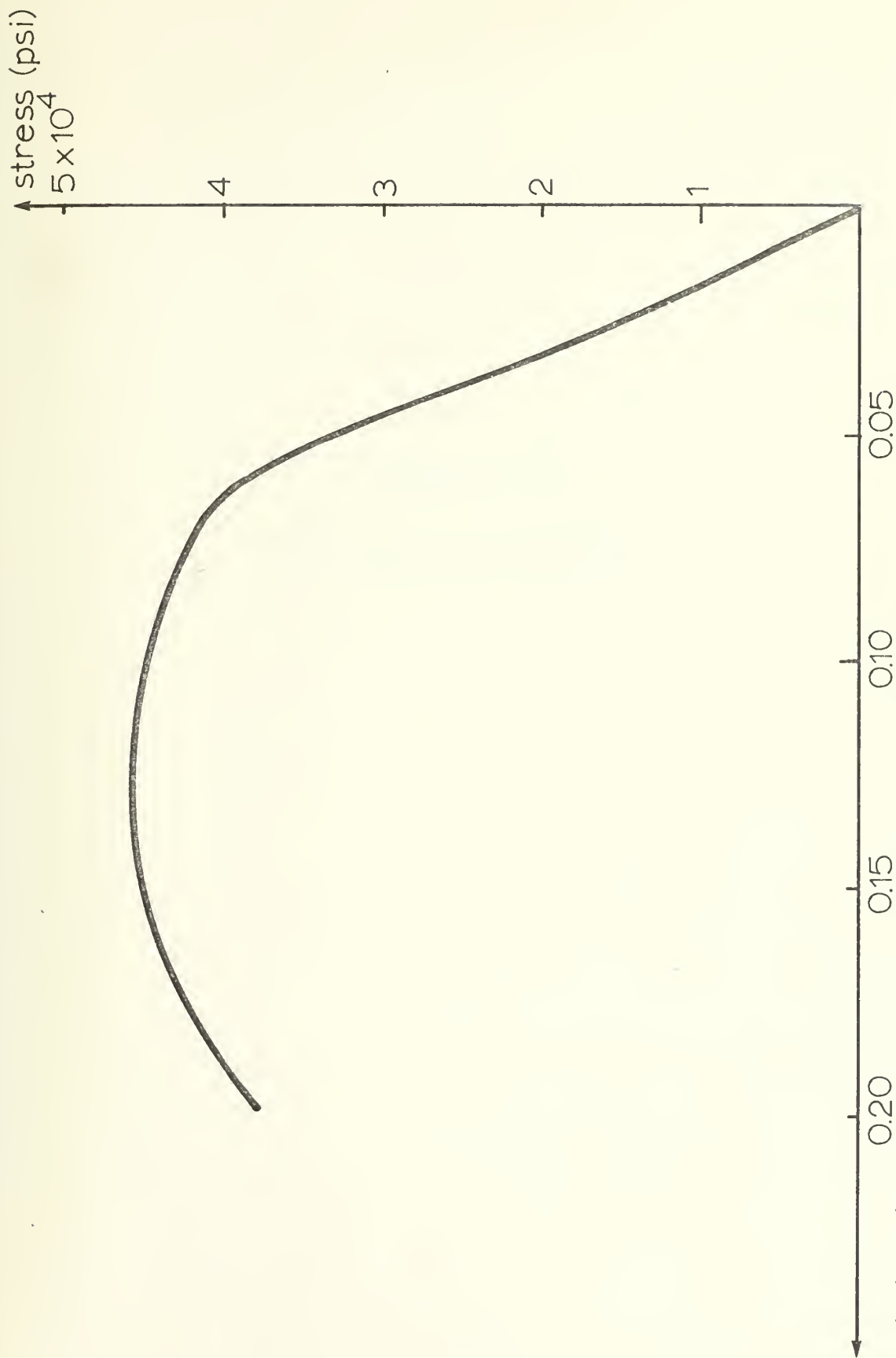
strain (in/in)

stress (psi)
5×10^4

strain (in/in) FIGURE III-2: Tensile test for specimen C13 (aluminum 6061-T6)

APPENDIX   IV

Explosive Specifications

Explosive Specifications

The explosive used was Du Pont "Detasheet" EL506D. Its composition is 63% pentaerythritol (PETN), 8% nitrocellulose and the remainder an elastomeric binder. It was delivered in rectangular sheets of 10 x 20 inches and thicknesses of 0.010", 0.015" and 0.030".

As mentioned in Reference 5, in the present experimental investigation a lot of problems were experienced when explosive thicknesses of 0.010" or 0.020" (which is a combination of 2 sheets of 0.010" thickness). In cases these thicknesses were used the explosion did not propagate all the way across the sheet of explosive used. After the tests pieces of the explosive were found intact, spread around the blasting chamber, or in other cases the explosive on the spherical shell was found burning. However, the sheets of explosive with thicknesses 0.015" and 0.030" presented no problems at all, as well as two sheets of 0.010" and 0.015" put together, the 0.015" thickness being on top.

The Detasheet characteristics according to the manufacturer are given in the following table.

Detonation velocity: 7,200 meters/sec

Density   1.45 grams/cm^3

Flexibility range   -30°F to 160°F

Thermal Stability

    25 hours   250°F

    1 hour   275°F

Hot Bar Ignition Temperature

    Instantaneous   565°F

    30 seconds   353°F